Brain Vital Signs: Towards Next Generation Neurotechnologies for Rapid Brain Function Assessments at Point-of-Care

by

Sujoy Ghosh Hajra

Thesis Submitted in Partial Fulfillment of the

Requirements for the Degree of

Doctor of Philosophy

in the

School of Engineering Science

Faculty of Applied Sciences

© Sujoy Ghosh Hajra 2019

SIMON FRASER UNIVERSITY

Fall 2019

Approval

Name:	**Sujoy Ghosh Hajra**
Degree:	**Doctor of Philosophy**
Title:	**Brain Vital Signs: Towards Next Generation Neurotechnologies for Rapid Brain Function Assessments at Point-of-Care**

Examining Committee: **Chair:** Kamal Gupta
Professor

Ryan D'Arcy
Senior Supervisor
Professor

Carolyn Sparrey
Supervisor
Associate Professor
Mechatronic Systems Engineering

Edward Park
Supervisor
Professor
Mechatronic Systems Engineering

Xiaowei Song
Supervisor
Adjunct Professor
Biomedical Physiology and Kinesiology

Carlo Menon
Internal Examiner
Professor

Erik Scheme
External Examiner
Associate Professor
Electrical and Computer Engineering
University of New Brunswick

Date Defended/Approved: November 18, 2019

Ethics Statement

The author, whose name appears on the title page of this work, has obtained, for the research described in this work, either:

   a.   human research ethics approval from the Simon Fraser University Office of Research Ethics

or

   b.   advance approval of the animal care protocol from the University Animal Care Committee of Simon Fraser University

or has conducted the research

   c.   as a co-investigator, collaborator, or research assistant in a research project approved in advance.

A copy of the approval letter has been filed with the Theses Office of the University Library at the time of submission of this thesis or project.

The original application for approval and letter of approval are filed with the relevant offices. Inquiries may be directed to those authorities.

<div align="right">

Simon Fraser University Library
Burnaby, British Columbia, Canada

Update Spring 2016

</div>

Abstract

Vital signs such as heart rate, blood pressure and body temperature have revolutionized medical care by providing rapidly assessed, physiology-based, non-invasive and easy-to-understand standardized metrics of different body functions. However, no such vital sign exists for the brain; instead, assessments of the brain are largely reliant on surrogate measures such as observations of behaviour or questionnaire-based measurements, which have been shown to be subjective and unreliable. This research aims to fill this key scientific, clinical, and technological gap by developing a brainwave-based technology platform to evaluate 'vital sign' metrics for the brain. A series of studies were undertaken to create and demonstrate a 'brain vital signs' platform that is capable of assessing a broad spectrum of functions ranging from the lower-level functions (i.e. sensation) to the highest-level cognition domains (i.e. contextual orientation). In particular, the first study focused on development and initial demonstration of the methods and apparatus for the brain vital signs technology; the next study focused on characterizing the brain vital sign responses to ensure scientific validity; the third study focused on creating a previously non-existant neurophysiology-based neural marker capable of capturing contextual orientation – which is the highest level cognitive domain known to be crucial to frontline clinical assessments; and finally, the last study focused on developing an advanced data analytic technique for maximizing signal capture under noisy environments typical of point-of-care evaluation settings. This research represents the first time that a 'vital sign'-like metric has been developed for the brain that embodies the key characteristics of existing vital signs, enabling brain function measures that are rapid (~5 minute testing time), easy to use, portable, non-invasive, and standardized with automated analysis. Crucially, these vital sign metrics directly measure the brain's electrical activity and do not depend on any responses from the test participant, thus providing much more objective information about brain function. The development of portable and objective 'vital sign'-like metrics for the brain not only advances the scientific understanding of brain function through novel metrics like orientation, but also creates significant opportunities for enhancing clinical diagnosis through improved brain function assessments at the point-of-care.

Acknowledgements

A big thank you to my primary supervisor, Dr. Ryan D'Arcy for believing in me and for supporting me, both during graduate school as well as previously at the National Research Council Canada where I first became interested in this area. I cannot believe everything we have created in the last 10-years – from Halifax Consciousness Scanner to Brain Vital Signs! Thank you also to Dr. Carolyn Sparrey and Dr. Edward Park for their guidance over the years as part of my supervisory committee. I am especially grateful to Dr. Xiaowei Song for teaching me a great deal about brain imaging and scientific research over the years, and Dr. Teresa Cheung for sharing her extensive knowledge of all things MEG. Additionally, I want to acknowledge the outstanding salary support from Simon Fraser University's Multi-Year Funding Award as well as the financial contributions from MITACS, Surrey Memorial Hospital Foundation, NSERC, CFI, and CIHR, without which this work would not have been possible.

I am grateful and would like to express my gratitude for all the colleagues and collaborators spanning academic, industrial, and clinical worlds who have made this journey so much better. I am extremely fortunate to have had the privilege of working with such wonderful collaborators as CfP at the University of Alberta, AK at BC Cancer, and RP at Safe Software. A thank you to the HealthTech Connex Inc. crew for bringing brain vital signs to the world and into the hands of those who need it most – I am excited to see where this goes over the next few years! I also want to acknowledge the various families and patients that I have worked with over the years – thank you for allowing me into your lives and providing me with the inspiration when the going got tough.

Ultimately, I want to thank my family and friends for their patience and support over the years – I could not have done this without you. My parents and my brother have been excellent role models – thank you for your love and guidance. Most importantly, I want to thank my partner as well as SL for their wonderful love and support over the years.

Table of Contents

List of Tables

List of Figures

List of Acronyms

ABI	Acquired Brain Injury
ANOVA	Analysis of Variance
AP	Action Potentials
AR	Auto Regressive
BA	Brodmann Area
BEM	Boundary Element Method
BOLD	Blood-Oxygenation Level Dependent
CRS-R	Coma Recovery Scale-Revised
CT	Computed Tomography
CWT	Continuous Wavelet Transform
DOC	Disorders of Consciousness
dSNRw	Dynamic SNR Weighted
EBS	Elemental Brain Score
EEG	Electroencephalography
ENE	Early Negative Enhancement
EOG	Electrooculogram
ERF	Event Related Fields
ERP	Event Related Potential
ES	Effect Size
FEM	Finite Element Method
fMRI	Functional Magnetic Resonance Imaging
fNIRS	Functional Near-Infrared Spectroscopy
FP	False Positive
GCS	Glasgow Coma Scale
GFP	Global Field Power
GLM	General Linear Model
GOAT	Galveston Orientation and Amnesia Test
HCS	Halifax Consciousness Scanner
HPI	Head Position Indicator
ICA	Independent Component Analysis
IFG	Inferior Frontal Gyrus

IPL	Inferior Parietal Lobule
LCFS	Levels of Cognitive Functioning Scale
LIS	Locked-In Syndrome
MCS	Minimally Conscious State
MCI	Mild Cognitive Impairment
MEG	Magnetoencephalography
MMN	Mismatch Negativity
MMSE	Mini-Mental State Examination
MNE	Minimum Norm Estimate
MoCA	Montreal Cognitive Assessment
MRI	Magnetic Resonance Imaging
NTBI	Non-Traumatic Brain Injury
PDF	Probability Density Function
PET	Positron Emission Tomography
pMTG	Posterior Middle Temporal Gyrus
POC	Point of Care
PRC	Peri-rhinal Cortex
PSP	Post Synaptic Potential
RMS	Root Mean Square
rN400	Rapidly elicited N400
SCAT	Sport Concussion Assessment Tool
SD	Standard Deviation
SEM	Standard Error of Mean
SNR	Signal-to-Noise Ratio
SQUID	Superconducting Quantum Interference Device
SVM	Support Vector Machine
TBI	Traumatic Brain Injury
TL	Temporal Lobe
TP	True Positive
UWS	Unresponsive Wakefulness State
VS	Vegetative State
WHIM	Wessex Head Injury Matrix

Chapter 1. Introduction

1.1. Overview

Vital signs such as heart rate and blood pressure have revolutionized the assessment of many different body systems and improved the level of care by providing easy-to-use, clinically-accessible, physiology-driven and standardized metrics of body function. Yet no such vital sign metric currently exists for the brain; instead, brain function measures typically require behavioural or questionnaire-based assessments that are highly indirect and prone to subjectivity and bias [1], [2]. The present dissertation aims to address this important scientific, clinical, and technological gap by developing and demonstrating a brainwave-based vital sign metric for the brain that is capable of assessing a broad spectrum of functions ranging from the lower-level domains (i.e. sensation) to the highest-level cognition measures (i.e. contextual orientation). This research represents the first time that such a vital sign metric for the brain has been possible, enabling measures that are rapid (~5 minute testing time), easy to use, portable, non-invasive, and standardized with automated analysis. Crucially, these vital sign metrics measure the brain's electrical activity and do not depend on any responses from the test participant, thus providing much more objective information about brain function.

1.2. Background and Motivation

1.2.1. Acquired Brain Injury

Brain diseases and disorders leading to disability and death are a worldwide concern, with substantial increase in global burden of neurological disorders over the last 25 years [3]. Studies have repeatedly demonstrated the staggering economic and societal impacts of brain-related disorders – with one study estimating the European cost of brain disorders at €798 billion per year (for comparison, the cost of cancer was estimated at €150-250 billion per year), and attributing 35% of years lost due to premature death or disability to neurological disorders [4]. In Canada, one in three Canadians will be negatively impacted by a brain-related disorder during their lifetime.

Among brain-related disorders, acquired brain injury (ABI) presents a particularly daunting challenge. ABI is defined as damage to the brain that is not of congenital or degenerative disease origin [5]. While people are more likely to survive an ABI due to improvements in critical care medicine [6], ABI survivors often face devastating personal consequences such as physical limitations and cognitive impairments [5]. Within the larger societal context, estimates suggest that the economic burden of ABI is $12.7B annually in Canada, with healthcare costs of up to $1M per new case at injury, and $400,000 in annual recurring direct and indirect costs [7].

ABI has two primary etiologies: 1) traumatic brain injury (TBI) caused by insults to the head and/or brain by objects or events external to the body (e.g. motor vehicle accident), and 2) non-traumatic brain injury (NTBI) occurring due to events internal to the body or the introduction of substances that negatively impact bodily functions (e.g. cardiac arrest). Due to the heterogeneity of ABIs, impact and outcomes can vary widely based on the type and severity of injury. For example, whereas mild TBI (also known as concussion) can result in changes in neural function that are transient in nature [8], severe ABI often has 1-year mortality rates as high as 90% for NTBI [9], [10] and 76-89% for TBI [11], [12], and usually results in patients suffering from disorders of consciousness (DOC).

While describing consciousness is considered a daunting task with several theories and schools of thoughts [13], operationally, consciousness is defined based on two main constituent components: 1) arousal (or consciousness level), referring to wakefulness, and 2) awareness (or consciousness content), referring to awareness of self and the external world [14]. In cases of DOC, one or both components of consciousness can be impacted. To enable diagnosis and treatment of patients with DOC, ascending tiered levels of disordered consciousness have been adopted in order to provide common taxonomy and frame of reference. The first level (lowest tier), occurring in the immediate post-injury phase, is coma which is characterized by lack of arousal and awareness as well as lack of sleep-wake cycles with no demonstrated response to stimulus [15]. If a patient survives, they generally progress to the next tier within 2-4 weeks. This next tier, called vegetative state (VS) or unresponsive wakefulness syndrome (UWS), is characterized by presence of wakefulness with at-least partial preservation of life-sustaining functions and closure and re-opening of eyelids similar to sleep-wake cycles, although no evidence of purposeful behaviour or language

comprehension/expression is present. VS or UWS is considered persistent if it continues for more than 4 weeks and permanent if it lasts more than 3 month for NTBI or more than 12 months for TBI [16]. Emergence from VS/UWS into the next tier, called Minimally Conscious State (MCS), is characterized by evidence of self or environmental awareness, in one of the following forms: 1) simple command following, 2) yes/no verbal or gestural responses (does not have to be accurate), 3) intelligent articulation/verbalization, or 4) movement or behaviour in response to stimuli. MCS is considered to be a continuum that can be sub-divided into MCS+ and MCS- tiers, with patients in MCS+ providing inconsistent but reproducible responses, and MCS- patients providing lower degree, but still some evidence, of responses. Evidence of further recovery and emergence from MCS is characterized by reliable demonstration of communication in the form of accurate yes/no responses as well as goal-directed object use [17].

While a relatively linear trajectory of recovery from DOC is presented above, it is important to note that other tiers also exist, specifically, in the form of locked-in syndrome (LIS, [15]). Much like MCS, LIS in turn can be separated into at least three distinct types [18]: 1) complete, where patients have no movement (including eyes) resulting in frequent misdiagnosis as unresponsive, 2) incomplete, where patients retain the ability to make some voluntary movements, and 3) classic, where patients are fully conscious and retain the ability for eye movement. In summary, recovery from DOC exists on a continuum, with patients potentially remaining in coma, or awakening but remaining unresponsive, or regaining the ability to interact with the environment, or even regaining full consciousness [14].

Unresponsive   **Responsive**

Coma   **VS/UWS**   **MCS+**

Figure 1.1.   General progression of responsiveness of patients

Accurate diagnosis of brain function is crucial for brain-injured patients with DOC, as patients diagnosed as unresponsive (i.e. not consciously aware) generally have lower

access to rehabilitation and other treatments compared to those deemed to be responsive (i.e. with some degree of conscious awareness) [19]. Access to rehabilitation is in turn a key determinant of patient outcomes, months or even years after the injury [20].

1.2.2. Current Clinical Assessments

Diagnosis of brain function is currently heavily reliant on clinical observations and behaviour-based assessments [21] [22]. A commonly used technique is the Glasgow Coma Scale (GCS, [23], Figure 1.2), which assesses ocular, motor, and verbal behaviours on a 15-point scale. The GCS was first proposed in 1974 and continues to be widely used in the clinic today. GCS scores of 3-8 suggest a severe brain injury, scores of 9-12 suggest a moderate brain injury, and scores of 13-15 represent a mild brain injury [24]. Another popular technique is the Coma Recovery Scale – Revised (CRS-R [25]), which assesses a variety of visual, auditory and motor responses as well as oral communication and arousal levels. On the other hand, the Level of Cognitive Functioning Scale (LCFS [26]) mainly assesses verbal responses to cues, while the Wessex Head Injury Matrix (WHIM [27], Figure 1.3) assesses basic behaviours and also targets higher-level cognitive functions such as memory and orientation.

Although behaviour-based brain function assessments have the advantages of practicality and wide scale accessibility, they are also hindered by critical limitations that lead to misdiagnosis rates of between 39% and 43% [35] [36] [30] [31]. Studies have shown that reliance on behaviour-based observations cannot produce accurate assessments in situations of mind-motor disconnect (also known as cognitive motor disassociation), in which patients with covert cognitive capacities are unable to demonstrate it through meaningful action [32]. These tests are also highly dependent on the administrator's subjective judgment in assigning scores [2], [30], [33]. Indeed, 70% of the patients misclassified as vegetative in one study were later shown to have the ability to spell, and 90% were able to make choices [33]. Unfortunately, recent studies from both 2009 and 2015 found that the diagnostic accuracy has not improved in the past two decades [30] [31], highlighting the critical need to develop better brain function assessments.

Eye opening

Criterion	Observed	Rating	Score
Open before stimulus	✔	Spontaneous	4
After spoken or shouted request	✔	To sound	3
After finger tip stimulus	✔	To pressure	2
No opening at any time, no interfering factor	✔	None	1
Closed by local factor	✔	Non testable	NT

Verbal response

Criterion	Observed	Rating	Score
Correctly gives name, place and date	✔	Orientated	5
Not orientated but communication coherently	✔	Confused	4
Intelligible single words	✔	Words	3
Only moans / groans	✔	Sounds	2
No audible response, no interfering factor	✔	None	1
Factor interferring with communication	✔	Non testable	NT

Best motor response

Criterion	Observed	Rating	Score
Obey 2-part request	✔	Obeys commands	6
Brings hand above clavicle to stimulus on head neck	✔	Localising	5
Bends arm at elbow rapidly but features not predominantly abnormal	✔	Normal flexion	4
Bends arm at elbow, features clearly predominantly abnormal	✔	Abnormal flexion	3
Extends arm at elbow	✔	Extension	2
No movement in arms / legs, no interfering factor	✔	None	1
Paralysed or other limiting factor	✔	Non testable	NT

Figure 1.2.   Sample GCS Examination
Source: glasgowcomascale.org

Lowest Order Items

Table 1   Items of behaviour 1–15

1) Eyes open briefly
2) Eyes open for extended period
3) Eyes open and move but do not focus on object/person
4) Attention held momentarily by dominant stimulus
5) Looks at person briefly
6) Volitional vocalization, to express feelings
7) Distressed when cloth put on face
8) Makes eye contact
9) Looks at person talking
10) Expletive utterance ('Get off!', etc.)
11) Eyes follow person moving in line of vision
12) Looks at person giving attention
13) Closes eyes and becomes quiescent when cloth put on face
14) Mechanical vocalization (with yawn, sigh, etc.)
15) Performs physical movement on verbal request

Highest Order Items

Table 4   Items of behaviour 47–58

47) Conventional speech usage but with very few words
48) Uses one or two gestures
49) 1 or 2 orientation items correct (day of week, month, year, age, place)
50) Knows the price of three common objects
51) Recognizes coins (eye-point or touch named coin)
52) Knows the name of one member of staff
53) Names or indicates left and right on self
54) Uses writing, typing or other communication aid fluently
55) 3–5 orientation items correct
56) Remembers something from the day before (e.g. show a coin, key, watch, etc. from your pocket and say you will ask them to remember it tomorrow)
57) Remembers something from earlier in the day (e.g. 'Have you been to physio yet?')
58) Completes PTA test

Figure 1.3.   Sample of Wessex Head Injury Matrix Assessment
Source: Adapted from [27]

5

1.2.3. Technology-Based Assessments

Neuroimaging technologies provide information about brain structure and function, and have increasingly enabled more objective, physiology-based measures of brain function that can augment purely behaviour-based assessments. There are now calls for composite approaches in brain function assessment that integrate behavioural scales with neuroimaging technologies [34].

Neuroimaging techniques can be divided into two groups depending upon whether they focus on evaluating brain structure or function: Structural techniques such as magnetic resonance imaging (MRI) and computed tomography (CT) enable direct assessments of extent of neural tissue damage [35]. Similarly, diffusion-weighted imaging, which can provide a measure of white matter tract integrity has been able to predict non-recovery in a group of TBI patients with 86% sensitivity and 97% specificity [36].

Functional assessment technologies such as functional magnetic resonance imaging (fMRI) and positron emission tomography (PET) have also shown promise. fMRI relies on the blood-oxygen-level-dependent (BOLD) contrast, and has demonstrated strong potential evidence of residual cognition in individuals considered to be in VS by showcasing similar activation patterns for imagining playing tennis and navigating their homes as observed in healthy individuals [37]. Similarly, a study utilized fMRI to demonstrate similar brain responses while watching a movie in healthy adults and a patient who was behaviourally unresponsive for 16 years [38]. PET, on the other hand, assesses brain function by measuring the activity of positrons from radioactive molecules injected into the body, and has also been shown to differentiate between different states of DOC [39].

Table 1.1.   Comparison of functional neuroimaging technologies

Information derived from [40], [41].

Criteria	fMRI	EEG	MEG	fNIRS	PET
Portability	Not portable	Portable	Not portable	Portable	Not portable
Cost	$2M	$300-80K	$2-3M	$20-40K	$8M
Spatial Resolution	Millimeters	Centimeters	Centimeters	Centimeters	Tens of Millimeters
Temporal Resolution	Seconds	Milliseconds	Milliseconds	Seconds	Minutes
Invasiveness	Mildly invasive	Not invasive	Not invasive	Mildly invasive	Very invasive
Type of measurement	Indirect (hemodynamic)	Direct (neuroelectric potentials)	Direct (neuromagnetic fields)	Indirect (hemodynamic)	Indirect (metabolic)

Despite their promising findings, these technologies do have important drawbacks. For instance, f/MRI, PET, and CT are all physically quite large and located in specialist centres, and cannot be readily deployed to the patient bedside or into community settings. In addition, the use of ionizing radiation and radioactive materials in CT and PET also preclude repeated measurements, rendering these techniques not useful in monitoring brain function changes for DOC patients given the need for serial testing in order to obtain accurate diagnostic or prognostic information [42]. Indeed, studies have recommended that patients be assessed at least five times within a two-week period in order to accurately monitor changes in brain function, making the use of CT or PET not feasible [43]. On the other hand, fMRI is non-invasive but relies on the neural hemodynamic response which takes seconds to peak [44]. Given that neural activity in the brain occurs on the order of milliseconds, the low temporal resolution of fMRI makes this technique less than ideal in measuring brain function. Other imaging technologies such as functional near infrared spectroscopy (fNIRS) are more portable compared to fMRI, but fNIRS also relies on the hemodynamic response (as it depends on measuring the relative differences in absorption of light of specific wavelengths by oxy- and deoxy- haemoglobin) and consequently has low temporal resolution [45].

Techniques that measure the electrical activity of the brain, such as electroencephalography (EEG) which records the scalp electrical potentials, and magnetoencephalography (MEG) which records the magnetic fields associated with neural electrical activity, do have temporal resolution on the order of milliseconds which are highly suited to measuring neural activity [46]. MEG also has good spatial resolution on the order of 1cm (though not superior to that of fMRI), while EEG has poorer spatial resolution on the order of several centimeters [46]. Nonetheless, MEG is fixed-infrastructure and cannot be deployed to point-of-care settings, whereas EEG has the advantage of portability and greater accessibility (Table 1.1).

To provide objective measures of brain function and aid in the clinical diagnosis and evaluation of brain-injured patients, an ideal imaging modality should embody the following characteristics: 1) non-invasiveness to facilitate repeated measurements [43], 2) portability to enable deployment to point-of-care settings, 3) high temporal resolution to provide information about neural temporal dynamics which occur on the order of milliseconds, and 4) relatively low cost to enable widespread clinical access. EEG meets all these requirements and is thus ideally suited for point-of-care evaluations of brain function [47].

1.2.4. Event-Related Potentials

Event-related potentials (ERPs) are derived from EEG, and measure the brain's responses to external sensory stimuli. ERPs exhibit characteristic features known as components which correspond to different brain functions spanning the entire information processing spectrum, ranging from low-level sensation to higher level cognitive functions such as language processing [48]. Since ERP responses are much smaller in amplitude compared to background EEG signals, ERP measurements typically require large numbers of repeated stimuli (also known as trials). ERPs are derived by first grouping together EEG data segments that are time-locked to each type of stimulus, averaging together the grouped segments or epochs, then comparing the trial-averaged waveforms between different stimulus conditions [47], [48]. ERP components are commonly identified based on their polarity (i.e. positive or negative voltage), latency (i.e. timing with respect to stimulus presentation), and topography (i.e. distribution of the signal across different regions of the scalp). For instance, the well-known N100 ERP component can be observed in response to auditory input as a

8

negative-going waveform peaking around 100ms post-stimulus presentation, and is maximal at fronto-central scalp locations (i.e. near the anterior and central regions of the scalp) [49].

ERPs have numerous advantages as a platform for brain function assessments: 1) their millisecond resolution enables tracking of temporal dynamics of brain information processing; 2) they have been shown to be sensitive to subtle cognitive dysfunctions in various clinical disorders [50], [51]; and 3) they have enhanced test-retest reliability compared to many standardized behaviour-based cognitive tests [52]–[55]. Indeed, ERPs have demonstrated enormous potential in assessing a range of brain functions in both healthy individuals [48] and patients with brain injury [56]–[60]. Among various ERP markers, three ERP components have been shown to have tremendous clinical utility in brain function evaluations: these include the N100 indexing sensation [61], P300 indexing attention [62], and N400 indexing language processing [63].

N100 ERP

The N100 ERP component is an obligatory response generated by the primary sensory cortices upon arrival of external stimuli through the corresponding sensory pathways. In the case of auditory stimuli, the N100 ERP component is generated when external sounds arrive at the primary auditory cortex via the auditory pathway, and occurs approximately 100ms after stimulus presentation [59], [64]. The auditory N100 ERP is generally considered to be an objective, physiological measure of auditory function [65], and is commonly elicited and assessed through the "oddball paradigm" which comprises a frequently occurring tone (i.e. *standard* condition) interspersed with a rarely occurring different tone (i.e. *deviant* condition). The N100 component is present in both conditions, but has larger amplitude in the deviant condition compared to standard [65].

P300 ERP

The P300 ERP component reflects the attentional mechanisms of the brain, and is independent of the stimulus input modality [65]. The P300 ERP comprises two sub-components P3a and P3b, with the former reflecting the switching of attention toward novel stimuli, while the latter reflects processes that allow updating of the existing contextual framework based on the new input [66]. The P300 ERP can be generated

using several paradigms, one of the most robust of which is the "oddball paradigm" in which participants are presented with a series of frequently appearing stimuli interspersed with a rare, different stimulus. Though typically occurring around 300ms after stimulus presentation, the P300 latency can also occur later depending on the specific task/paradigm used. The P300 amplitude becomes larger for more improbable targets (i.e. lower probability of occurrence), and the latency increases with increasing difficulty of detection (i.e. more similarity between frequent and rare stimuli) [67].

N400 ERP

The N400 ERP was first reported as a differential response between sentences that ended with semantically related words (*congruent* condition, e.g. "The pizza is too hot to *eat*.") compared to sentences that ended with semantically unrelated words (*incongruent* condition, e.g. "The pizza is too hot to *sing*.") [63]. The N400 ERP consists of a negative deflection in the *incongruent* relative to *congruent* condition waveform, occurring at around 400ms after stimulus onset [68]. While initially primarily studied within the context of language processing, the N400 ERP has since been shown to occur in many other situations such as mathematical errors (e.g. 10 + 3 = 17), violations of real-world knowledge (e.g. "The color of the ocean is yellow"), and violations of tool-use context (e.g. toothbrush used for cutting vegetable) [68], [69]. Nonetheless, the N400 component is believed to reflect the degree of violation between the expected and actual stimulus input, irrespective of the specific context [68].

1.2.5. Clinical Applications of ERPs

To date, numerous studies have demonstrated the clinical utility of the N100, P300, and N400 ERP components in brain function assessment for ABI patients, with efficacy in capturing injury severity [70], predicting recovery [71], and tracking improvements due to recovery/rehabilitation [72], [73]. For instance, Connolly et al. demonstrated the possibility of using the N400 ERP for improved assessments in a very small sample of patients with brain injury following stroke [74], which D'Arcy et. al. further extended by showing in a larger sample of stroke patients that the N400 ERP facilitated improved clinical management [58]. Other studies have highlighted the ability to assess a spectrum of brain functions by measuring multiple ERPs within the same experimental paradigm, and demonstrated the utility of this approach in measuring the

overall level of brain function [75], [76]. Crucially, ERP outcomes have been shown to exhibit comparable test-retest reliability relative to well-established clinical vital sign measures such as blood pressure and heart rate [52], [53] [77], further supporting the use of ERP-based measures to augment existing clinical metrics.

Yet despite their clinical potential, ERP assessments continue to be restricted primarily to specialized centres within the research domain, due largely to their requirements for cumbersome equipment and prolonged testing procedures. Measuring a single ERP component typically requires at least 1-2 hours in testing time due to the need for large numbers of repeated trials to obtain sufficient signal-to-noise ratio (SNR) [48], [65], with higher-level cognitive measures like P300 and N400 components requiring even more trials compared to lower-level sensory components like N100 [78]. Moreover, typical ERP measurements utilize large EEG systems that have multiple electrode sensors covering the scalp (e.g. 32- or 64-channel), requiring extensive setup time to ensure sufficient conductivity at the electrode-scalp interface. Indeed, even studies that specifically investigated the possibility of shortening ERP testing time for clinical applications were only able to shorten testing times to 30-90 minutes in order to measure 3-4 ERP components including the P300 and N400 [71], [75], [79], which is still too time-consuming for routine clinical use at the bedside. In fact, a recent survey of clinician attitudes towards ERP use in clinical settings showed that, of the 54 clinicians surveyed across 22 care centres in France, 79% felt that the cumbersome methodology of ERP testing precluded their routine use in clinical care, and 63% felt that the lack of standardization and reference values in ERP outputs was also a major hindrance to their clinical uptake [80].

To leverage the known advantages of ERPs in their high temporal resolution, potential for portability, and clinical salience in brain function assessments, a new technology platform is needed that is capable of obtaining ERP-based brain function measurements in a manner that facilitates routine clinical application. To maximize clinical utility, the new technology should enable measurements that are rapid to assess, easy to use, provide objective, physiology-based information about brain function, and produce standardized outputs for easy interpretation. Since these characteristics are all features of existing well-established clinical vital sign metrics such as body temperature and heart rate which are used to evaluate cardiovascular and overall health, the desired

technology also represents a new method of obtaining vital sign like measurements – for the brain.

1.2.6. Key Challenges

ERPs have well-established relevance in clinical assessments of brain function, but are currently hindered by critical limitations that preclude their widespread usage outside the research setting. The creation of an ERP-based technology platform that provides physiology-driven information about brain health while enabling rapid application and ease of use at the point-of-care would represent a significant step forward in improving brain function assessments for ABI patients. However, as an initial step, such a technology would need to be developed and assessed in healthy individuals.

To develop and demonstrate the first ERP-based 'vital sign' metrics for the brain, four key challenges must be addressed: 1) A technology platform must first be created that embodies the main features of existing widely-used vital signs like heart rate, with characteristics that include portability, rapid and user-friendly testing protocol, standardized and easy-to-interpret output, and the ability to capture key salient features that provide physiology-driven information about the health of the underlying body system. 2) The measurement outputs must be physiologically and clinically salient, with features that are consistent with known characteristics of established ERP-based metrics obtained using traditional research-based testing paradigms. 3) To maximize its clinical utility, the new brain vital signs measurements should encompass a variety of factors that provide cumulative information about a range of brain functions, with particular emphasis on the highest-level cognition measures that are known to have high clinical salience. 4) Finally, given that ERP testing is known to have SNR challenges that lead to low effect sizes (especially in situations involving rapid testing protocols that necessitate low trial numbers), new data analytic strategies and techniques must be developed to address these concerns to maximize effect size and improve signal capture for the new brain vital signs technology.

1.2.7. Proposed Research

The overall goal of this research program is to create and demonstrate a technology platform that utilizes the known clinical salience of ERPs to provide rapid, objective, physiology-driven measurements for a wide range of brain functions that enable the assessment of brain health. Crucially, the technology will target a variety of brain functions that range from the lowest level sensory processes to the highest level cognition and integration domains – with the latter never before having been measurable using ERPs.

The overall hypothesis of this work is that an ERP-based technology platform can capture clinically salient information about brain health using a rapid testing protocol, and successfully produce scientifically valid results that are standardized relative to normative values. Specifically, the research involves four components (Figure 1.4) that address each of the key challenges mentioned above:

Study I: Develop a prototype technology for brain vital signs and demonstrate its scientific applicability in measuring a spectrum of brain functions in healthy adults across a broad age range

Study II: Investigate the scientific validity of brain vital sign outputs compared to established ERP techniques

Study III: Create a novel ERP-based metric to capture the highest-level cognition and integration functions known to be crucial in clinical brain function evaluations

Study IV: Develop a new data analytic approach that addresses the SNR challenges of short ERP testing protocols and enhances ERP signal capture in the new brain vital signs technology

```
                    ┌────────────────────────────────┐
                    │      Develop Brain Vital Signs  │
                    └────────────────────────────────┘
```

Study I
- Develop prototype
- Initial demonstration - experimental & biological salience?

Study IV
- Develop technique to maximize signal capture in low-SNR, noisy environments

Study II
- Are results real?
- How does brain process rapid stimuli?

Study III
- Expand platform to measure highest-level cognition (orientation)
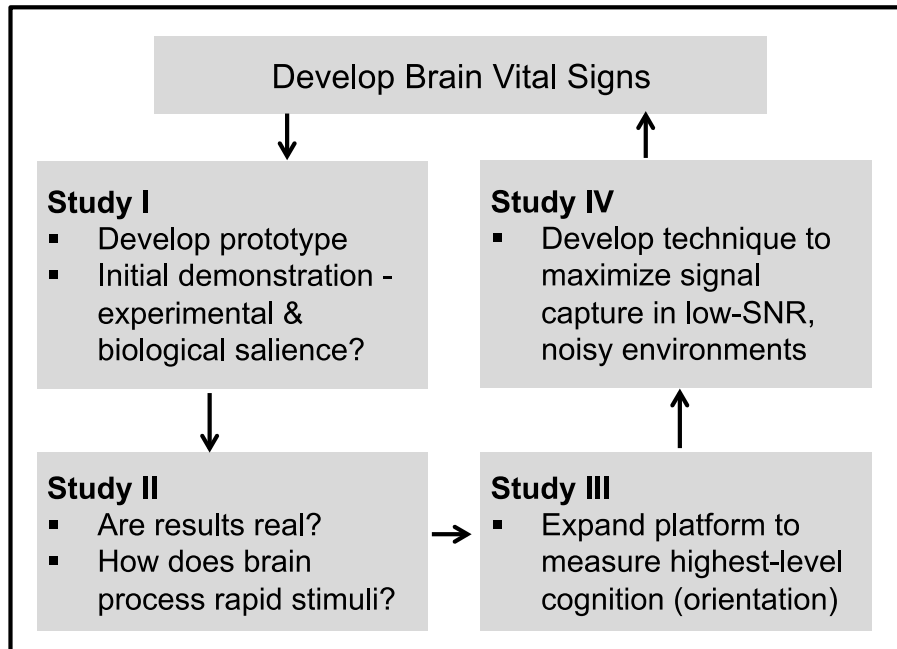
Figure 1.4.   Overview of research program and component studies

Study I. Develop brain vital signs technology and demonstrate in healthy adults

This study aims to develop and demonstrate in healthy adults a prototype brain vital sign technology that embodies the key features of existing widely used clinical vital signs like body temperature and heart rate. The requirements for brain vital sign technology are thus as follows: 1) it should have portable hardware, 2) be easy to apply, 3) have rapid testing protocol (typical vital sign measurements require no more than 5 minutes testing time), 4) provide physiology-based measurements, 5) not require responses from the testing subject, 6) be non-invasive and amenable to repeated measurements, and 7) produce standardized and easy-to-interpret outputs. Although previous research did make some initial progress towards a portable ERP-based brain function assessment technology through development of the Halifax Consciousness Scanner (HCS) [81], there were crucial limitations in the HCS technology design that led to cross-contamination between brain responses to adjacent stimuli. In contrast, the brain vital sign technology not only addresses the limitations of the previous HCS, but also meets all the other scientific and clinical requirements as well. Moreover, to demonstrate the biological validity of the brain vital sign metrics in capturing known effects across a highly varied participant sample, the current research also provides the

first study of rapid, multi-ERP measurements in healthy adult volunteers across a broad age range. Critical clinical comparisons are also made using established behaviour-based metrics like the Mini-Mental State Examination (MMSE, [82]) and Montreal Cognitive Assessment (MoCA, [83]). The specific hypotheses are as follows:

1) The new rapid testing brain vital signs platform can successfully elicit N100, P300, and N400 ERP components in healthy adults across a wide age range

2) The ERP components elicited by the brain vital signs platform can capture aging-related brain function changes such as increase in P300 latency in the older compared to younger adults

3) Any observed differences in ERP responses will be preserved in the standardization framework used to normalize brain vital sign outputs for easy interpretation

Study II. Investigate scientific validity of brain vital sign outputs

This study aims to investigate the temporal, spectral, topographic, and neuroanatomical characteristics of the brain vital sign measurements in healthy adults using MEG, which has superior spatial resolution compared to EEG. Given that ERP components that measure higher-level cognitive functions (e.g. N400 for language processing) are especially sensitive to loss of SNR due to reduction in trial numbers, it is crucial to closely examine the brain responses elicited by the rapid brain vital signs paradigm to determine whether their features are consistent with those observed using traditional, well-established testing protocols. This helps ensure that the neural responses elicited using the new brain vital signs technology are scientifically valid compared to established literature, and demonstrate the scientific utility of the new rapid ERP testing framework. The specific hypotheses are as follows:

1) The rapidly elicited brain vital sign N400 component (rN400) will exhibit temporal characteristics consistent with known features of N400 from established literature

2) The rN400 response will exhibit scalp topography consistent with that of the established N400 response

3) The rN400 response will exhibit spectral effects consistent with the time-frequency characteristics of the established N400 response

4) The rN400 component will activate brain regions of the language network, consistent with that of the established N400 response

Study III. Create new ERP-based measure for orientation processing

This study aims to develop a novel ERP-based measure to capture neurophysiological responses associated with orientation, which is defined as the brain's knowledge of the current context in space, time, and person. Specifically, orientation refers to the brain's knowledge of the "here and now", and represents the highest level of cognition involving the integration of multiple neural subsystems [84]. Orientation is one of the earliest brain functions impacted by injury and disease such as concussion and dementia [85], and its evaluation forms a key cornerstone of many frontline clinical assessment tools that screen for cases of potential dysfunction [86], [87]. Sadly, the only clinical tests currently available for orientation assessment are behaviour-based metrics that utilize questionnaires, such as the Sport Concussion Assessment Tool for concussion [88], WHIM and Galveston Orientation and Amnesia Test for severe brain injury [27], [86], MMSE and MoCA which both screen for dementia [82], [83]. These measures are subjective and highly reliant on administrator judgement, and are susceptible to potential bias and lack of standardization in output [1], [2]. No physiology-based measures currently exist, and no study to date has investigated the possibility to create an ERP-based measure of orientation processing.

Vital sign metrics should provide information about the overall health of the underlying body system. In creating a vital sign platform for the brain, it is essential to incorporate measures that capture a broad range of neural functions to help elucidate brain health, particularly functions that are known to be clinically salient in brain health monitoring and assessment. Given that orientation represents the highest level of cognition that is also crucial to frontline clinical tests, its assessment naturally forms a key component of an ERP-based technology platform that aims to provide 'vital sign' information about brain health. Moreover, incorporating an ERP-based measure of orientation processing into the brain vital sign platform would represent the first time that a neurophysiology-based marker of this high-level cognitive function has been

demonstrated. The ability to capture this response through such an objective measure will also help to significantly advance our understanding of brain function.

This study aims to develop an ERP-based metric of orientation processing by designing a unique stimulus paradigm that allows the capture of orientation responses, along with all the other ERP components (N100, P300, N400), within the same rapid testing protocol. The brain vital sign platform is demonstrated in healthy adults using portable EEG with 5 channels. Moreover, additional evaluations are also performed in a separate sample of healthy adults using MEG with concurrent EEG to allow for localization of cortical sources as well as signal comparisons with outcomes from the portable EEG system. The responses are evaluated for their temporal and neuroanatomical characteristics. The specific hypotheses for this study are as follows:

1) Neural responses to stimuli irrelevant to the current context will exhibit characteristics that represent violation of the expected input

2) Neural responses to stimuli that are relevant to the current context will be different from those of the irrelevant condition

Study IV. Create new signal processing technique for addressing low-SNR challenge of ERP assessments

This study aims to create and evaluate a new signal processing approach to address the low SNR challenges of ERP-based measurements. Specifically, the brain's response to a specific stimulus usually has very low SNR, and therefore responses to several repetitions of the stimuli (trials) are averaged together to generate discernable ERPs [47], [48]. Since the SNR of the ERP response increases with number of trials, many ERP studies collect hundreds of trials and thereby require hours of testing time. SNR is especially a concern when assessments are undertaken in non-idealized conditions (e.g. few trials, collections outside shielded rooms etc.) such as those envisioned for brain vital signs collections due to potential contamination from several sources of noise which are generally orders of magnitude larger than the signals of interest [89]. Given the constraints of rapid assessment for the development of brain vital signs, instead of simply adding more trial numbers (and therefore increasing the testing time), this study instead envisions boosting the SNR of the ERP response by combining data from multiple sensors while accounting for their inherent SNR differences.

Evaluations using simulation and experimental data focus on the impact of the data combination on the capture of ERP effects of interest. The specific hypotheses are as follows:

1) The new technique will perform better than simple combination of data from multiple sensors in situations of unequal noise among the sensors being combined.

2) The new technique will capture significantly more ERP effects of interest compared to individual sensors.

Chapter 2.   Technical Background

2.1. Signal Origin

As shown in Figure 2.1(A), neurons generally consist of dendrites to receive information, soma/cell body for processing the information, and axons for communicating information to other neurons. Action potentials (AP) are generated when a neuron is sufficiently excited, and this AP travels down the axon in the form of an electrical impulse to the axon terminal where neurotransmitters enable the transfer of information (from the pre-synaptic neuron) across the synapse to the dendritic extensions of the adjacent neuron (post-synaptic neuron) as shown in Figure 2.1(B). This in turn produces post-synaptic potentials (PSP), which generate intracellular flow of charges (e.g. positive charges from the dendrite to the soma for excitatory PSP) and are then processed by the post-synaptic neuron.
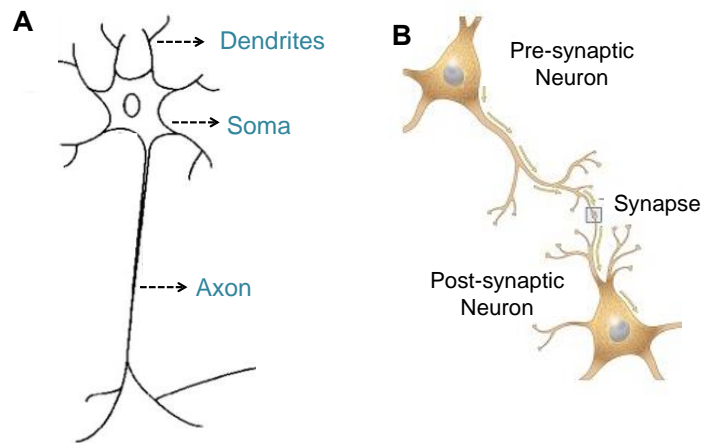
Figure 2.1.   Schematic of Neuron
A) Schematic of an individual neuron showing dendrites for receiving information, cell body (soma) for processing information and axons for communicating information to other neurons. B) Schematic of connection between two adjacent neurons with one neuron sending information (pre-synaptic neuron) via its axon to the recipient (post-synaptic neuron) across the synaptic cleft. Adapted from images taken from http://ffden-2.phys.uaf.edu/212_fall2003.web.dir/Keith_Palchikoff/Neural%20Networks.html and https://lifesciences.umaryland.edu/neuroscience/Research-Focus-Groups/Synapses--Circuits/ .

The flow of charges within the dendrite creates a primary current (shown in yellow in Figure 2.2B), which induces magnetic fields (per the right hand rule) and associated electric fields in the surrounding extracellular tissues in turn creating a cascade of charge flow resulting in secondary or volume current [90]. While the above-mentioned processes occur in all neurons, they are of particular interest within the pyramidal neurons due the unique geometric arrangement of these cells. Specifically, pyramidal cells have elongated apical dendrites that form a parallel arrangement perpendicular to the cortex (Figure 2.2A). As present non-invasive neuroimaging technologies are unable to register the activity of individual neurons, the particular geometry of pyramidal cells enables the summation of activity from many adjacent neurons (Figure 2.2B) that can indeed be registered by neuroimaging technologies and form the primary generators of signals measured by EEG and MEG [91].
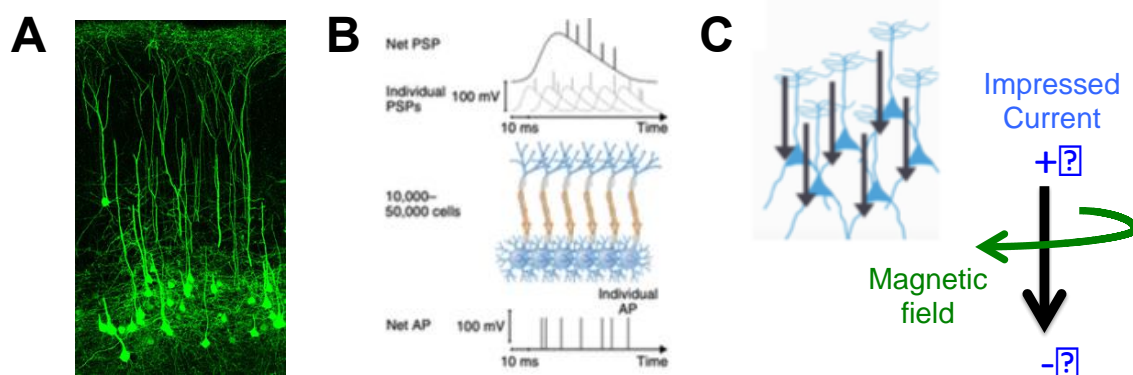
Figure 2.2.   Origins of Measured Signals
A) Pyramidal neurons within the somatosensory cortex with upwards-aligned apical dendrites and soma at the bottom, stained with yellow florescent protein and imaged at 40X resolution. Source: https://www.uthsc.edu/neuroscience/imaging-center/. B) PSPs from many adjacent pyramidal cells summate to form net PSP, whereas APs do not summate. Summation of 10,000-50,000 neurons needed for activity to be registered by MEG. Image adapted from [92]. C) Primary currents/PSP from individual neurons summate to form impressed current with associated magnetic field.

As shown in Figure 2.2(B) & (C), since APs are biphasic, large and rapid (~100mV, ~1ms), the activity from many adjacent neurons generally do not overlap to produce a net effect, whereas PSPs are monophasic, smaller and slower (~10mV, ~20ms) and therefore the activity of adjacent neuron assemblies can summate to produce a cumulative net PSP that forms the source or impressed current [92]. In summary, the signals measured by MEG and EEG are the effect of cumulative primary currents from many pyramidal neurons in close proximity. These primary currents induce

electromagnetic fields that traverse through the conductive tissues of the head (e.g. brain, cerebrospinal fluid etc.). Since these tissues have uniform magnetic permeability [93], passage through differing tissues does not distort the magnetic fields. However, as the tissues have widely varying electrical conductivities [93], passage of electrical fields through the tissue layers introduces secondary currents (return or volume currents). Since MEG can measure the magnetic fields due to both the primary and the secondary currents, whereas EEG mainly measures the volume-conducted currents, EEG is highly susceptible to signal distortions due to conductivity differences and this leads to poorer spatial resolution of EEG compared to MEG [46].

Furthermore, the differences in sensing techniques between MEG and EEG introduce one key distinction in the signals that are measurable by the two modalities. In particular, given the brain's geometry of cortical surface with outer and inner folds (gyri and sulci respectively) and the arrangement of pyramidal neuron perpendicular to the cortical surface, primary current sources can align in radial or tangential directions. Since MEG relies upon measuring the magnetic fields that extend beyond the surface of the head, perfectly radial sources do not register on MEG. On the other hand, since EEG measures the potential due to volume-conducted currents, EEG can measure contributions from both radial and tangential sources.

2.2. MEG Instrumentation

As shown in Figure 2.3(A), the magnetic fields produced by the human brain are very small, and in fact are similar to those generated by a car 2km away. Consequently, to enable MEG measurements of brain activity, the equipment is housed within a magnetically shielded room made up of layers of μ-metal (nickel-iron alloy) and aluminum as μ-metal has high magnetic permeability and provides protection against low-frequency magnetic fields, whereas aluminum attenuates the impact of high-frequency magnetic fields.

Within the shielded room, the primary components of MEG instrumentation are the super-conducting quantum interference devices (SQUIDs) immersed within a dewar filled with liquid helium at -269°C. SQUIDs are superconducting loops with Josephson junction(s), and are in turn coupled to flux transformers in the form of superconducting wire loops (usually made of niobium) which are also immersed in liquid He. There are

several types of flux transformers (Figure 2.3E), but they all primarily pick up magnetic fields perpendicular to the plane of the loop. The simplest kind of flux transformer is the magnetometer consisting of a single wire loop. Further to magnetometers, axial gradiometers consist of two wire loops wound in opposite directions but aligned along the central axis perpendicular to the measurement surface, and planar gradiometers are similar to axial gradiometers but the two loops are parallel to the measurement surface. The key reason for the use of gradiometers over magnetometers is their ability to suppress unwanted noise. In particular, the opposite windings of the gradiometers enable cancellation of the environmental noise (generated father away and therefore more constant across both loops) compared to brain signals (generated closer and therefore unequal pickup among the loops).
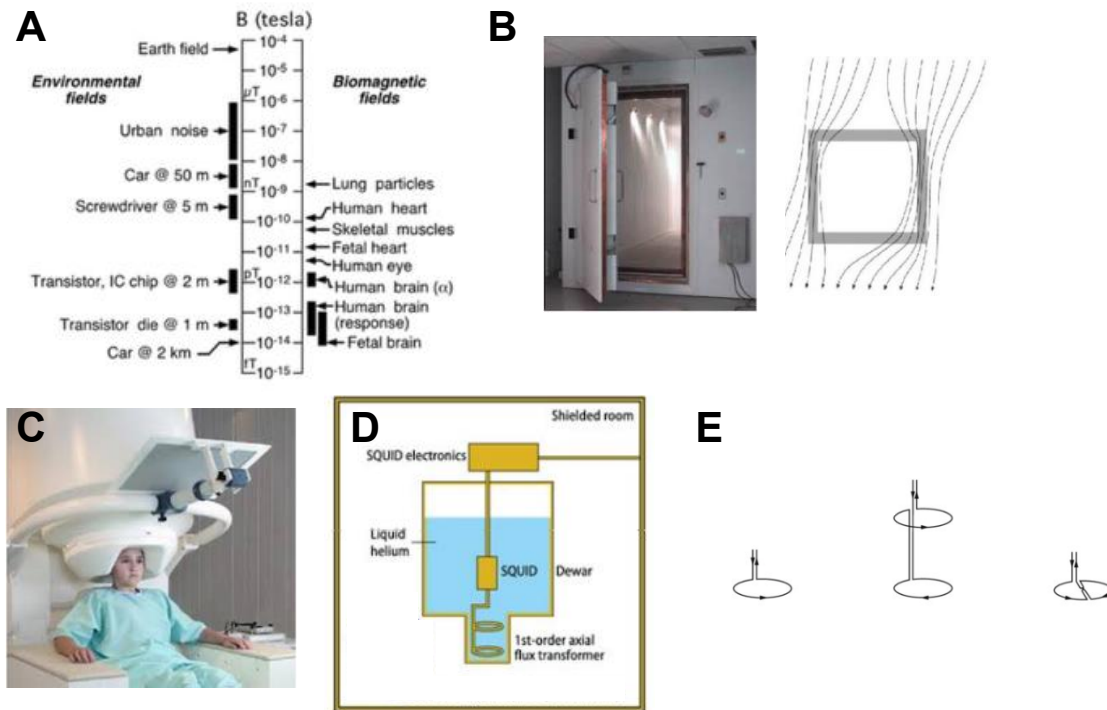
Figure 2.3.   MEG Signal Characterisitics and Instrumentation
A) Magnetic fields due to environmental and biological sources. Adapted from [94]. B) Image of shielded room and its effect on external magnetic fields. Adapted from [95]. C) Image of participant in MEG. D) Schematic of MEG instrumentation showing flux transformer and SQUID immersed in liquid helium within dewar. E) Types of flux transformers – magnetometer (left), axial gradiometer (middle) and planar gradiometer (right).

2.3. EEG Instrumentation

In order to convert the volume-conducted ionic currents into measurable electrical current, EEG utilizes electrodes and electrolytic gel placed on the scalp. While several types of electrode materials are available, silver-silver chloride (Ag/AgCl), consisting of a silver base layer coated with silver-chloride compound, is among the most commonly used EEG electrodes, and is paired with aqueous electrolyte containing high concentrations of chloride ions. The popularity of Ag/AgCl electrodes can be attributed primarily to its low half-cell potential and its operating characteristics close to a true nonpolarizable electrode. High half-cell potential, i.e. the voltage exhibited by the electrode at equilibrium, can cause drifts in the signal over time, and thus the low half-cell potential of Ag/AgCl is well suited for biological measurements [96]. Furthermore, Ag/AgCl electrodes, while being relatively easy to fabricate, also closely approximate a nonpolarizable electrode, thereby enabling the free flow of charges across the electrode-electrolyte interface [97]. The following oxidation-reduction reactions maintain the equilibrium at the electrode-electrolyte boundary:

$$Ag \leftrightarrow Ag^+ + e^-$$

$$Ag + Cl^- \leftrightarrow AgCl + e^-$$
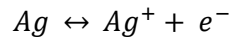
However, this balance is disturbed when the volume-conducted ionic currents reach the scalp, and the excess charges produce an imbalance in the skin-electrolyte boundary, in turn producing movement of ions within the electrolyte, and ultimately disrupting the chemical and charge equilibrium at the electrode-electrolyte interface. As processes try to re-establish equilibrium at the electrode-electrolyte interface, this results in net movement of charge through the electrode and gives rise to current flow.

It is important to note however that EEG is always measured as potential difference between a recording electrode (placed on the scalp) and a reference electrode (usually placed at mastoid, earlobe, nose etc.). This is in contrast to MEG recordings that provide reference-free measurements. The voltage difference between recording electrode(s) and the reference electrode is amplified through an instrumentation amplifier (to help remove common mode voltage), followed by several stages of further amplification, filtering (optional in some hardware), and ultimately conversion from analog to digital signal.

While the general principles of EEG recording have not changed much in the many decades of its existence, two relatively recent advancements have significantly boosted the abilities of EEG amplifiers: 1) extremely high amplifier input impedances, and 2) use of active electrodes. Since the amplifier input impedance, wire (connecting the electrode to the amplifier) impedance and skin-electrode impedance are all in series, high amplifier input impedance allows it to tolerate higher skin-electrode impedances than has traditionally been possible and retain better signal-to-noise ratio [98]. Similarly, the use of amplification circuitry within active electrodes (sometimes referred to as preamplifiers) help boost the signal prior to transmission along the wire to the EEG amplifier, and this in turn helps minimize the impact of the noise introduced during that transmission, thereby allowing the EEG amplifier to operate in noisier environments [99].

2.4. From Data to Event Related Brain Responses

Once the raw data has been collected by the EEG and MEG instrumentation, in order to obtain EEG-derived ERPs and MEG-derived event related fields (ERFs), several processing steps need to be undertaken. These usually include, at the minimum, filtering, artefact removal or correction, segmentation of the continuous data into epochs time-locked to stimulus presentation and conditional averaging to generate waveforms of time evolving average brain response (i.e. ERP/ERF) [47], [48].

While EEG and MEG are collected with high sampling rates (250-1200Hz), since ERPs and ERFs of interest generally reside within specific (usually low) frequency bands of interest (e.g. 0.1-20Hz) that may be non-overlapping with the spectrum of certain noise sources (e.g. muscle activity at 40Hz), an effective technique to extract the information of interest is simply the application of appropriate filters. Butterworth filters are commonly chosen since they have flat response in the pass band and more linear phase delay compared to other filters [100]. Additionally, to remove specific frequencies (e.g. line noise (60Hz in North America), or the head localization coil frequencies in MEG) from the data, notch filters are commonly applied. While filtering helps remove some noise, it is often not enough by itself and additional techniques (some discussed below) are often applied in conjunction to remove both internal/biological and external/environmental contaminations [89].

2.4.1. Regression Based Technique

Some of the largest contaminants for EEG and MEG data are of biological origin, in particular the signals generated by the eyes. For example, blinking creates a large positive spike as the eyelids slide over the more positively charged corneal surface and is registered by the electrodes in EEG [101]. Similarly, while smaller than signals generated by blinking, the constant potential difference among the cornea and the ocular fundus results in shifting electrical fields when eyes move (e.g. horizontal saccades) and again give rise to potential changes that are registered by EEG electrodes [101]. Specialized techniques have been created to deal with the issue to ocular contamination, with a commonly used technique being the Gratton & Coles method [102]. This regression-based technique involves initially computing a signal propagation factor to capture the spatial propagation of the contaminating ocular signal in the frontal-posterior direction, and subsequently the application of the propagation factor to remove the contaminating signals from each recorded EEG channel. The correction procedure for each trial is as follows:

$$\tilde{y}_{i,j} = y_{i,j} - k \cdot x_{i,j}$$

where $\tilde{y}_{i,j}$ is the corrected EEG signal in the i-th trial and j-th channel, $y_{i,j}$ is the corresponding raw EEG, and $x_{i,j}$ the raw EOG typically recorded using electrodes positioned at the outer canthus for horizontal EOG and supra-orbital ridge for vertical EOG. K is the propagation factor.

The propagation factor is computed for each channel separately by averaging across all trials for each condition to derive an averaged response, and then subtracting the averaged response from each trial in both EEG channels and electroculogram (EOG) channels to derive the residual background signal. Thereafter, per-trial and per-channel propagation factors are derived by computing the correlation coefficient between the residual background signal in EOG and each EEG channel as follows:

$$k_{i,j} = \text{corr}\left(\frac{y_{i,j} - \bar{y}_j}{x_{i,j} - \bar{x}_j}\right)$$

where $k_{i,j}$ is the propagation factor for the i-th trial and j-th channel, $y_{i,j}$ denotes the raw EEG signal in the i-th trial and j-th channel, xi,j the corresponding raw EOG signal,

and $\bar{y}_j$ and $\bar{x}_j$ represent the trial-averaged ERP signals for the j-th channel in EEG and EOG traces, respectively.

2.4.2. Adaptive Filtering Technique

Another common technique for de-noising, which also utilizes a reference input like the regression technique above, is the adaptive filtering approach. In this technique, a linear filter with parameters that can be adjusted based on an optimization algorithm is used. Specifically, if s(n) is the recorded contaminated EEG signal with x(n) as the "true" EEG portion and r(n) as a noise contamination; and v(n) is the recorded signal of the reference channel corresponding to the artefact source (e.g. EOG channel) then the goal is to utilize an optimization technique (e.g. least squares) to alter the parameters of the filter processing the v(n) input to provide a contamination free recording x'(n) [89]. For the current research, a two reference input version of the adaptive filter algorithm [103] is used with the vertical and horizontal EOG channels as reference inputs.

2.4.3. Independent Component Analysis

While the above-mentioned techniques primarily target ocular contamination, blind source separation based independent component analysis (ICA) can account for additional contaminating sources. While both EOG recordings and ocular-artifact-contaminated EEG data contain portions of ocular and neural signals, the two traces generally tend to be statistically independent in the time domain. Thus, ICA is ideally suited to separate EEG neural signals from EOG artifacts as this technique decomposes complex, multivariate data into statistically independent component sources [104]. If **x** denotes the observed signals in a multi-channel recording comprised of a linear mixture of independent source signals **s**, the data model can be expressed as:

$$\mathbf{x} = \mathbf{A} \cdot \mathbf{s}$$

where, $\mathbf{x} = \{x_1, ..., x_N\}$ is the measured data, $\mathbf{A}$ is a mixing matrix, and $\mathbf{s} = \{s_1, ..., s_N\}$ represents the independent source signals. The goal of ICA is to recover a close representation of the original source signals with the process modelled as:

$$\mathbf{u} = \mathbf{W} \cdot \mathbf{x}$$

where, $\mathbf{u}$ is a scaled and permuted version of $\mathbf{s}$, and $\mathbf{W}$ is an unmixing matrix specifying a spatial filter to invert the original mixing process.

The first step in ICA is a whitening procedure which demeans the data and removes correlations among the channels. Subsequently, the whitened data is transformed into independent sources by minimizing Gaussianity of the signals. This is due to the Central Limit Theorem which states that any linear combination of two random variables is more Gaussian that either of them. While Gaussianity is commonly measured using kurtosis, defined below, this technique is vulnerable to outliers and therefore is not well suited for application with experimental outcomes [105].

$$\text{kurt}(f) = E\{f^4\} - 3(E\{f^2\})^2$$

An alternate approach, used by many ICA algorithms including the infomax technique used in this research, is the application of mutual information for ICA estimation. Mutual information provides a measure of the amount of information that can be obtained about one random variable through observations of another, and is defined as:

$$I(\mathbf{f}; \mathbf{g}) = H(\mathbf{f}) - H(\mathbf{f}|\mathbf{g})$$

where, H(f) is the Shannon entropy and H(f|g) is the conditional entropy defined as:

$$H(\mathbf{f}|\mathbf{g}) = H(\mathbf{f}, \mathbf{g}) - H(\mathbf{g})$$

where, H(f,g) is the joint entropy of f and g calculated using the joint probability distribution [104], [106]. Therefore, within the context of the ICA estimations, maximizing the joint entropy of the sources minimizes mutual information.

2.5. Machine Learning Analysis

Subsequent to de-noising, ERP/ERF waveforms are derived as detailed previously in Section 2.4. ERP components are examined by contrasting one or more experimental conditions such as a "standard" or baseline condition and a "deviant" or test condition. ERP components normally occur when the test condition displays deviations from the baseline condition within specific latency windows, and several techniques are applied to objectively validate the existence of ERP components.

Examples of such techniques include the application of t-test and analysis of variance (ANOVA) for assessing features of interest such as amplitude differences among conditions [107] or spectral content of the conditions [108], as well as techniques that do not assume an underlying distribution and instead use permutation based non-parametric techniques [109]. An emerging technique is the use of machine learning approaches to detect ERPs in individual participants [110]. In particular, prior work using data from 100 healthy individuals collected using the HCS device has demonstrated that support vector machines (SVMs) paired with permutation-based non-parametric approaches can distinguish between experimental conditions with high accuracy for both P300 (99.0%) and N400 (92.3%) ERPs [65].

Machine learning classification often involves the application of an algorithmic model to assess an input and classify it as having membership in one category/group or another ("classes"). Within supervised learning approaches, the model is first trained using data with known classes ("labelled data"), and then tested using data with unknown class. SVM is a supervised nonparametric statistical learning technique, which given two classes of data, aims to form a decision boundary (hyperplane) dividing the two classes by maximizing the distance between the hyperplane and the nearest data points (support vectors) [110]. This reliance on support vectors which represent a small portion of the data set makes SVM models more generalizable and less susceptible to over fitting compared to other techniques [111]. Additionally, SVM techniques have also been shown to be well suited to sparse learning scenarios, i.e., situations where a large number of features are present in the data but the number of available training data sets is relatively small [112]. These properties together make SVM especially attractive for use with ERP data and indeed, empirical results also support this sentiment. A comparison of three supervised machine learning approaches (SVM, Naïve Bayes [113], and Binary Logistic Regression [114]) using the ERPs generated from the HCS data from 100 healthy controls confirms the superior performance of SVM (Figure 2.4).

Condition/Algorithm	Accuracy	TPR	FPR	Sensitivity	Specificity
N400_bayes	62.63%	0.50505	0.25253	0.50505	0.74747
N400_lr	71.38%	0.70707	0.27946	0.70707	0.72054
N400_svm	91.25%	0.89899	0.074074	0.89899	0.92593
P300_bayes	95.96%	0.96633	0.047138	0.96633	0.95286
P300_lr	95.45%	0.92929	0.020202	0.92929	0.9798
P300_svm	98.99%	0.99327	0.013468	0.99327	0.98653

Bayes = Naïve Bayes; lr = logistic regression; TPR = true positive rate; FPR = false positive rate.

Figure 2.4.   Results of three machine learning techniques classifying ERP data
Source: Technical Report by C. Liu 2015.

The results founds that while all classifiers were able to distinguish the experimental conditions for the P300 ERP very well (with accuracies >95%), only the SVM technique was able to distinguish the conditions associated with N400 ERP well. The SVM approach was utilized for this research with the details provided within each study.

2.6. Forward Modelling

The goal of many MEG and EEG studies is to understand the distribution and activity of current sources within the brain based on the data collected on or near the scalp. This process of estimating sources in the brain based on measurement of signals outside the head is called the inverse problem. However, the solution to the inverse problem requires knowledge of how a known current source would manifest as scalp potential or external field given a specific set of geometry and conductive properties, and calculating this is called the forward problem. The interlinked processes of forward and inverse modeling are shown in Figure 2.5.
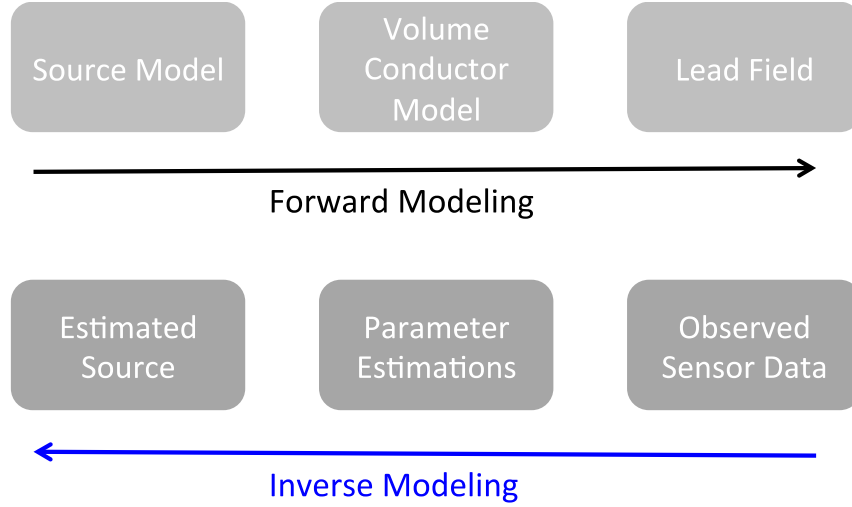
Figure 2.5. **Schematic of Forward and Inverse Modelling**

Maxwell's Equations, shown below, are the fundamental guiding principles for MEG and EEG:

$$\nabla \cdot \mathbf{E} = \frac{\rho}{\varepsilon_0}$$

$$\nabla \cdot \mathbf{B} = 0$$

$$\nabla \times \mathbf{E} = -\frac{\partial \mathbf{B}}{\partial t}$$

$$\nabla \times \mathbf{B} = \mu_0 (\mathbf{J} + \varepsilon_0 \frac{\partial \mathbf{E}}{\partial t})$$

where, ρ is the charge density, $\mathbf{J}$ is the current density, $\mathbf{E}$ is the electric field, and $\mathbf{B}$ is the magnetic field. The constant ε_0 is the permittivity of free space, and μ_0 the permeability of free space.

Within the context of the current research, the focus is on MEG source localization, and since the magnetic permeability of tissue is considered the same as free space [115] and fields generated by biological sources occur below 1kHz, the quasi-static approximations (i.e. $\frac{\partial \mathbf{B}}{\partial t} = 0$ and $\frac{\partial \mathbf{E}}{\partial t} = 0$) of Maxwell's Equations, stated below, are applicable [90], [115].

$$\nabla \cdot \mathbf{E} = \frac{\rho}{\varepsilon_0}$$

$$\nabla \cdot \mathbf{B} = 0$$

$$\nabla \times \mathbf{E} = 0$$

$$\nabla \times \mathbf{B} = \mu_0 \mathbf{J}$$

The above equations in turn help derive the Biot-Savart Law for describing the behaviour of magnetic fields generated by source **J** at location **r'** as described below:

$$\mathbf{B}(\mathbf{r}) = \frac{\mu_0}{4\pi} \int_{R^3} \mathbf{J}(\mathbf{r}') \times \frac{\mathbf{r}'}{|\mathbf{r} - \mathbf{r}'|^3} d\mathbf{r}'$$

Since MEG measures a combination of magnetic fields due to primary and secondary currents, the Biot-Savart Law can be extended, with the simplifying assumption of isotropic conductivities for brain, scalp and skull, to include contributions of magnetic field component due to primary and volume-conducted currents as shown below.

$$\mathbf{B}(\mathbf{r}) = \mathbf{B_0}(\mathbf{r}) + \frac{\mu_0}{4\pi} \sum_{ij} (\sigma_i - \sigma_j) \int_{S_{ij}} V(\mathbf{r}') \times \frac{\mathbf{r} - \mathbf{r}'}{\|\mathbf{r} - \mathbf{r}'\|^3} \times d\mathbf{S}'_{ij}$$

where, $\mathbf{B_0}(\mathbf{r}) = \frac{\mu_0}{4\pi} \int_{R^3} \mathbf{J}^P(\mathbf{r}') \times \frac{\mathbf{r}'}{|\mathbf{r}-\mathbf{r}'|^3} d\mathbf{r}'$ is the magnetic field due to the primary current $\mathbf{J}^P$, and the second term represents the contributions of volume currents calculated as surface integrals over the brain-skull, skull-scalp, and scalp-air boundaries [115], [116] with $V(\mathbf{r}')$ representing the surface potential of the various tissue layers, $\mathbf{V_0}(\mathbf{r}) = \frac{1}{4\pi\sigma_0} \int_{R^3} \mathbf{J}^P(\mathbf{r}') \times \frac{\mathbf{r}'}{|\mathbf{r}-\mathbf{r}'|^3} d\mathbf{r}'$ is the potential at **r** due to the primary current, and σ is the conductivity of the tissue.

As mentioned in Section 2.1, MEG measures the concurrent activity of a population of pyramidal neurons, and thus equivalent current dipoles are used to model the activity of patches of cortex (Figure 2.6). Propagation of fields from the cortex to the scalp and outside the head is governed by the electrical and geometric properties of the

conducting medium (i.e. brain, skull, skin/scalp), and several volume conductor models can be defined.

Physiological   Source
Source   Model
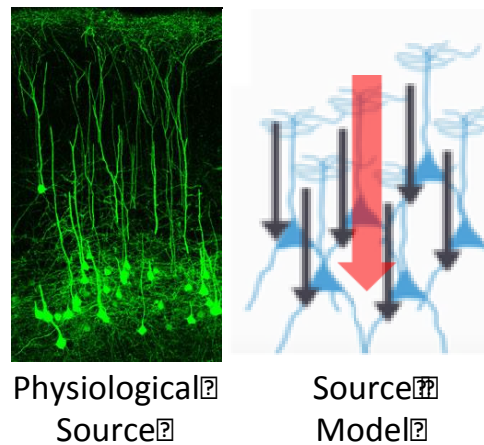
Figure 2.6.   **Equivalent Current Dipole Model**
Pyramidal neurons (physiological source of signal) modeled as dipoles with the equivalent current dipole (red arrow) modelling a patch of cortex.

Specifically, the electrical properties of the tissues are derived from ex-vivo experimentation [90], while the geometric properties require analytical or numerical solutions to help define the volume conductor model to solve the forward problem. The geometry of volume conductor models can be defined either with simple geometric shapes (e.g. single sphere or 3-shell concentric spheres) or more realistically by extracting the geometry from structural MRI images. For generation of realistic volume conductor geometries, boundary element method (BEM) is commonly used (especially for EEG). As shown in Figure 2.7, BEM tessellates the boundaries between different head tissues (e.g. skin, skull, brain) with triangular surfaces and assumes each compartment to be isotropic and homogenous [117]. An alternate technique for creating realistic volume conductor geometries is the finite element method (FEM), which models the volume with tetrahedrons. While FEM is more accurate than BEM, it is less commonly used due to its computational complexity [118].
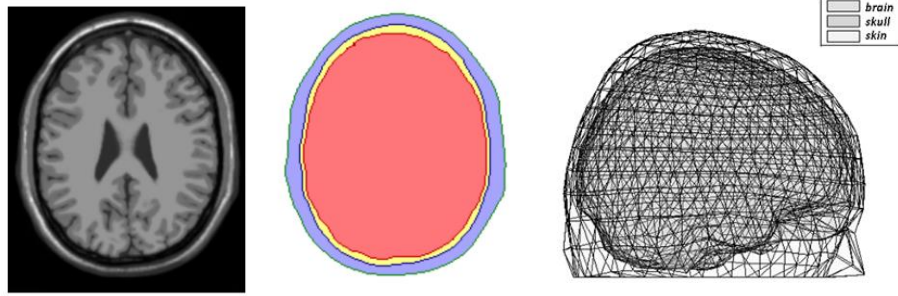
Figure 2.7. **Sample boundary element method extraction of realistic geometry**
Left: Structural MRI, Middle: Segmented head tissue, Right: BEM model with three compartments corresponding to brain, skull and skin/scalp. Source: Adapted from FieldTrip Toolbox tutorial.

2.7. Inverse Modelling

Once the forward modelling step is completed, the goal of estimating the sources in the brain based on the observed/recorded MEG and EEG sensor data is accomplished via inverse modelling. Three main categories of inverse modelling techniques are available: single and multiple dipole fitting, distributed source modelling, and spatial filtering methods.

2.7.1. Dipole Fitting

The basic tenet of dipole fitting is to manipulate the source parameters of dipole orientation, strength and location in order to minimize the error between the modelled and the actual measured data. Generally, the orientation and strength are modelled together as 3D vectors in space, and the location is modelled separately. The dipole fitting procedure involves iteratively generating modelled data for sets of orientation, strength and location parameters and then minimizing the difference between the model and the measured data.

For a given set of orientation, strength and location parameters, the modelled data can be described as:

$$\mathbf{m} = \mathbf{A} \cdot \mathbf{q}$$

where $\mathbf{m} = \{m_1 \dots m_S\}$ is a vector containing modeled data for S sensors, $\mathbf{q} = \{q_1 \dots q_k\}$ is the source vector containing k dipolar sources, and $\mathbf{A}$ is an $S \times K$ matrix known as the lead field or gain matrix, calculated during the forward modelling procedure describing

the propagation of unit dipole moment through the volume conductor with its particular conductivities and geometric properties. Multiple dipoles/sources are treated as linear superpositions of the contributions of each.

A parameter optimization technique is applied to determine the 'ideal' source location by minimizing the sum of squared error between the modelled and the actual measured data in the following manner:

$$min(\mathbf{Y} - \mathbf{A} \cdot \mathbf{q})^2$$

where, $\mathbf{A} \cdot \mathbf{q}$ is the modeled data, and $\mathbf{Y}$ denotes the actual sensor measurements.

Simple grid search based techniques can be employed to scan through the entire brain and identify optimal parameters, but this is not computationally feasible due to the large number of possible locations (especially challenging in the multiple dipole scenario) and thus dipole fitting is often applied when a-priori knowledge of the sources are available [90]. Some dipole fitting techniques use gradient decent approach but are prone to local minima and the results are thus highly dependent on the starting conditions. In such situations, several different starting conditions are applied in order to identify convergent solutions. Irrespective of the specific technique used, dipole fitting is largely confined to simple source localizations where only a small number of sources are expected to be active.

2.7.2. Distributed Source Modelling

Unlike dipole fitting, in distributed source modelling techniques, the location and orientation of current sources are fixed. Specifically, these techniques assume that the source currents originate in the cortical surface, modelled as a 3D mesh derived from structural MRI, with dipoles located orthogonal to the mesh surface. Having pre-defined the location and orientation of the sources, distributed source modelling techniques only need to estimate the strength of the dipole sources throughout the cortical surface. However, since the number of available sensors is much lower than the number of cortical sources, this is a severely underdetermined problem [90], with a large number of possible combinations able to explain the measured data equally well.

In order to find a unique solution, distributed source modelling algorithms thus need additional constraints and incorporate knowledge of the source or desired property of the solution via a regularization term. This involves the following procedure:

$$min_q \{\|\mathbf{Y} - \mathbf{A} \cdot \mathbf{q}\|^2 + \lambda\|\mathbf{D} \cdot \mathbf{q}\|^2\}$$

where, $\mathbf{Y}$ is the data measured by sensors, $\mathbf{q}$ is the source distribution, $\mathbf{A}$ is the lead field matrix calculated during forward modelling, $\mathbf{D}$ is a matrix describing knowledge of the sources, and λ is the regularization factor.

Minimum norm estimates (MNE) is a widely used source localization technique that relies upon minimizing the L2-norm [119]. Unfortunately, this tends to bias the results towards the cortical surface, but since MNE requires few assumptions about the source characteristics it is widely used for studying neural responses that may not be well characterized [120]. As parts of the present research involved the development of a new technique for brain function assessment (detailed in Chapter 5), little prior knowledge of the neural source characteristics were available and thus the MNE technique was applied.

2.7.3. Spatial Filtering

In contrast to the above-mentioned techniques, spatial filtering approaches do not try to explain the observed data as a whole, but rather calculate the contributions of each source location. Spatial filtering techniques such as beamformers calculate sets of filter weights for each location such that signals from that location are passed with unity gain and contributions from other sources are nulled. Unfortunately, this leads to the primary disadvantage of beamforming techniques, in that correlated sources are suppressed and neural phenomena containing correlated sources cannot be accurately localized using this approach [90], [121]. As mentioned previously, given the lack of knowledge of source characteristics within the present research, beamforming was not deemed to be ideal and thus MNE was employed instead.

2.8. Time-Frequency Analysis

In addition to analysis of temporal (ERP, ERF) and neuroanatomic (source localization) features, often the spectral content of neural signals is of interest. The simplest frequency domain representation is achieved with the classic Fourier transform, which for a given function f is defined as:

$$F(\omega) = \int_{-\infty}^{\infty} f(t)\, e^{-j\omega t} dt$$

where, ω is frequency in radians, and the transformed signal can be converted back into time domain through the inverse Fourier transform as defined below.

$$f(t) = \frac{1}{2\pi} \int_{-\infty}^{\infty} F(\omega)\, e^{j\omega t} d\omega$$

However, as biological signals such as those measured by EEG and MEG are not stationary, they violate key assumptions of Fourier transform specifically in terms of the constancy of spectral content over time, rendering the Fourier technique unsuitable for use. In order to assess the time evolving spectral content of biological signals, alternate approaches such as continuous wavelet transform (CWT) are utilized instead. At its core, CWT involves using a template (called mother wavelet) and decomposing the signal of interest based on a set of basis functions created by stretching and compressing the mother wavelet. Mathematically, this can be expressed as shown below.

$$F(a, b) = (f, \psi_{a,b}) = \frac{1}{\sqrt{a}} \int_{-\infty}^{\infty} f(t)\, \psi\left(\frac{t - b}{a}\right) dt$$

where $\psi_{a,b}$ is a wavelet scaled by parameter a and time shifted by parameter b. This scaling (dilation) and time shifting (translation) enables the wavelet to provide greater temporal resolution at higher frequencies and lower temporal resolution at slower frequencies (Figure 2.8B).

While several wavelets have been defined, one of the most commonly used wavelet is the Morlet wavelet comprised of a complex exponential and a Gaussian taper (Figure 2.8A) as defined below:

$$\psi_\sigma(t) = c_\sigma \pi^{-\frac{1}{4}} e^{-\frac{1}{2}t^2} \left(e^{i\sigma t} - \kappa_\sigma \right)$$

where $\kappa_\sigma = e^{-\frac{1}{2}\sigma^2}$ and $c_\sigma = \left(1 + e^{-\sigma^2} - 2e^{-\frac{3}{4}\sigma^2} \right)^{-\frac{1}{2}}$ and the parameter σ is a constant governing time and frequency resolution trade-off.
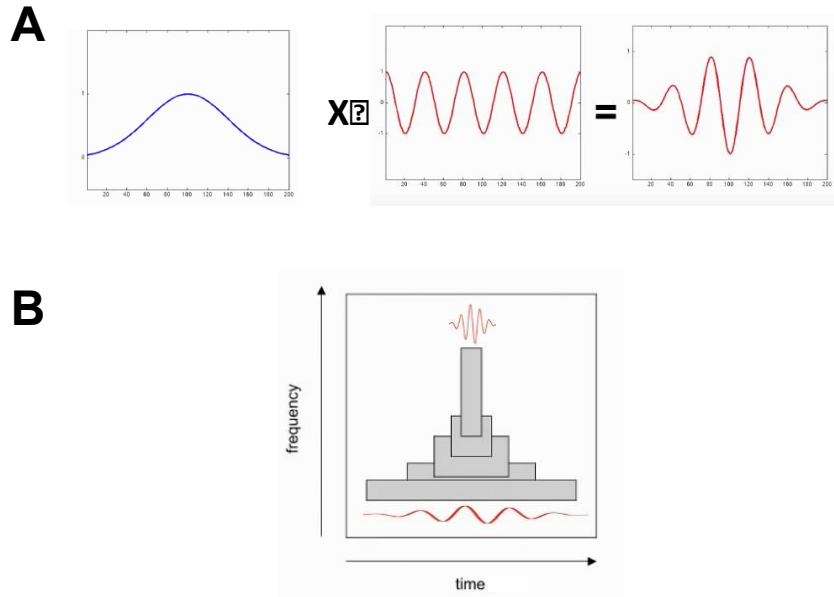
Figure 2.8.   Morlet Wavelet Generation and Application
A) Morlet wavelet (right) is comprised of a complex exponential (middle) and a Gaussian taper (left). B) Mother wavelets like Morlet can be used to generate basis functions that provide differing frequency and temporal resolution. Source: FieldTrip tutorial.

Trade-off between time and frequency resolution is necessary at all times due to the constraints of Heisenberg's uncertainty principle. The Morlet wavelet provides better trade-off between time and frequency resolution, and is thus widely used to analyze bioelectric and biomagnetic signals [122], [123].

Chapter 3.　　Study I: Developing Brain Vital Signs Platform

3.1.　Abstract

Clinical assessment of brain function relies heavily on indirect behavior-based tests. Unfortunately, behavior-based assessments are subjective and therefore susceptible to several confounding factors. Event-related brain potentials (ERPs), derived from electroencephalography (EEG), are often used to provide objective, physiological measures of brain function. Historically, ERPs have been characterized extensively within research settings, with limited but growing clinical applications. Over the past 20 years, we have developed clinical ERP applications for the evaluation of functional status following serious injury and/or disease. This work has identified an important gap: the need for a clinically accessible framework to evaluate ERP measures. Crucially, this enables baseline measures before brain dysfunction occurs, and might enable the routine collection of brain function metrics in the future much like blood pressure measures today. Here, we propose such a framework for extracting specific ERPs as potential "brain vital signs". This framework enabled the translation/transformation of complex ERP data into accessible metrics of brain function for wider clinical utilization. To formalize the framework, three essential ERPs were selected as initial indicators: 1) the auditory N100 (Auditory sensation); 2) the auditory oddball P300 (Basic attention); and 3) the auditory speech processing N400 (Cognitive processing). First step validation was conducted on healthy younger and older adults (age range: 22-82 years). Results confirmed specific ERPs at the individual level (86.81%-98.96%), verified predictable age-related differences (P300 latency delays in older adults, $p<0.05$), and demonstrated successful linear transformation into the proposed brain vital sign (BVS) framework (basic attention latency sub-component of BVS framework reflects delays in older adults, $p<0.05$). The findings represent an initial

critical step in developing, extracting, and characterizing ERPs as vital signs, critical for subsequent evaluation of dysfunction in conditions like concussion and/or dementia.

3.2. Introduction

Vital signs such as heart rate, pulse oxygenation, and blood pressure are essential to monitoring and managing the health of various body systems. Yet there are no such vital signs identified for brain function – despite the clearly instrumental role such vital signs could play. Current clinical assessments for screening brain functional status relies largely on subjective, behavior-based measures, such as the Glasgow Coma Scale (GCS), to evaluate level of conscious awareness following brain injury [2], [23]. However, subjective behaviour-based tests of this nature have been reported to have misdiagnosis rates as high as 43% [30], [47]. More detailed clinical evaluation of cognitive function and associated impairments are often reliant on neuropsychological assessment [82], [124]. These too are behavior-based measures, depending heavily on the patient's capacity to produce voluntary, on-demand motor and/or verbal responses to stimuli [125]. Unfortunately, confounding factors, such as motoric and communicative limitations, often hamper greatly the clinical effectiveness for many of these measures.

Over the last 20 years, our group has demonstrated the critical need for a physiological, objective brain function assessment that utilizes event-related potentials or ERPs [58], [65], [126]. ERPs are derived from long-standing electroencephalography (EEG; [127]). They can be recorded using minimal non-invasive scalp electrodes, combined with time-locked stimulation, to reflect target brain responses during information processing [1], [47]. EEG combines practical features of being accessible, available, low cost, and portable [14], which makes the technology well suited for point-of-care applications [1]. Work to date has demonstrated that ERPs can provide specific information across a spectrum of brain functioning, from low-level sensory to higher level cognitive processing [48]. Moreover, ERPs have been shown to have robust diagnostic and prognostic capabilities [56]–[59], [128], [129].

In recent years, clinical ERP integration has focused on developing rapid, automated approaches in order to successfully utilize key ERPs that can be robustly recorded at the individual-level. The initial effort focused on developing a rapid evaluation framework for neurological status after severe acquired brain injuries, called

the Halifax Consciousness Scanner (HCS; [81]). The HCS was developed to examine the presence or absence of five key ERP responses linked to sensation (N100), perception (mismatch negativity, MMN), attention (P300), memory for one's own name (early negative enhancement, ENE), and semantic speech processing (N400). These ERPs were validated across a large sample of healthy individuals and clinically applied in neurological status assessment [65], [130]. However, it has become increasingly clear that mere assessments of presence or absence of a particular ERP does not fundamentally address the need to measure healthy individual brain function over time. Effective longitudinal monitoring of brain functional changes requires the establishment of individual functional 'baselines' of brain vitality prior to conditions of dysfunction. Specifically, there is no framework for establishing and monitoring well established ERPs that can serve as indicators for an individual's healthy brain function, in spite of the evidence for relatively stable within-subject variance over time [52], [53]. This gap is essential to address in order to successfully assess the significance of any ERP-related change in which questions arise about possible dysfunction, which are increasingly arising as a potential application and common challenge in the evaluation of, for example, concussion and/or dementia.

Accordingly, the objective of the current study was to begin developing an initial framework to translate/transform ERPs into practical and accessible brain vital signs. The conceptual development of such a framework required a systematic process anchored to other existing vital sign frameworks. Therefore, the current paper is divided into two main sections: (i) a proposed conceptual framework for brain vital signs; and (ii) a first step evaluation of practical implementation in a test sample of healthy adults across the lifespan.

(i). Brain vital sign framework: As with other vital signs, a potential brain vital sign framework must satisfy some fundamental requirements: 1) the responses should be EEG hardware platform independent; 2) each response should be extensively characterized within the literature; 3) responses should be recorded reliably within healthy adult individuals[1]; 4) they should be accessible to normative data comparisons for essential response characteristics (e.g., amplitudes and latencies); and 5)

---

[1] Most ERP responses are also well characterized across brain development, but require increasing reliance on age specific norms and caveats that are not discussed here.

importantly, the responses should be translated into a clinically accessible framework, which can be readily communicated.
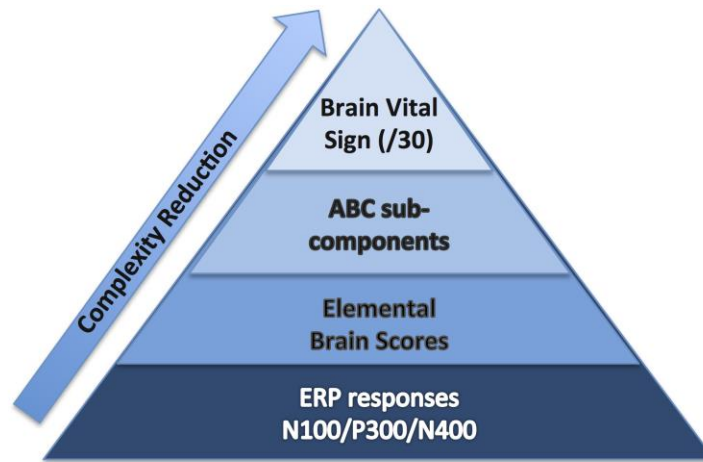
Figure 3.1.   Brain Vital Sign Framework.
1) Overall brain vital sign score: highest 30; 2) ABC break down into **A**uditory sensation, **B**asic attention, and **C**ognitive processing; and 3) Elemental Brain Scores linearly transformed from N100, P300, and N400 response amplitudes and latencies (3 responses*2 measures= 6 scores).

To start, we selected well-established sensation-to-cognition ERPs[2]: the N100, P300, and N400[3]. A complex-to-basic pyramidal approach provided an overview of the translation from technical ERP nomenclature to easy to communicate brain vital signs (Figure 3.1). Sub-scores reflective of specific brain functions were derived from the mean and standard deviations (Figure 3.2). Lastly, linearly transformed scores normalized to the best possible results for each amplitude and latency measure were created and referred to as elemental brain scores (EBS).

---

[2] While the main focus is on auditory ERP responses, all three are present across both auditory and visual modalities.

[3] Note that the mismatch negativity (MMN;[137]) may also be considered a potential ERP response for a brain vital sign framework. As the MMN can also be derived from the same auditory stimuli that elicit the N100/P300, it remains possible candidate for future expansion.

BVS (/30) = A(/10)+B(/10)+C(/10)
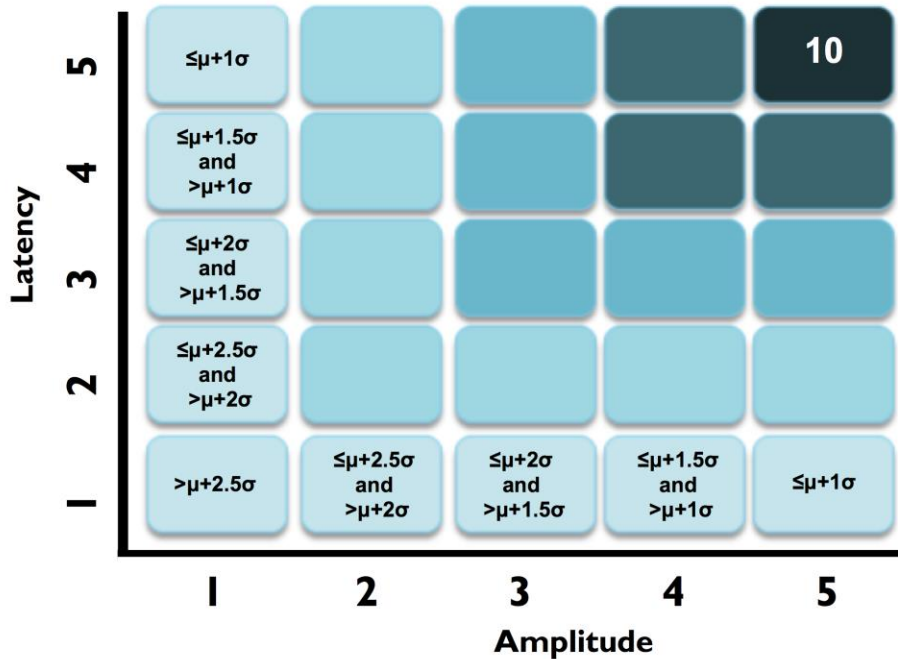
Figure 3.2.   ABC Breakdown Demonstrating Graded Measures.
Calculation shown for BVS sub-components 'A'. Similar calculations undertaken for 'B' and 'C'.

(ii). Practical implementation in healthy adults: To address implementation, the following steps were undertaken: 1) Hardware performance characterization was critical for platform independence. While some studies have compared hardware system performance for one time point analysis [99], analysis of performance over time was conducted to characterize instrument noise levels for longitudinal monitoring. 2) Stimulus sequence optimization was crucial to balance the trade-off between short testing times and highest possible response signal-to-noise ratio (SNR). 3) Response extraction and identification required an expert-independent, quality-checked approach. 4) Response results then required translation/transformation into the brain vital sign framework for interpretation and reporting. 5) A test sample of ERP data, with an age-related difference comparison embedded, provided initial validation across the adult life span (i.e., younger versus older adults).

The current study utilized a healthy sample data set to test three hypotheses: 1) The three ERPs would be detectable at the individual level (Hypothesis 1); 2)

Comparison between younger and older adults will show predictable age-related changes (Hypothesis 2); and 3) Because the brain vital sign framework is generated by applying a linear transformation to the raw ERP responses, we anticipate the pattern of age-related ERP changes would be preserved in the EBS results. With this initial step, it would then be possible to expand the brain vital sign framework into more extensive normative development along with applications in possible dysfunction related to conditions like concussion and dementia.

3.3. Methods

3.3.1. Characterizing and calibration of EEG hardware performance

Four candidate EEG systems (gNautilus and gMobiLab systems manufactured by g.Tec Medical Engineering, and two Enobio systems manufactured by Neuroelectrics) were evaluated in order to identify the most reliable hardware. Hardware evaluation used a 5-minute known input calibration signal ("ground truth"), derived from a combination of sinusoidal waves with frequencies of 5, 10, 15 and 30Hz (in MATLAB software). The test signal was delivered through the audio output port (at maximum volume setting) and recorded on 2 channels of the EEG systems as well as a Tektronix oscilloscope (model # 795-TBS1052B). Testing was conducted 2 times per day over 3 consecutive days (6 total).

Stability and reliability was assessed using inter-channel stability (correlation between channels at each time point of test), day-over-day stability (percentage change in peak voltage over the 3 days), peak-to-peak voltage recorded, and SNR (defined as ratio of sum of spectral power surrounding the 5, 10, 15, 30Hz ['signal'] and 60Hz ['noise']). The g.Nautilus device, provided maximal SNR and had the best recording stability over the 3 days (average change 1.45% over 3 days, see Supplementary Material for full results), and was therefore utilized for subsequent human data collection.

Scalp-recorded ERPs were recorded from 3 midline electrodes (Fz, Cz, & Pz, embedded within a cap), insert earphones, g.Nautilus EEG acquisition hardware (bandpass: dc-250Hz, 500Hz sampling, 3 axis head motion accelerometers), and a portable computing platform. Four additional electrodes provide ground (forehead), reference (ear lobe) and eye monitoring (electro-oculogram, EOG).

Following signal amplification, conditioning, and digitization, the data were transmitted over Bluetooth link to the portable host computer. Time-stamping signals were sent from the host computer using a custom-designed USB-to-TTL converter subsystem to mark stimulus presentation events. These TTL pulses were logged by the amplifier along with the EEG data and later used for signal averaging to derive ERPs.

3.3.2. Stimulus sequence balancing SNR and short testing time

Auditory tone and spoken word pair stimuli were presented through the insert earphones. Tone stimuli elicited the N100 and P300 responses and spoken word pairs elicited the N400 (Figure. 3). Tones (100ms duration) were divided into standard (75dB, 80%) and deviant (100dB, 20%) conditions, with the N100 and the P300 derived from the deviant condition. Paired spoken words were divided into congruent prime pairs (e.g., bread-butter, 50%) and incongruent prime pairs (Romeo-table, 50%). The N400 was derived from the incongruent prime word pairs. The interlacing of tones and word pair stimuli enabled full optimization of near maximum trials per unit time (e.g., 5s / stimulus cycle × 60 cycles = 5mins).
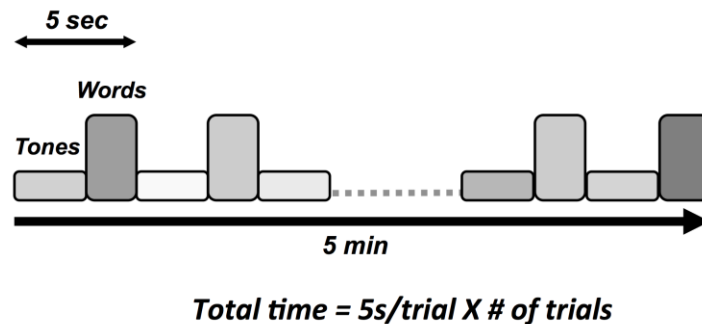
Figure 3.3.   Brain Vital Sign Stimulus Sequence
Schematic illustration of auditory stimulus sequence consisting of tones and word pairs.

3.3.3. ERP response elicitation, extraction and identification

EEG scans were conducted with minimal preparation compared to conventional EEG techniques (<5 minute setup). Each participant was fitted with an elastic cap with embedded electrodes, and g.GAMMAsys electrode gel was injected at each location for conductivity. EOG channels were recorded using disposable Ag/AgCl electrodes on the

supra-orbital ridge and outer canthus of the left eye. Skin-electrode impedances were maintained at <30kΩ impedance at each site. Acoustic stimuli were delivered binaurally through Etymotic ER4 insert earphones. Participants were instructed to pay attention to the auditory stimuli while maintaining visual fixation on a cross located 2.0m away (black on white background). Three runs of the 5-minute stimulus sequence were collected on each participant (approximately 15 min total run time).

Automated ERP pre-processing used established methods, including spectral filtering, segmentation, baseline correction, and conditional averaging [48]. Signal-to-noise optimizations include ocular correction to remove eye artifact, jittered stimulus timing to minimize potential alpha contamination, and artifact de-noising using pattern recognition. ERP processing parameters were as follows: 1-20Hz bandpass filter, 60Hz notch filter, -100ms to 900ms epoch length for segmentation relative to stimulus onset. ERP response identification was undertaken through a template matching process in which N100, P300, and N400 peaks were identified by specifying expected polarity within expected temporal ranges[131]. Each ERP response value was measured as peak-to-peak measure relative to the preceding peak of opposite polarity.

Machine learning methods such as support vector machine (SVM), allow training of two-category classifiers to distinguish contrasting experimental conditions (see [110] and [65]). The best results were obtained using single run, trial-averaged data from all three-electrode sites as inputs to the SVM with a radial kernel. 90% of the available data were randomly selected to train a two-category classifier to distinguish between the two stimulus conditions for each experiment (i.e. standard vs. deviant tones for N100 & P300, congruent vs. incongruent words for N400). The trained classifier was then applied to the remaining 10% of datasets to test the accuracy of classification. Under 10-fold cross-validation with contiguous divisions, this process is repeated 10 times such that the classifier is trained and tested on all available data. The total instances of correct group classification (ex. number of correct standard and deviant classifications) relative to the total number of classifications provide an accuracy number. Standard statistical measures including true positive (TP), false positive (FP), sensitivity, and specificity are derived from the confusion matrix. The SVM analyses were further verified using non-parametric permutation statistics to assess if the observed performance could be obtained by chance [132]. This involved randomly redistributing the class labels in the training sets and observing the performance of the new SVM solution. After 1000

permutations, the observed classification accuracies were used as a null distribution against which the significance of the true SVM solution was determined.

3.3.4. Translation/transformation of ERP responses to brain vital sign framework

First, similar to neuropsychology assessment, a total brain vital sign score of 30 was defined to represent the most basic result: all responses fall with the normative range, bounded by standard deviation. The highest level of brain vital sign framework combines all three ERP peak amplitude (µV) and latency (ms) measures, ranked in terms of standard deviations from the mean (M/SDs), into one composite score of 30. The total brain vital sign score of 30 reflects overall healthy brain processing[4]. The total scores for each participant were generated by comparing the amplitude (X) and latency (L) measures of each of the 3 components to the normative database, with scoring criteria determined using the mean (µ) and standard deviation (σ) of the corresponding measures in the normative database. Details are shown in Table 3.1.

A standard clinical scheme of "ABC" was implemented for the breakdown of individual responses, with the N100 as an indicator for Auditory sensation (A) [61]; the P300 as an indicator for Basic attention (B) [62]; and the N400 as an indicator for Cognitive processing during speech perception (C) [63]. Within the ABC scheme 5 points for amplitude and latency each were awarded. In addition to establishing a healthy brain vital sign range (A=10, B=10, C=10; Total 30), it was also possible to derive metrics for monitoring ABC amplitude and latency changes over time. Amplitude and latency metrics for ABC were used to calculate 6 elemental brain scores (EBS). Each EBS was normalized to the best possible response measurement. Therefore, for each EBS, it is possible to rank ABC amplitude and latency results relative to the largest normative ERP response amplitude and shortest normative ERP response latency, with scores ranging from 0 to 1. A score of 1 matched the outer bounds for best possible measurement.

---

[4] Note that the initial SD cut-off can be customized and optimized in accordance with the enhanced development of normative databases.

Table 3.1.   BVS scoring criteria for the three ERP components.

P300		N400 & N100	
Amplitude (X) / Latency (L)	BVS Score	Amplitude (X) / Latency (L)	BVS Score
X > μ – σ L < μ + σ	5	X < μ + σ L < μ + σ	5
μ – 1.5σ < X < μ – σ μ + 1.5σ > L > μ + σ	4	μ + 1.5σ > X > μ + σ μ + 1.5σ > L > μ + σ	4
μ – 2σ < X < μ – 1.5σ μ + 2σ > L > μ + 1.5σ	3	μ + 2σ > X > μ + 1.5σ μ + 2σ > L > μ + 1.5σ	3
μ – 2.5σ < X < μ – 2σ μ + 2.5σ > L > μ + 2σ	2	μ + 2.5σ > X > μ + 2σ μ + 2.5σ > L > μ + 2σ	2
X < μ – 2.5σ L > μ + 2.5σ	1	X > μ + 2.5σ L > μ + 2.5σ	1

Mathematically, EBS measures can be expressed as shown in equations 1 and 2 below:

$$\text{Score} = 1 - \text{abs}\left(\frac{M - \text{best}}{\text{max} - \text{min}}\right) \text{ -- Eq (1)}$$

$$\text{Score} = 1 - \text{abs}\left(\frac{\text{best} - M}{\text{max} - \text{min}}\right) \text{ -- Eq (2)}$$

Where, *M* is the mean value of the amplitude/latency, *max* is the maximum value and *min* is the minimum value and *best* is the 'ideal' value that should be achieved. Best value can either be the max or the min value depending on whether the lowest or the highest value represents the ideal situation – generally for latency the lowest (smallest) value represents faster (better) processing, whereas for amplitude the highest positive value or lowest negative value is thought to represent ideal processing.

Equation 1 was utilized for N100 and N400 amplitude and latency as well as P300 latency, whereas equation 2 was used for P300 amplitude. All EBS calculations were undertaken using an existing database of 100 healthy controls [65] containing information about N100, P300 and N400 components. To account for outliers in the normative database, all data values were ranked, and the interquartile range between 75th and 25th percentiles calculated. Extremity thresholds were determined by calculating the points corresponding to 1.5-times the interquartile range above the 75th

percentile, and 1.5-times the interquartile range below the 25th percentile. Data points beyond the boundary formed by these thresholds were excluded as outliers from the normative database prior to BVS and EBS extraction. This process resulted in the removal of 6 participants (out of 100) from the N100 amplitude database, 2 participants from the N100 latency database, 1 participant from the N400 amplitude, 6 participants from the P300 amplitude database and 1 participant from the P300 latency database. No participants were excluded from the N400 latency database.

3.3.5. Initial validation across the healthy adult lifespan

Sixteen (16) participants ranging in age from 22-82 years were recruited (46.81 ± 22.14, 8 females). A bimodally distributed sample was selected across lifespan, with 8 in the 20-35 year-old range (26.13 ± 4.00, 4 females) and 8 in the 50-85 year-old range (67.5 ± 11.25, 4 females). Participants had no history of neurological problems or psychoactive medications. All individuals were fluent in English and had normal or corrected-to-normal hearing. Visual inspection of the data led to removal of 2 participants from subsequent analysis due to noisy data. Furthermore, to ensure analyses used a minimum of a 20-year age separation with controlled age-appropriate cognitively matched samples, data from 2 participants were not included (1 from each sub-sample). The final matched analysis therefore included 6 in the 20-30 year range and 6 in the 50-85 year range. Research Ethics Boards at Simon Fraser University and Fraser Health Authority approved the study.

Each participant underwent neuropsychological screening along with EEG/ERP testing using Mini Mental State Exam (MMSE) [82] and Montreal Cognitive Assessment (MoCA) [83]. MMSE examines 5 areas of cognition (orientation, registration, attention and calculation, recall, and language), with scores below 23 suggestive of cognitive impairment (maximum score 30) [82]. MoCA examines a multitude of high-level cognitive functions (e.g. short-term memory recall, delayed recall, visuospatial abilities, working memory, and language etc.).

ERP results were divided into the two groups (20-30 and 50-85 age ranges). Quantitative group-level ERP response characteristics were compared using two-tailed independent samples t-test. Results are presented as mean ± SD. Moreover, to assess the performance of the expert-independent method (SVM) across the age ranges, a sub-

analysis was undertaken for each group to compare and contrast any performance differences.

ERP responses were also transformed into the brain vital sign framework, generating an overall brain vital sign score and the 6 EBS scores for each participant. EBS scores were compared at the group-level. Normality was assessed using the Shapiro-Wilk W test. Only the EBS measures for amplitude in the "C" component of the framework did not pass the normality test, and they were therefore compared using the Wilcoxon test. All others were compared using two-tailed independent-samples t-test. Results are presented as mean ± SD.

3.4. Results

3.4.1. Participant cognitive status evaluation

Participant characteristics and MMSE/MoCA scores are presented in Table 3.2. Both the younger (age 20-30) and older (age 50-85) groups scored in the healthy range. All individuals in the younger group obtained full scores (30/30) for both MMSE and MoCA. Participants in the older group scored 30 for MMSE and 29.3±0.5 for MoCA.

Table 3.2.   Sample characteristics and cognitive test scores

	Age 20-30	Age 50-85
Sample Size (n)	6	6
Education (years)	18.3 ± 1.9	17.8 ± 5.6
MMSE (/30)	30	30
MoCA (/30)	30	29.3 ± 0.5
Sex (M:F)	1:1	1:2

3.4.2. ERP response extraction and expert-independent identification

Figure 3.4 shows the ERP components evoked using the stimulus sequence in representative individuals for the 20-30 and 50-85 age ranges. The N100 component was elicited during Auditory sensation (-6.74 ± 2.13µV). The P300 was elicited during Basic attention to deviant tones (10.72 ± 2.66µV). The N400 was elicited during Cognitive processing of semantically incongruent word pairs (-5.09 ± 2.67µV). All

components were present in all participants. Figure 3.5 presents group-averaged ERP results.
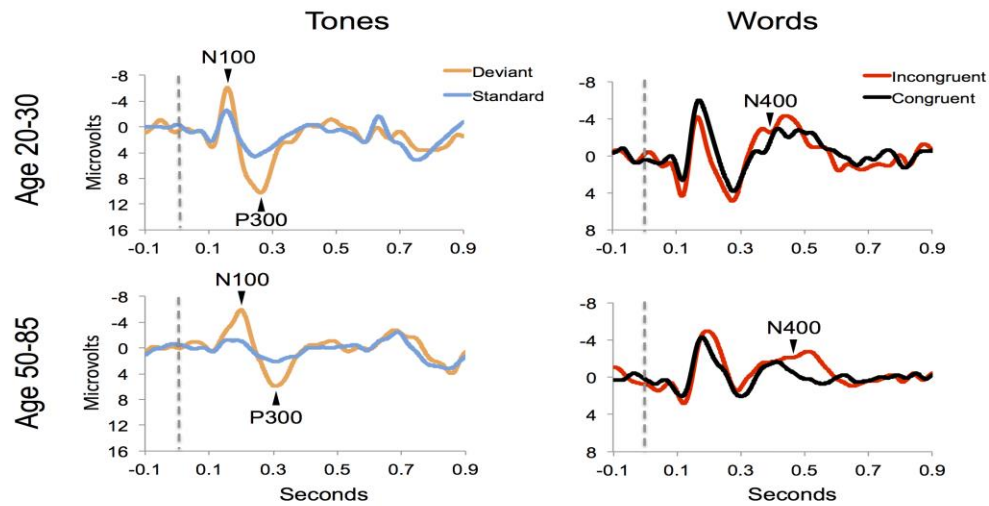
Figure 3.4.   Representative Participant ERP Waveforms.
ERP waveforms for a representative participant in the younger (age 20-30, participant age = 30) and middle-aged/older (age 50-85, participant age=60) age ranges. Data were averaged across 3 runs.
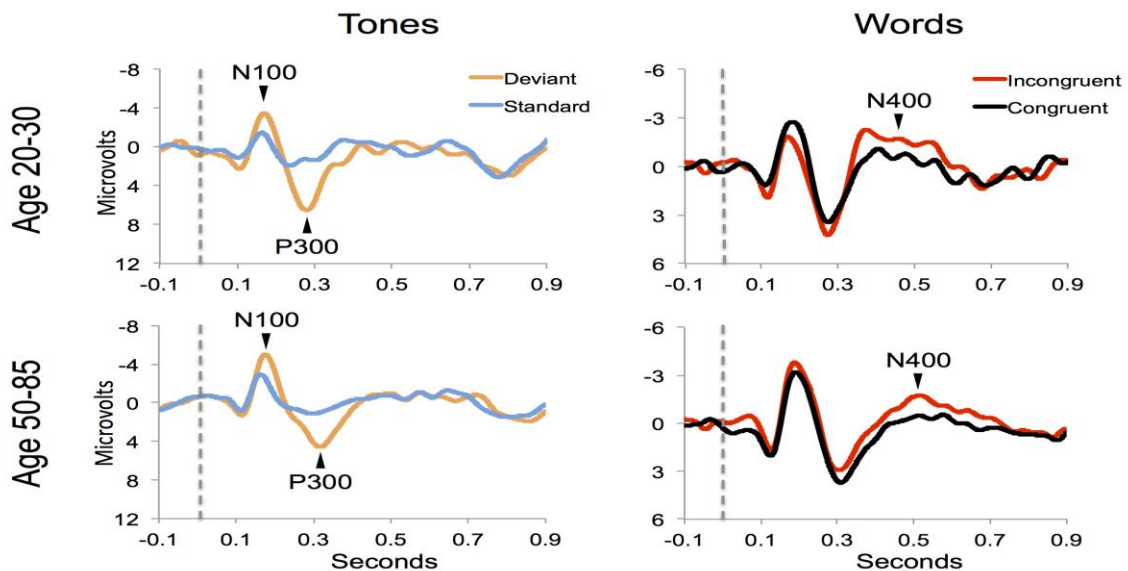
Figure 3.5.   Grand Averaged ERP Waveforms.
ERP waveforms for group averages in the younger (age 20-30) and middle-aged/older (age 50-85) age ranges.

ERP response results indicate that the trained SVM classifier successfully identified predicted response differences. For the P300, the SVM classification included deviant vs. standard tones. The individual-level accuracy of P300 classification is 98.96% across all ages, with 0.98 sensitivity and 1.00 specificity (Table 3.3). For the N400, the SVM classification included incongruent vs. congruent word pairs. The individual-level classification accuracy for N400 is 86.81% across all ages, with 0.84 sensitivity and 0.90 specificity (Table 3.3). Permutation analysis verified the accuracy of the SVM classification for P300 (p<0.001) and N400 (p=0.05).

Table 3.3.   **SVM classification for P300 and N400**

	P300	*N400*
Accuracy	98.96%	86.81%
True positive	0.98	0.84
False positive	0.00	0.10
Sensitivity	0.98	0.84
Specificity	1.00	0.90

3.4.3. Translation to the brain vital sign framework

The participant responses were successfully translated into the brain vital sign framework. Relative to norms, the representative participants in Figure 3.5 both scored full 30, allocated the maximum 10 for each of the A, B and C components. All individuals achieved scores of 30. EBS scores were also calculated: A) amplitude (0.56 ± 0.17) and latency (0.41 ± 0.25) for the N100 using N=99 norms; B) amplitude (0.59 ± 0.11) and latency (0.59 ± 0.14) for the P300 using N=100 norms; and C) amplitude (0.50 ± 0.24) and latency (0.36 ± 0.16) for the N400 using N=100 norms. As anticipated, each of the EBS measures straddled the 50th percentile mark (=0.5, representing average performance) within the mean ± 1 standard deviation segment.

3.4.4. Initial validation across the healthy adult lifespan

Table 3.4 presents quantitative group-level component ERP response characteristics. Table 3.4 shows that P300 latencies increased significantly between younger and older groups (p<0.05), with a similar trend for the N400 latencies (p=0.07). Table 3.5 shows that SVM classification undertaken separately for the younger and older age groups, showed comparable results between the two groups. Figure 3.6 and

Table 3.6 shows group-level EBS scores between younger and older groups.

Similar to P300 latency measures, the corresponding EBS score ('B' latency) demonstrated a significant group difference (p<0.05) between old and young. Additionally, the 'C' latency EBS also showed a trend (p=0.07) for group differences, again in agreement with the corresponding N400 latency trends.

Table 3.4.   Quantitative measures for group-level ERP characteristics.

Mean ± SD. *p<0.05 between groups.

		Age 20-30	Age 50-85
P300	Amplitude (μV)	11.09 ± 3.39	10.36 ± 1.91
	Latency (ms)	276.00 ± 20.59	310.00± 15.02*
N400	Amplitude (μV)	5.93 ± 3.60	4.51 ± 1.00
	Latency (ms)	460.67 ± 65.11	516.67 ± 57.53

Table 3.5.   SVM classification comparisons between the two age groups.

TP=True Positive; FP=False Positive.

	P300, Younger	*P300, Older*	*N400, Younger*	*N400, Older*
Accuracy	99.31%	98.61%	86.11%	86.11%
TP	0.99	0.97	0.88	0.85
FP	0.00	0.00	0.15	0.13
Sensitivity	0.99	0.97	0.88	0.85
Specificity	1.00	1.00	0.85	0.88

Table 3.6.   EBS values for group-level characteristics.

Mean ± SD. *p<0.05 between groups.

	Age 20-30	Age 50-85

N100	Amplitude	0.57±0.22	0.55±0.13
	Latency	0.47±0.29	0.34±0.20
P300	Amplitude	0.62 ± 0.14	0.56 ± 0.07
	Latency	0.69 ± 0.12	0.49± 0.09*
N400	Amplitude	0.55 ± 0.32	0.44 ± 0.13
	Latency	0.43 ± 0.16	0.30 ± 0.14
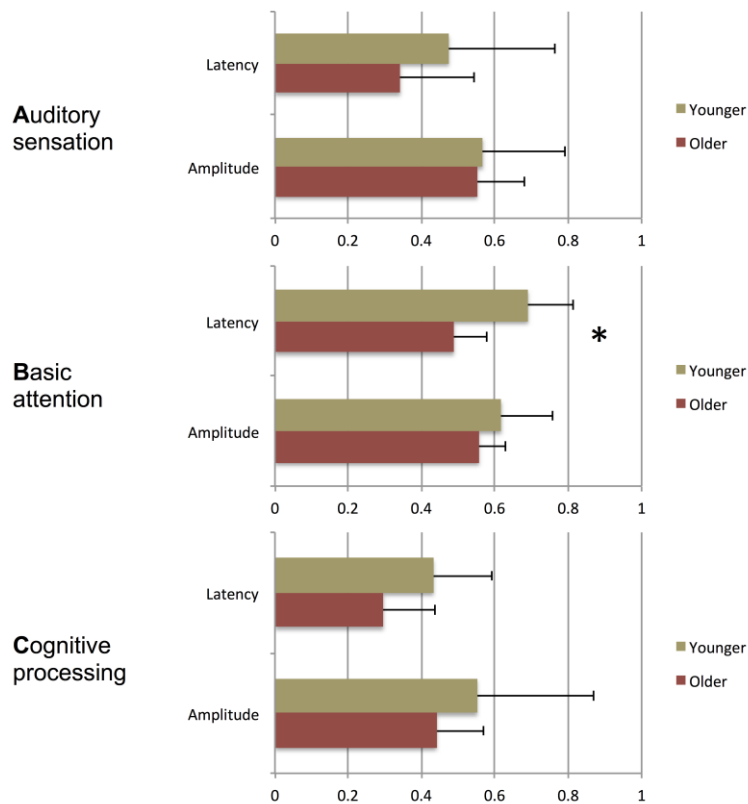
Figure 3.6.   EBS for Group-level Comparison.
Mean ± SD. * denotes p<0.05 across groups.

3.5. Discussion

The current study had two objectives: 1) to describe a conceptual framework for brain vital signs, which can provide an objective physiological evaluation of healthy baseline brain function; and 2) to conduct an initial practical evaluation in a test sample of healthy adults across the lifespan. The results demonstrated the successful detection of the three key ERPs at the individual level (Hypothesis 1), confirmed the expected

pattern of age-related ERP changes (Hypothesis 2), and enabled the translation of ERPs into the brain vital sign framework (Hypothesis 3). Importantly, this provided the initial step towards a brain vital sign approach that preserves and simplifies the essential valuable ERP results, but enables practical, accessible 'vital sign' attributes.

Robust individual level detection of ERPs like the N100, P300, and N400 has become possible through machine learning advances [65], [110]. Indeed, even within the current small initial validation sample, the ERPs were successfully detected for individuals across the life span (Figure 3.4 & Figure 3.5). SVM-based analysis allowed expert-independent validation with high accuracy, sensitivity, and specificity. SVM-based methods are generally considered extremely well suited for use in biomedical data due to their ability to deal with sparse learning scenarios [112]. Traditionally, SVM-based techniques for ERP are restricted to within-subject training and classification for brain machine interface applications [110]. By contrast, in the current application the SVM-based methods involved between-subject training and classification, further demonstrating potential for robust clinical applications. Moreover, permutation analysis based verification of performance provides further confidence regarding the robustness of these approaches.

As an initial validity check, predictable age-related changes in ERPs were examined and verified within the brain vital sign framework. To demonstrate the relative sensitivity differences between subjective behavioural tests and objective physiological measures, standard mental status assessments were compared to that of the ERP results. Results from MMSE and MoCA were both in the healthy range for the younger (age 20-30) and older (age 50-85) groups. While the ERP results generally matched this pattern, it was possible to show subtle age-related P300 latency delays (p=0.008) in older adults, consistent with previous studies [133]. A similar trend was observed for N400 latency delays (p=0.07). Thus, while both behavior and brain - based testing showed intact cognitive status, only the ERP evidence showed enhanced sensitivity to age-related changes in healthy brain function. Future work will further characterize standard factors in larger normative samples. These include characterization of aging related confounds, effects of education levels, impact of concurrent changes in other vital signs such as heart rate and blood pressure, and correlations between specific EBS components and traditional behavioural measures. Similarly, planned future work will also explore the opportunity to include both resting state as well as other stimulus-

related brain response measures (such as event related spectral perturbations) into the BVS framework.

To translate ERP results into the brain vital sign framework, we applied a linear transformation to reduce complexity and create a standard clinical schematic of ABC: A) N100=Auditory sensation; B) P300=Basic attention; and C) N400=Cognitive processing (Figure 3.1). Brain vital sign scores were then derived through comparison to the mean and standard deviation of the normative data. All participants showed an overall brain vital sign score of 30, derived from perfect 10-point ABC sub-scores (Figure 3.2). This component provided a normative evaluation for healthy brain function. As an initial development and to retain applicability over a wide range of potential dysfunction, all components were weighted equally in this framework. Future work may create variations/improvements that weigh the components differently for applications in specific disorders.

To transform ERP results into measurements of individual changes over time, the amplitude and latency measurements for all three responses were converted into 6 elemental brain scores (EBS: 3 responses × 2 measurements). Importantly, the EBS transformation involved a normative comparison against the best possible measurement, resulting in scores ranging from 0 to 1. During initial validation, EBS transformation preserved the pattern of age-related changes, with significant change in the 'B' component latency (p=0.004) and a similar trend in 'C' component latency (p=0.07).

The justification for a brain vital sign framework is strongly within the need for a practical and objective physiological measure of healthy brain function, combined with the capability for portable EEG/ERPs to meet the practical requirements and utilize well-established neural responses (i.e., studied extensively for 35-70 years). The challenge has related to translating/transforming ERPs to begin addressing the clinical requirements for vital signs.

Accordingly, the current study represents only an initial development effort, with a number of steps and caveats remaining: 1) the initial validation used a relatively small sample size, with further validation work currently being conducted; 2) the critical need for hardware platform independence remains to be systematically examined in order to understand differences between EEG acquisition systems; 3) the development of

standardized normative databases represents an on-going improvement and refinement; 4) the continuing development of analyses to characterize sensitivity, specificity, reliability, and other standard metrics are needed; and 5) more comprehensive evaluations anchored to standard vital sign developmental approaches must also be conducted. Nonetheless, the ability to move beyond the traditional and heavily expert-dependent ERP research setting to a more clinically-oriented brain vital sign framework allows for a systematic method of assessing healthy brain function. The current study provides an initial demonstration of the framework, but the small sample size necessitates that the results should be further validated in a larger sample. Furthermore, it should be noted that there are several approaches available for eliciting the ERP components. We have demonstrated one approach that we believe makes the oddball discrimination task easier in order to maximize applicability across age groups and brain functional status. Establishing a baseline measurement approach for healthy brain function is critical, particularly when questions of dysfunction arise due to conditions such as concussion and dementia. This study represents the initial steps towards such an approach.

3.6. Conclusion

Clinical evaluations of healthy brain functioning is moving from indirect subjective behavior-based tests, to objective, physiological measures of brain function, such as those derived from ERPs. We have previously demonstrated the essential role for clinical ERPs to evaluate functional status following serious injury and/or disease. The current study addressed an important gap: the need for a clinical-accessible brain vital sign framework that utilizes well-established ERPs. As an initial step, the framework was used to evaluate healthy brain function across the life span. The findings confirmed the ERPs at the individual level, verified predictable age-related differences, and demonstrated successful linear transformation to create the brain vital sign framework.

3.7. Supplementary Material

3.7.1. Device assessment and hardware selection

Several EEG systems (g.Tec g.Nautilus, Neuroelectrics Enobio, B-Alert X-10, Emotiv Epoc, InterXon Muse, g.Tec g.MobiLab, Mindo 4S) were identified as potential

candidates. They were qualified based on the following criterion: 1) ability to provide time-stamping signal to mark timing of stimulus presentation, 2) form factor (i.e. light-weight, portable), 3) number of sensors (>=5 but <=8), 4) type of sensor (gel-based preferred over saline or dry electrode), and 5) pricing (lower preferred). Based on the above criterion, the g.Nautilus and Enobio systems were chosen for further assessments as they met the criterion of having dedicated time-stamping capabilities, portability (165 and 68g respectively), 8-channels for measurements and operations with gel-electrodes at a relatively low cost per device.

Table 3.7.   Comparison of candidate EEG systems.

System	Qualified	Reason/Notes
g.Nautilus	Yes	Criterion met
Enobio	Yes	Criterion met
X-10	No	Pricing high
Epoc	No	Saline-based, not gel
Muse	No	Dry-electrode, not gel
g.MobiLab	Yes	Criterion met, but not used due to individual-lead setup
4S	No	Too few channels

No-input assessment of device

Data from the two candidate 8-channel EEG systems (g.Nautilus manufactured by g.Tec, Austria and Enobio manufactured by Neuroelectrics, Spain) were assessed within both electro-magnetically shielded environment, and in more realistic non-pristine environment. Specifically, this entailed collecting 30-seconds of ambient 'noise' data on both systems with the EEG and reference leads enabled for collection, first outside and then within the shielded room. The middle 10-second segment of the 30-second data collection is used for temporal and spectral domain analysis and comparison among the systems. As the 10-second noise signals could be considered quasi-static, a fast-Fourier transform (FFT) was applied to the data to assess the frequency content of the signal. Raw data were filtered using a notch filter at 60Hz (5Hz bandwidth) to remove the line noise followed by a 4th-order Butterworth filter with high-pass cut-off at 0.1Hz and low-pass cut-off at 20Hz in order to review the response within the usual ERP frequency ranges. Figure 2.7 and 2.8 highlight the data collected on the Enobio and g.Nautilus

systems in a non-shielded environment, whereas Figures 2.9 and 2.10 show the data collected on the same systems within the shielded room.

Key features of interest that become apparent (qualitatively) are: 1) for the data collected outside the shielded room, overall raw data quality appears less noisy for g.Nautilus compared to Enobio, 2) 60Hz peak prominent in g.Nautilus but buried within noise spectrum for Enobio, 3) the 60Hz peak becomes prominent within shielded room in Enobio data (possibly due to lack of overall background noise levels), and 4) g.Nautilus has lower noise floor both inside and outside shielded room.
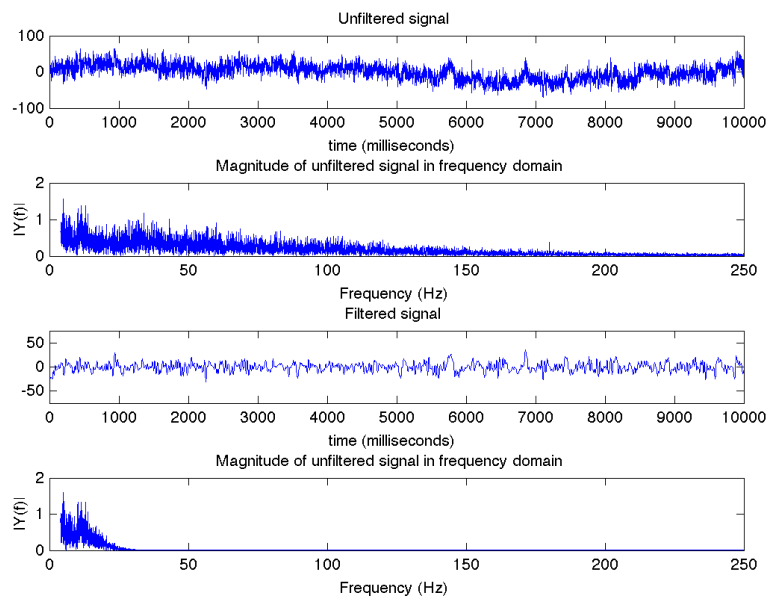
Figure 3.7.   Data from Enobio System (Non-shielded Room)
Top panel shows raw data in time domain, second panel shows the frequency content of raw data following FFT, third panel shows the time domain signal post-filtering, and the bottom panel shows the frequency content of the filtered data.
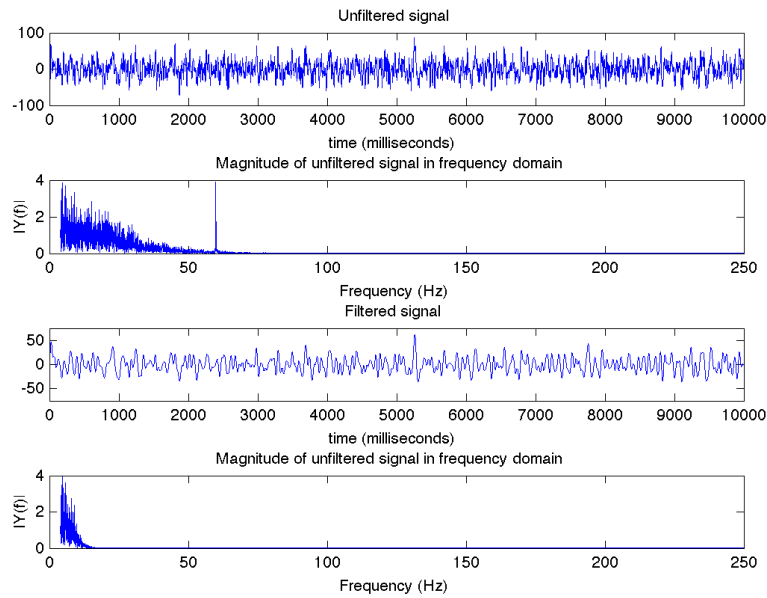
Figure 3.8.   Data from gNautilus System (Non-shielded Room)
Top panel shows raw data in time domain, second panel shows the frequency content of raw data following FFT, third panel shows the time domain signal post-filtering, and the bottom panel shows the frequency content of the filtered data.
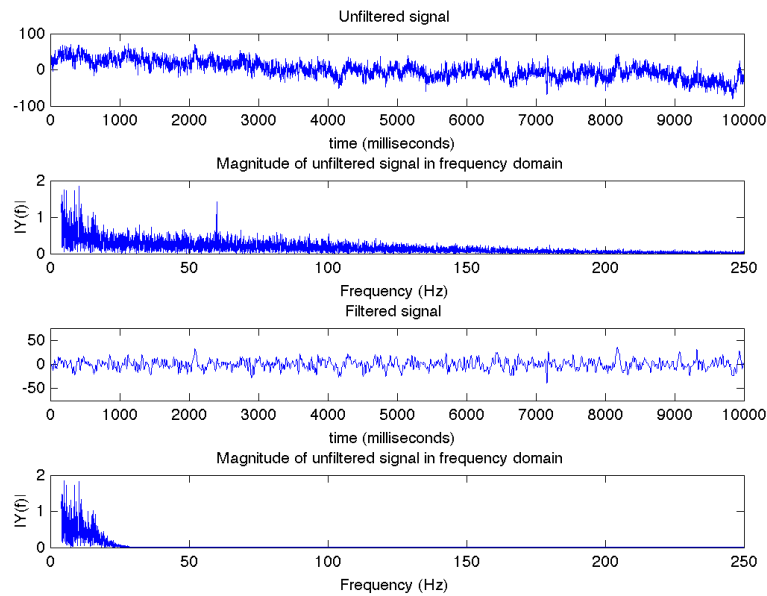
Figure 3.9.   Data from Enobio System (Shielded Room)
Top panel shows raw data in time domain, second panel shows the frequency content of raw data following FFT, third panel shows the time domain signal post-filtering, and the bottom panel shows the frequency content of the filtered data.
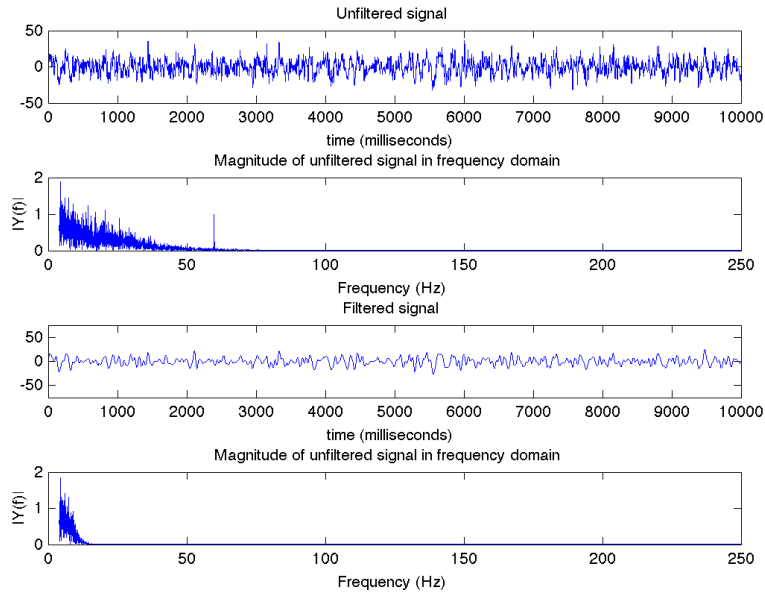
Figure 3.10.   Data from gNautilus System (Shielded Room)
Top panel shows raw data in time domain, second panel shows the frequency content of raw data following FFT, third panel shows the time domain signal post-filtering, and the bottom panel shows the frequency content of the filtered data.

Known-input assessment of device

Further to the assessments of the devices with ambient noise collections, in order to assess the response of the EEG devices under known input situations, additional analyses were undertaken. Specifically, this entailed creating a synthetic input signal, *s(t),* as shown in Equation 3 below. This synthetic signal was used as "ground truth" input and injected into two channels of the EEG systems as shown in Figure 2.11. Subsequently, the data collected by the EEG systems were analyzed using: 1) signal-to-noise ratio assessments, specifically by quantifying the spectral power in the 5,10,15 and 30Hz ('signal') and dividing by the spectral power at 60Hz ('noise') as shown in Equation 4, 2) inter-channel correlation by assessing the correlation of the signals collected at the two channels as shown in Equation 5, and 3) inter-session reliability by assessing the stability of the peak-to-peak voltage of signals collected over 3 days of collections as shown in Equation 6.

60
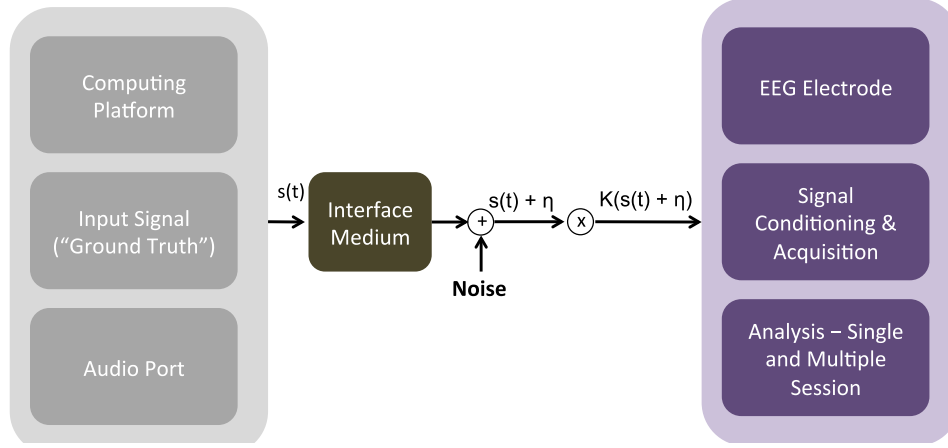
Figure 3.11.   Flowchart of Setup for Assessing EEG Devices with Known Input.
The known signal ('ground truth') is created using a combination of sinosoids and outputted from the audio port of a computing platform. The output from the audio port is fed into a conductive gel medium which also contains the electrodes from the EEG device where it is picked up, conditioned and recorded for further analysis. The 'ground truth' signal, s(t), combines with noise signal, n, and is attenuated by passage through the conductive medium by a factor, K, before being recorded by the EEG system.

$$s(t) = \sum_j A_j \, \sin(2\,\pi\,f_j\,t)$$ where, f_j = 5, 10, 15, 30 and 60Hz and A_j =1   --Eq. (3)

$$SNR = \frac{\sum F^2 \, (2*\pi*f)}{F^2 \, (2*\pi*60)}$$ where, f = 5, 10, 15, 30 and $F(\omega) = \int_{-\alpha}^{\alpha} f(t) e^{-i\omega t} \, dt$--Eq. (4)

$$Corr\,(X,Y) = \frac{N \sum XY - (\sum X)(\sum Y)}{\sqrt{[N\sum X^2 - (\sum X)^2][N\sum Y^2 - (\sum Y)^2]}}$$ where, N is number of samples   --Eq. (5)

$$\Delta V_{pp} = \frac{(V_{pp2} - V_{pp1}) + (V_{pp3} - V_{pp1}) + (V_{pp3} - V_{pp2})}{3}$$ where, V_{pp} is peak-to-peak voltage --Eq. (6)

As shown in Figure 2.12, the gNautilus system compared to the Enobio system provided significantly better SNR. Additionally, the g.Nautilus system also provided better stability of signals across test sessions (with a 1.45% change over 3 test sessions, calculated as $\Delta V_{pp}/V_{pp1}$ * 100). Consequently, the g.Nautilus system was chosen for development of the brain vital signs platform. More recent work by Raduntz et. al. has also again reiterated the superior performance of the g.Nautilus system compared to other available EEG platforms [134].
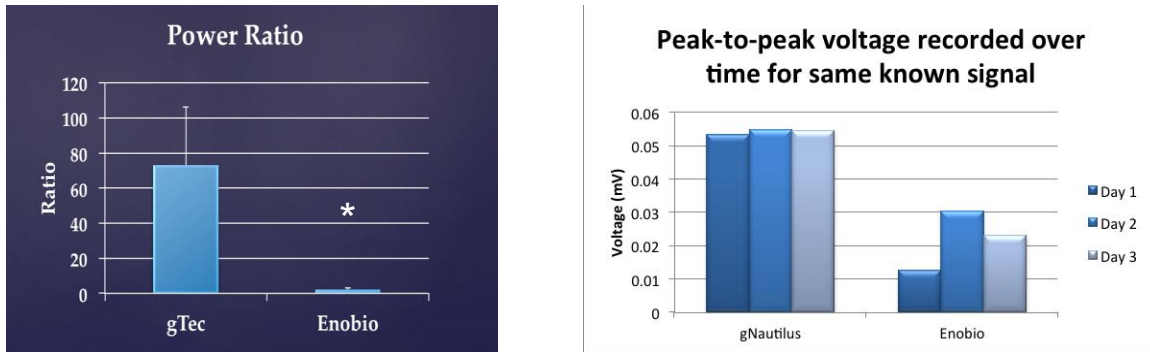
Figure 3.12.   Results of Known Input Signal EEG System Testing.
Results from assessments of g.Nautilus and Enobio systems are shown. ***Left:*** SNR was significantly higher for g.Nautilus relative to Enobio, *p<0.05. ***Right:*** The g.Nautilus system also had higher inter-session stability with change of 1.45%.

3.7.2. Synchronization timing assessment

The brain vital signs platform depends upon the successful elicitation and analysis of event related potentials (ERPs). As ERPs are a record of the brain's response to specific stimuli and occur within a few hundred milliseconds of the brain being presented with the stimuli, recording the precise timing of the presentation of stimuli is vital to the success of the ERP experiment. A crucial feature of any good ERP experimental apparatus is the ability to deliver stimuli and record the timing of that delivery within the recorded EEG data with high *precision* to enable proper analysis for extraction of ERPs.

There are a series of software and hardware components that make precise stimulus presentation possible: 1) the software-based stimulus presentation module first reads in the auditory stimulus file from disk; 2) the module then presents the stimulus to participants via earphones while also commanding the software-based time stamping module to initiate the trigger signal; 3) the trigger information passes through a hardware solution (e.g. USB or Parallel port) to the paired hardware solution on the EEG device (e.g. TTL input line or Parallel port); 4) the triggering signals are then acquired in hardware in conjunction with the EEG channel data; and 5) both EEG data and triggers are recorded by the software-based acquisition module. Thus, in order to ensure the ERP test apparatus is recording precise timing information, it is crucial to test the entire chain as latency delays may occur anywhere along the path. As shown in Figure 3.13, a test setup was created with the following specifics: 1) earphones were modified to enable connection to the EEG channels via conductive gel electrodes, 2) modified audio

62

signals were generated (frequency (50Hz and 100Hz) and voltage limited to be recordable by the EEG device) and delivered using in-house software developed with Python, 3) two version of custom USB-to-TTL subsystem were developed using hardware components from Future Technologies Devices International (part #s TTL-232RG-VSW3V3-WE and DLP-USB245M-G) and Amphenol ICC (part # L77HDA26SOL2) paired with in-house software (using D2XX driver and Java wrapper) to control the specific bit voltage levels, and 4) custom software was created to enable acquisition of data and control of the overall system within a portable computing platform.
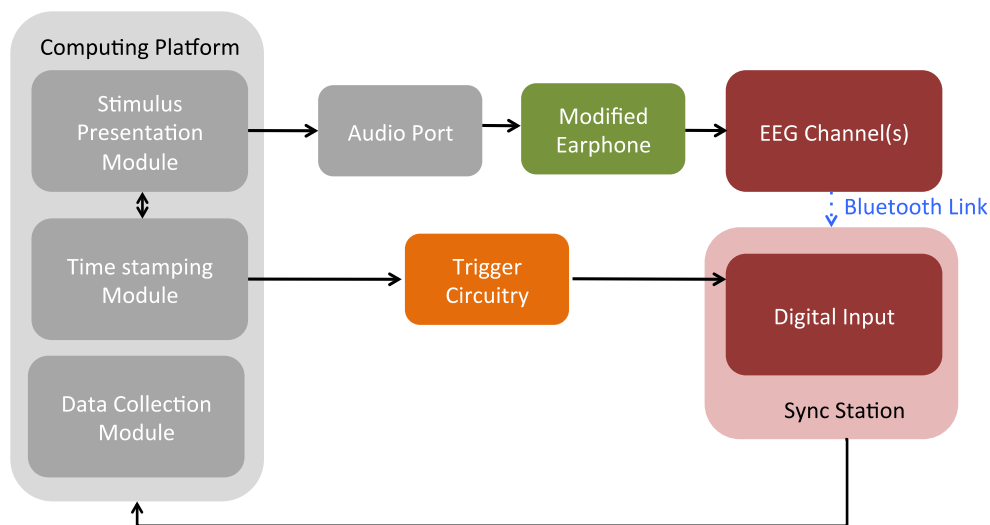
Figure 3.13.   Flowchart Depicting Assessment of Trigger/Timestamping Timing
Audio file with 50Hz and 100Hz bursts were presented by the stimulus module via the audio port and then passed through the modified earphones to interface with the EEG channel leads. Simultaneously, the computing platform also initiated a time-stamping signal that was passed through the trigger mechanism to create TTL pulses recorded by the digital input port of the synchronization (base) station of the g.Nautilus EEG system concurrently with the EEG channel data. The synchronized data stream consisting of the EEG channel and digital input data is read and stored in memory by the data collection module of the computing platform.

The time stamping sub-assembly was first tested in isolation, as shown in Figure 3.14, whereby the output from the sub-system was connected to LEDs to ensure that the desired bit control was achieved via the software and hardware combinations.
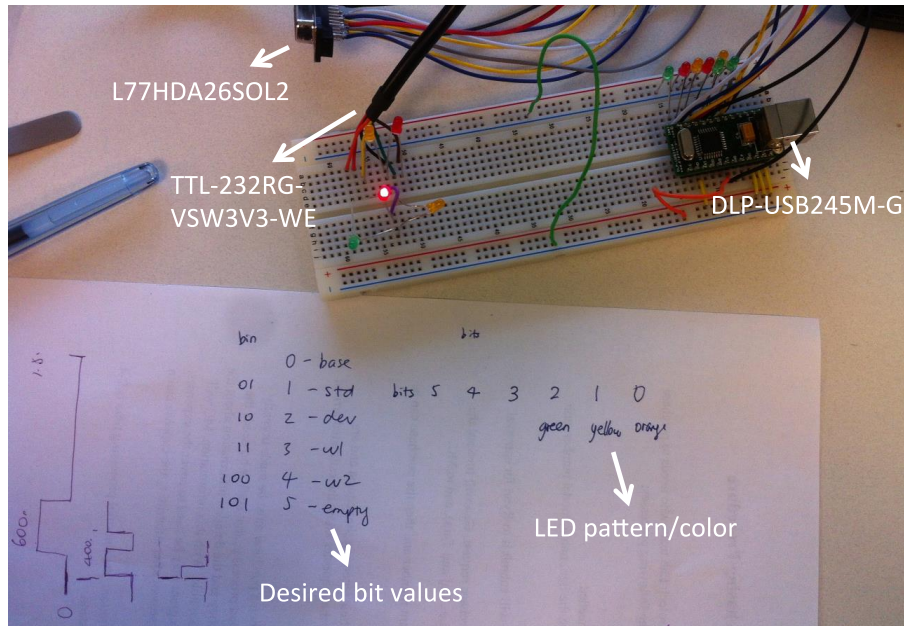
Figure 3.14.   Setup for Standalone Testing of Trigger (time-stamping) Assembly

Thereafter the trigger (time stamping) assembly was placed within the entire chain of systems (as shown in Figure 3.13), and stimuli (audio bursts) were recorded using the EEG channels and the corresponding time-stamping/trigger signal was recorded via the digital I/O port. Subsequent analysis compared the onset time of the audio burst and the trigger signal, as shown in Figure 3.14. Testing was conducted in two stages, first by using Simulink to record the EEG data and the output from the soundcard via the microphone input, and then by using Python along with the two trigger sub-assembly hardware setups (using TTL-232RG-VSW3V3-WE vs. DLP-USB245M-G). Two versions of the brain vital signs platforms were assessed – 1) as shown in Figure 3.16(B), g.Nautilus paired with Dell laptop and running a Simulink based acquisition software, and 2) as shown in Figure 3.16(C), g.Nautilus paired HP laptop running a C++ based acquisition software. Final timing results are shown in Figure 3.15. Table 3.8 and Table 3.9 show the results from the testing. Since precision, i.e., lower variance of the difference in onset times for the stimulus and trigger from instance to instance is crucial, the setup with the lowest mean difference and variance was chosen for brain vital signs platform development.
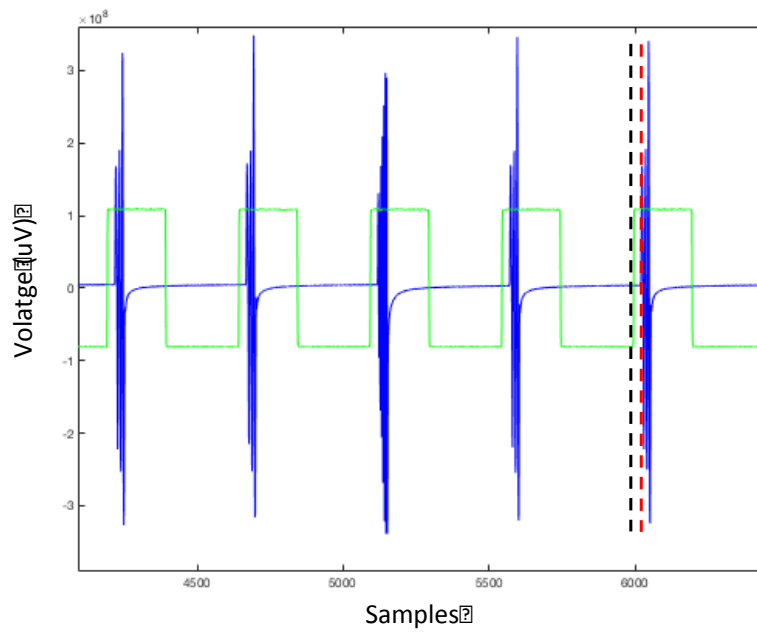
Figure 3.15.   Sample Data from Trigger Timing Test
Blue waveform corresponds to data recorded by the EEG channel, with bursts corresponding to audio stimulus presented by computing platform. Green square waves correspond to data recorded by the digital I/O port corresponding to trigger signals. Analysis compared the onset times of stimulus presentation (red dotted line) and trigger delivery (black dotted line).
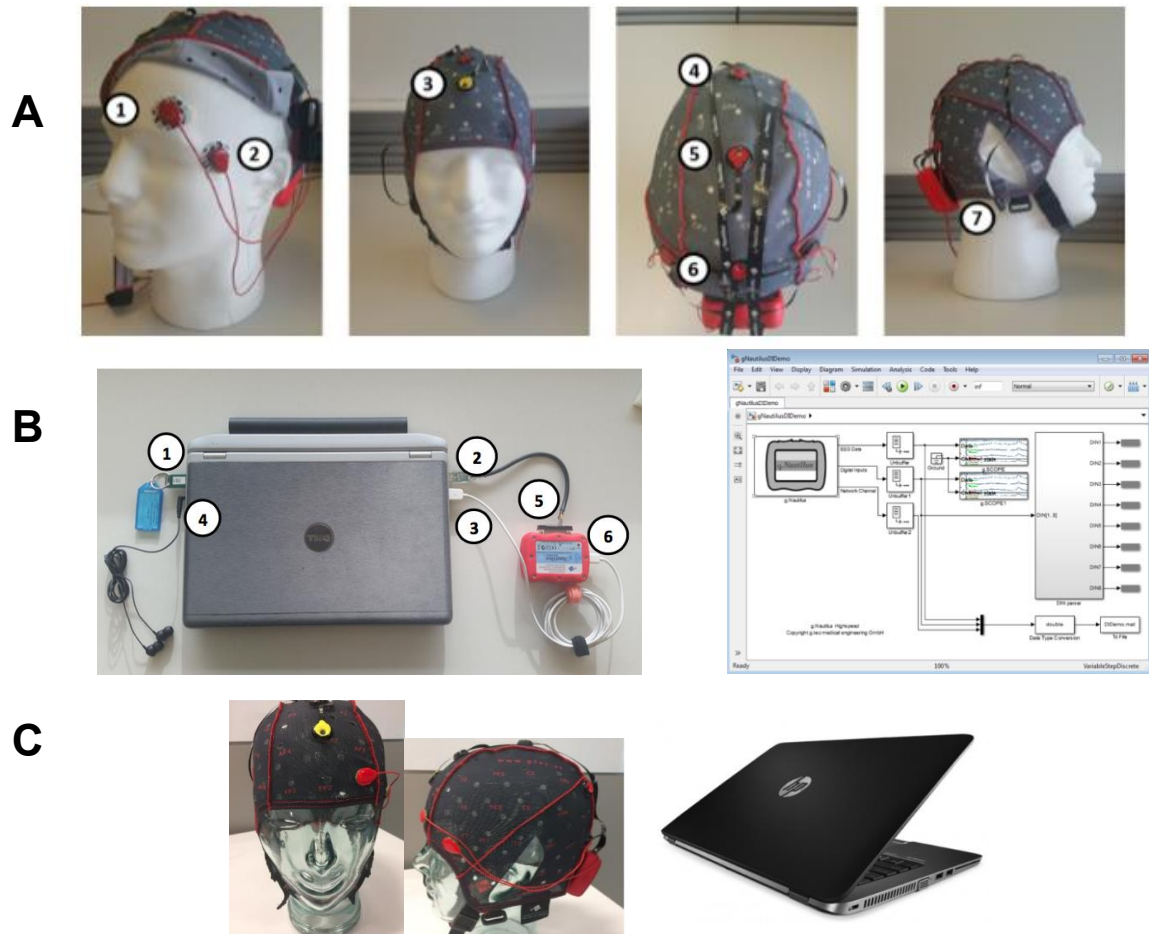
Figure 3.16.   Versions of Brain Vital Signs Platform
(A) The g.Nautilus EEG device is shown, with locations for vertical EOG (1), horizontal EOG (2), ground (3), Fz, Cz and Pz EEG collection sites (4-6), and reference electrode (7). **(B)** First version of the brain vital signs platform hardware pairing g.Nautilus with Dell laptop is shown with g.Tec's Simulink acquisition software license dongle (1), custom USB-to-TTL trigger system (2 & 5), connection to base station (3 and 6), and earphones for audio stimulation (7). **(C)** Second version of the brain vital signs platform is shown with two main differences from (B) being the change to improved HP laptop and the use of C++ based acquisition software API from g.Tec. Subsequent versions of brain vital signs have been created with the primary changes attributable to the stimulus sequence used.

Table 3.8.   Results from trigger timing test with version 1.

Setup	Timing value (mean ±std. dev.)
Simulink Acquisition & Soundcard output read through microphone input	400ms ± 100ms
Simulink Acquisition, Python Stimulation & DLP-USB245M	90ms ± 46ms
Simulink Acquisition, Python Stimulation & TTL-232RG	73ms ± 36ms

Table 3.9.   **Results from trigger timing test with version 2.**

Setup	Timing value (mean ±std. dev.)
Python & DLP-USB245M	64ms ± 9.6ms
Python & TTL-232RG	36ms ± 5.5ms *

3.7.3. Creation and refinement of stimulus sequence

Several auditory stimulus sequences were created and tested prior to finalization of the version ultimately chosen (described in section 2.3.2) for use within the brain vital sign platform. Towards the goal of creating the stimulus sequence, two key streams of work were undertaken – 1) the selection of specific stimuli (e.g. words to be used), and 2) the arrangement and timing of the stimulus sequence.

For stream 1, a large database of candidate semantically related word pairs (>700 pairs) were assembled using both publically available databases (e.g. University of South Florida Free Association Norm database) and prior semantic language literature [135]. A subset of word pairs were chosen (~120 pairs) based on minimum association frequency/Cloze score [136] of 0.7 and by balancing the word types (e.g. nouns vs. action), and this subset of words was subjected to Cloze probability testing locally to confirm association among word pairs (example shown in Figure 3.17). Subsequently, specific choice of word pairs included within the stimulus sequence were guided by the need to balance characteristics such as word length and frequency (as derived from MRC Linguistics database) among the groups of interest (e.g. semantic congruent and semantic incongruent) and for maintenance of literacy level at grade 10 standard to ensure maximum applicability of the technology.

Cloze Score	Priming Word	Response	1	2	3
0.80	Answer	Question	question	question	question
0.10	Cracker	Saltine	saltine	cheese	cheese
0.40	Scratch	Itch	sniff	card	itch
0.60	West	East	coast	east	east
0.90	Right	Left	lane	left	left

Figure 3.17. Sample Data from Cloze Probability Testing
Portion of tabulated results from Cloze testing showing the prime/cue word ('Priming Word') as well as the most common response ('Response'), responses to each prime from 3 sample participants, as well as the Cloze score which represents the proportion of responses that match the most common response.

For Stream2, some key exemplars of the previous versions of the stimulus sequence are shown and discussed below. The first version is shown in Figure 3.18, and involved a repeating pattern of three tones and two words (so-called 'set'), with more frequent standard tones (unfilled oval) and rare deviant tones (filled oval) to elicit N100 and P300 ERP responses and word pairs that were either semantically related (blue rectangle, e.g. 'butter') or unrelated (green rectangle, e.g. 'desk') to the prime word (orange rectangle, e.g. 'bread') to generate N400 ERP response. The grey rectangles relate to the word pairs for contextual information (e.g. 'city' – 'Surrey') and are discussed in detail in Chapter 5. Unfortunately, when tested on human participants, this version did not elicit any discernable P300 ERP component. Thus, a new version of the stimulus sequence was generated which included 5 tones per set to better set up the pattern of regular tones with the goal of making the deviance more obvious, and also with increased numbers of overall deviant tones (Figure 3.19). While this second version of the stimulus sequence successfully elicited the target ERPs of N100, P300 and N400 in test participants (Figure 3.20, Table 3.10), the duration of the stimulus sequence (and therefore the test) was relatively long (~10minutes).

Set 1   Set 120

000 🟧🟦 ● ● ● 000 ⬜⬜ 000 🟧🟩 000 ⬜⬜

0.75 0.5 1.5

◯ Standard/Deviant Tone   ▢ Auditory Word
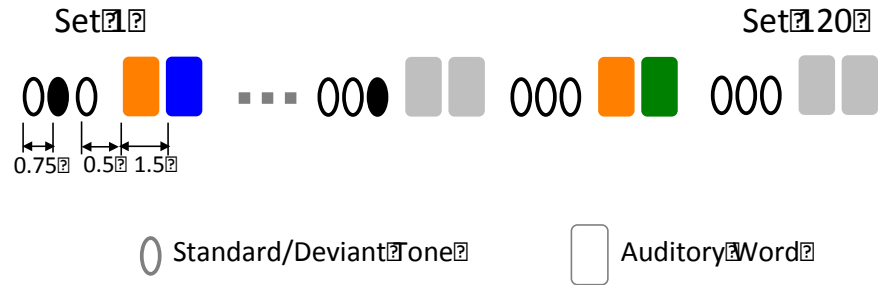
Figure 3.18.   Version 1 of Stimulus Sequence

Set 1   Set 120

00000 🟧🟦 ● ● ● 00000 ⬜⬜ 00000 🟧🟩 00000 ⬜⬜

0.4 0.4 1.5

◯ Standard/Deviant Tone   ▢ Auditory Word
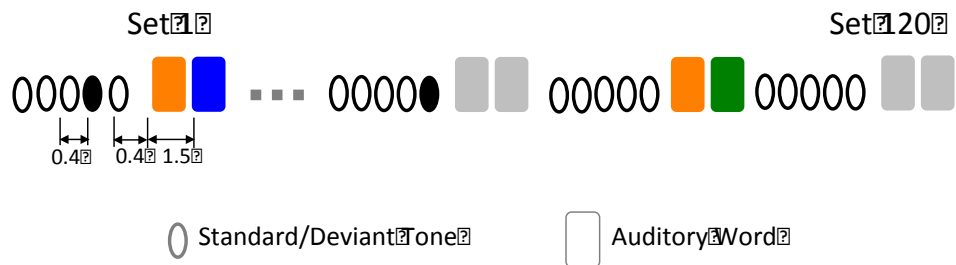
Figure 3.19.   Version 2 of Stimulus Sequence
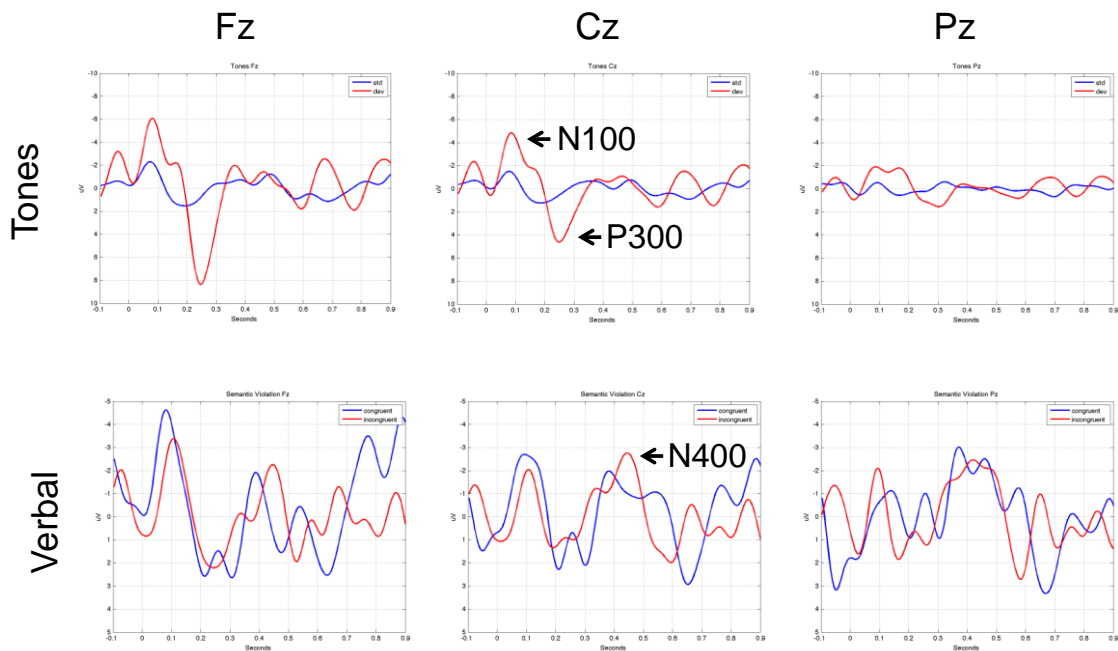
Figure 3.20.   ERP Waveforms Generated by Version 2 of Brain Vital Signs
Target ERPs corresponding to sensation (N100), attention (P300) and language processing
(N400) were successfully elicited by the stimulus sequence. Displayed are ERPs from frontal
(Fz), central (Cz) and posterior (Pz) electrode locations on the scalp.

69

Table 3.10   **Quantitative assessment of ERPs from Version 2**

p<0.05 paired conditions, Cz electrode

ERP	Condition	Amplitude
N100	Standard	-1.1 ± 0.34
	Deviant	-5.3 ± 1.5 *
P300	Standard	1.5 ± 0.36
	Deviant	9.2 ± 2.2 *
N400	Congruent	-1.2 ± 0.624
	Incongruent	-4.1 ± 2.1 *

Subsequently, version 3 of the stimulus sequence was created which was largely similar to version 2, but with two modifications: 1) the location of the deviant tone was constrained to tone 4 or 5 within a set, and 2) certain word pair slots were replaced with bursts of pink noise. The constraint of location for the deviant tone was introduced to ensure that in addition to the 'global' pattern of tones followed by words, sufficient 'local' pattern of standard tones was established to ensure better detection of the deviance and thereby create more robust P300 [66]. The pink noise bursts were introduced to provide an active baseline against which to measure the ERP markers, i.e., rather than measuring to background brain activity (captured in the pre-stimulus baseline), the goal was to enable calculation of the deflection generated by stimulus with respect to listening stimulus that did not contain information of interest.

Ultimately, the version used for brain vital signs platform showcased in this chapter was developed (Version 4) by retaining aspects from all three prior versions, but by multiplexing the role of the *prime* words in order to shorten the stimulus sequence (and therefore the test) to about 5 minutes. Details of the multiplexing innovation are provided in Chapter 5.

3.8. Author Contributions

This study was conducted in collaboration with co-authors who contributed to the data collection, analysis, and some study design.

Chapter 4.   Study II: Characterizing Brain Vital Signs Neural Markers

4.1. Abstract

Background: For nearly four decades, the N400 has been an important brainwave marker of semantic processing. It can be recorded non-invasively from the scalp using electrical and/or magnetic sensors, but largely within the restricted domain of research laboratories specialized to run specific N400 experiments. However, there is increasing evidence of significant clinical utility for the N400 in neurological evaluation, particularly at the individual level. To enable clinical applications, we recently reported a rapid evaluation framework known as "brain vital signs" that successfully incorporated the N400 response as one of the core components for cognitive function evaluation. The current study characterized the rapidly evoked N400 response to demonstrate that it shares consistent features with traditional N400 responses acquired in research laboratory settings – thereby enabling its translation into brain vital signs applications.

Methods: Data were collected from 17 healthy individuals using magnetoencephalography (MEG) and electroencephalography (EEG), with analysis of sensor-level effects as well as evaluation of brain sources. Individual-level N400 responses were classified using machine learning to determine the percentage of participants in whom the response was successfully detected.

Results: The N400 response was observed in both M/EEG modalities showing significant differences to incongruent versus congruent condition in the expected time range ($p < 0.05$). Also as expected, N400-related brain activity was observed in the temporal and inferior frontal cortical regions, with typical left-hemispheric asymmetry. Classification robustly confirmed the N400 effect at the individual level with high accuracy (89%), sensitivity (0.88) and specificity (0.90).

Conclusions: The brain vital sign N400 characteristics were highly consistent with features of the previously reported N400 responses acquired using traditional laboratory-based experiments. These results provide important evidence supporting clinical translation of the rapidly acquired N400 response as a potential tool for assessments of higher cognitive functions.

Keywords: N400, ERP, MEG, semantic language, clinical application

4.2. Background

Measurements of brainwave activity through event-related potentials (ERPs) are becoming increasingly useful in providing objective, physiology-based measures of brain function [48]. ERPs are derived from electroencephalography (EEG), and can provide information about cortical electrical activity corresponding to different aspects of neural processing [47], [137]. In particular, higher order cognitive functions like semantic processing indexed by the N400 ERP are among the most promising responses for emerging clinical applications [51], [71], [130], [138]. The N400 response was first described when Kutas and Hillyard presented participants with visual sentences that either had a semantically related (i.e. *congruent*) or semantically unrelated (i.e. *incongruent*) ending [63]. It was observed as a negative deflection of the incongruent relative to congruent condition waveforms which peaked at approximately 400ms latency following stimulus presentation, and the authors suggested that this differential was a neural marker of semantic language processing.

In the 38 years since its initial report, the N400 response has been studied extensively using a variety of stimulus paradigms in various healthy and clinical populations [139]–[144]. While the initial N400 work utilized sentence-based stimuli, subsequent studies showed that prime-target word pairs also successfully elicited this response [145], [146]. Additionally, non-language-based stimuli such as mental arithmetic and action sequences have also been shown to produce the N400 response [68], and the strength of this response has been found to be correlated with various stimulus properties [147]. Others have demonstrated overlapping features in the temporal and spatial characteristics of the N400 response when elicited using language- as well as non-language-based stimuli [68], with the spectral content in particular demonstrating potential in distinguishing between different neural processes [148]. In

fact, one of the key spectral features of the N400 response has been shown to be a reduction in beta band oscillations when processing incongruent relative to congruent stimuli in semantic language paradigms [149].

The cortical generators of the N400 response have been investigated using numerous noninvasive imaging modalities, such as functional magnetic resonance imaging (fMRI), electroencephalography (EEG), as well as magnetoencephalography (MEG). Results have revealed widespread cortical activations across the left temporal lobe, along with smaller areas of activity in the right temporal as well as bilateral inferior frontal and parietal regions [141], [150]–[152]. Specifically, areas of the bilateral temporal cortices (Brodmann Areas [BA] 20/21/22) and left inferior frontal gyrus (BA 45/47) have been shown to be key cortical regions within the distributed language network likely responsible for N400 [153], and these results are also supported by findings from lesion studies [154].

Further to its functional relevance as an indicator of neural processing in healthy individuals, the N400 response has also shown significant potential as a diagnostic and prognostic tool in clinical populations[58], [60], [68], [71], [73], [125], [131], [155]–[157]. Studies in brain-injured patients with disorders of consciousness showed that the N400 response was correlated with functional recovery [71]. Moreover, changes in N400 response also predicted cognitive decline in patients as they progressed from mild cognitive impairment (MCI) to dementia [51], [156]. Yet despite these promising findings, the use of the N400 ERP beyond the research setting has been hindered by two main challenges: First, given that ERPs are produced by averaging the neural response signals across a large number of trials, traditional N400 studies require prolonged testing paradigms [48], [65]. These paradigms are particularly problematic in clinical populations due to fluctuations in vigilance levels and lack of capability or motivation[155], [158]. In addition, rather than measuring only a single brain response in clinical populations (e.g. sensation, attention, or language), there are now calls for concurrent evaluations of a *spectrum* of brain responses which provide a more complete profile of brain function [65]. This is particularly crucial in longitudinal monitoring of brain function changes in clinical populations [76]. Under these circumstances, the traditional ERP testing paradigms may require hours to evaluate, which is impractical within most clinical settings.

To assess the N400 response within a short testing time while providing information about other brain function indicators, our group has been undertaking systematic development of rapid evaluation techniques in recent years. We previously demonstrated the successful evaluation of the N400 response in 100 healthy individuals using a point-of-care enabled device [65], then employed this device to track the progress of rehabilitation therapy in a brain-injured patient [130]. More recently, we demonstrated a rapid evaluation platform known as the brain vital sign framework [159], which enables the rapid assessment of several brain function indicators including the N400 (semantic language), N100 (sensory processing) [61] and P300 (attention orienting) [62]. The brain vital sign framework employs a portable, low-density EEG system, with automated, user-friendly software for easy clinical applications. The testing paradigm utilizes a short, 5-minute auditory stimulus sequence in which tone and word stimuli are interlaced to maximize the number of trials and signal-to-noise ratio. Results in healthy adults showed that, not only were the target responses successfully elicited at the individual level, but the platform also captured expected age-related changes in attention and cognition that were undetected using conventional clinical screening measures [159].

Although the rapid evaluation brain vital sign framework showed initial promise as a potential avenue for clinical application of the N400 ERP, the component characteristics of this rapidly elicited N400 (rN400) response have not yet been described. Given the short, complex stimulus paradigm, it is crucial to characterize this response with respect to its spatiotemporal, spectral, and neuroanatomical features, and compare them with known N400 characteristics reported in studies using more conventional approaches over the last few decades.

The current study utilized MEG with simultaneous EEG to investigate the temporal, spatial, spectral, and neuroanatomical characteristics of the rN400 response elicited within the brain vital sign framework. We hypothesized that the rN400 response will exhibit features consistent with known characteristics of the N400 response, including: 1) increased ERP negativity and MEG signal power for the incongruent relative to congruent condition during the 300-500ms post-stimulus interval; 2) decreased beta- band power for the incongruent relative to congruent condition during the same interval; and 3) increased activation of temporal and frontal cortices (BA 20, 21, 22, 45 and 47) for processing of incongruent relative to congruent stimuli.

74

4.3. Methods

4.3.1. Participant Details

Seventeen (17) right-handed healthy participants with no history of neurological problems or psychoactive medication were recruited (22.6 ± 2.4 years, 10 males). Participants were undergraduate or graduate students, had normal hearing, normal or corrected-to-normal vision, and were fluent in English. The study was approved by ethics boards at Fraser Health Authority and Simon Fraser University, and all participants provided written informed consent.

4.3.2. Auditory Stimuli

As introduced elsewhere [159], the rapid assessment framework utilizes a compressed auditory stimulus sequence with interlaced tones and words to elicit brain responses across four different functional domains – auditory sensation (N100 ERP), attention (P300 ERP), and semantic language (N400 ERP) - in approximately 5 minutes (Figure 4.1). The sequence comprised 60 blocks, with each block containing five tones and two words representing a prime-target pair. Semantic language processing responses were derived by conditionally averaging the trials corresponding to the target word in the pair. Semantically linked words (*congruent* condition, 50%, e.g. doctor-nurse) were contrasted with words not semantically linked (*incongruent* condition, 50%, e.g. doctor-egg) to generate the differential processing measures. Words in both groups were balanced for characteristics such as word frequency and length, and the words in the semantically linked group had a minimum Cloze probability of 0.8 [136]. The stimuli were recorded in a male voice and root-mean-square normalized using Audacity software. The stimulus sequence contained 30 trials each of the congruent and incongruent conditions.
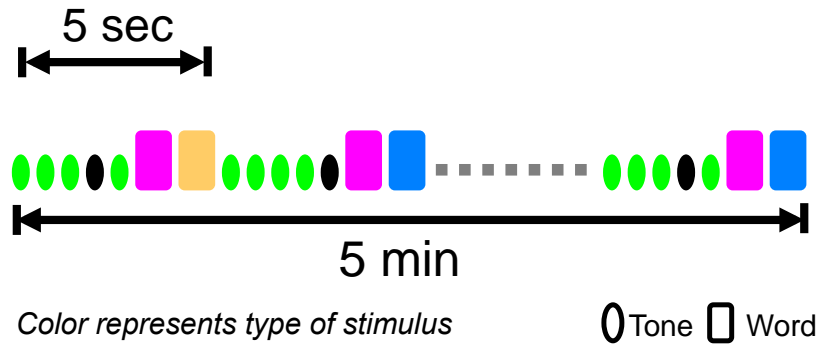
Figure 4.1.   Illustration of auditory stimulus sequence of the brain vital sign framework.

Blocks of five tones and two words repeated 60 times for a total scan time of about 5 minutes. Words represent prime-target pairs, containing both semantic congruent (pink-orange) and incongruent (pink-blue) pairs. Tones (standard=green and deviant=black) elicit sensory (N100) and attention (P300) measures.

4.3.3. MEG and EEG data acquisition

A 151-channel CTF MEG (MEG International Services Limited, Canada) was used with concurrent 3-channel EEG, both recorded in a magnetically shielded room with the participants in the supine position. Data were sampled at 1200Hz using axial gradiometers (5-cm baseline) with synthetic 3rd order gradients employed for noise cancellation. Continuous head position monitoring was undertaken by three head position indicator coils located at fiducial points (HPI, positioned at nasion, left and right pre-auricular points). In line with previous bran vital signs work, EEG recordings utilized Ag/AgCl scalp electrodes placed at Fz, Cz and Pz locations, with impedances kept below 5kOhms. Four additional electrodes were placed on the head corresponding to reference (left mastoid), ground (forehead), horizontal (outer canthus of left eye) and vertical (supra-oribtal ridge of left eye) electro-occulogram (EOG). To facilitate the alignment of MEG scanner and head coordinate systems, the shape of the participants' head and the 3-dimensional position of HPI coils and EEG/EOG electrodes were recorded using a Polhemus electromagnetic digitization system prior to data collection (Polhemus Incorporated, USA). Auditory stimulation was presented binaurally using insert earphones, and participants were instructed to maintain visual fixation on a crosshair displayed on the overhead screen (white cross on black background) throughout the session.

4.3.4. Data Preprocessing

Raw data for both MEG and EEG were first visually inspected, and artifactual channels removed from further analysis. Data were then down-sampled to 300Hz, notch filtered to remove frequencies corresponding to power line (60Hz) with its harmonics as well as HPI coils, and low-pass filtered to 100Hz. Data were visually inspected, and data from 2 of the 17 participants were excluded from subsequent analysis due to excessive noise.

4.3.5. MEG Analysis

Following band-pass filtering (0.5-45Hz), independent component analysis (ICA) was performed with the *runica* algorithm in EEGLAB [160] in order to remove artifact from ocular, cardiac, and muscular sources.

Temporal Effects

Since head position within the MEG helmet can vary across participants, global field power (GFP) was utilized to provide a measure of the overall activity across all channels [161]. Individual-level GFP was computed for the congruent and incongruent conditions using trial-averaged event-related fields. A bootstrapping approach was utilized to determine time intervals of significant difference between conditions, in which the GFP signals at each time point were permuted between the congruent and incongruent conditions across all subjects [109]. Using this approach, the interval of significance was identified to be 300-500ms and used as the window of interest in subsequent analyses, consistent with prior literature [162], [163]. The mean GFP value in this time interval was then calculated for each condition (congruent and incongruent) and participant, and compared using paired t-test at the group level.

Spectral Effects

Sensor level time-frequency analysis was undertaken by convolution of the data with Morlet wavelets (6 cycles) using the continuous wavelet transform function in MATLAB (The Mathworks Inc., USA). The coefficients corresponding to 0.5-45Hz frequency in the -200ms to 900ms time window relative to stimulus onset were extracted, and log power was computed as the square of the absolute value of the coefficients. To better understand the event-related spectral changes, the mean log

power in the baseline period (-100 to 0ms) was subtracted from the log power in the post-stimulus period for every trial within the frequency band. Significance was assessed using a bootstrapping approach by permuting the trial-averaged wavelet power in the congruent and incongruent conditions across participants in each frequency [109]. This entailed the calculation of T-statistic for each time point and frequency between the congruent and incongruent conditions in the 800ms following stimulus presentation. Thereafter, 1000 permutations were undertaken and new T-statistic calculated for every permutation leading to a null distribution against which the significance of the true T-statistic was assessed (with $p<0.05$ considered to be significant).

Neuroanatomical Effects

Source level analysis was performed using SPM8 (Wellcome Trust Centre for Neuroimaging, UK) with the forward and inverse modeling steps elaborated in previously published work [164]. Source analysis for localizing neural generators of the semantic language process was undertaken using minimum norm estimates (MNE) to maintain consistency with prior N400 studies in MEG [153], [162]. Group constraints were employed during inversion [165], and source reconstruction was based on trial-averaged data within the entire frequency range (0.5-45Hz) and active epoch (0 to 900ms relative to stimulus presentation). Source-level contrast images were derived using data in the 0.5-45Hz frequency range and previously identified window of 300-500ms. Statistical modeling employed a general linear model (GLM) with T-contrasts [166].

4.3.6. EEG Analysis

To facilitate future translation into point-of-care enabled platforms, concurrently collected EEG data were also analyzed to extract ERPs. Contamination from ocular sources was removed from the EEG signal using an adaptive filtering approach [103]. For this process, the recorded EOG signals were used as reference inputs and processed using finite impulse response filters (m=3), followed by recursive least squares-based removal from the EEG signal (λ=0.9999). Subsequent to artifact removal, standard analysis steps including filtering (1-10Hz), segmentation (-200 to 900ms) and conditional averaging were undertaken to generate ERPs [47], [48]. The mean value of the ERP waveform at the Cz electrode site in the 300-500ms time interval was

calculated for each condition and participant, and compared using paired t-test at the group level.

Individual-Level Analysis

To evaluate reliability of the rN400 ERP at the individual level, a machine learning-based approach was undertaken using a two-category support vector machine (SVM) classifier following previously published methods [110], [159]. Briefly, an SVM classifier with a radial kernel was trained to distinguish between the congruent and incongruent condition waveforms using single-run, trial-averaged data from all three electrode sites. During each session, 90% of the available data were randomly selected to train the classifier, while the remaining 10% were used for testing classification accuracy. This procedure was repeated 10 times under 10-fold cross-validation, such that the classifier was trained and tested on all available data. Results were averaged across all sessions, and measures were derived from the confusion matrix corresponding to accuracy, sensitivity, and specificity. To further assess the reliability of the analysis, results were verified using non-parametric permutation statistics [65], [132]. In short, this involved randomly redistributing the congruent and incongruent class labels among all datasets and performing the same classification procedures. This process was repeated 1000 times, and the resulting accuracies were used to create a null distribution against which the true classification accuracy was compared. Probabilities less than 0.05 were deemed to be significant for SVM classification outcome.

4.4. Results

4.4.1. Temporal and Spectral Effects in MEG

Sensor-level GFP demonstrated differential processing of the target word depending upon whether they were semantically related (*congruent* condition) or semantically unrelated (*incongruent* condition) to the first word. In particular, in the 300-500ms post-stimulus interval, there was increased power for the incongruent relative to congruent condition (p<0.05, Figure 4.2A,B). In addition, the processing of incongruent words resulted in a significant reduction in beta band power relative to the processing of congruent words (p<0.05, Figure 4.2C). This decrease was observed in the 335-440ms

time interval, overlapping in time with the N400 response. Although there appeared to be some differences also present in other frequency bands, none of them were statistically significant.
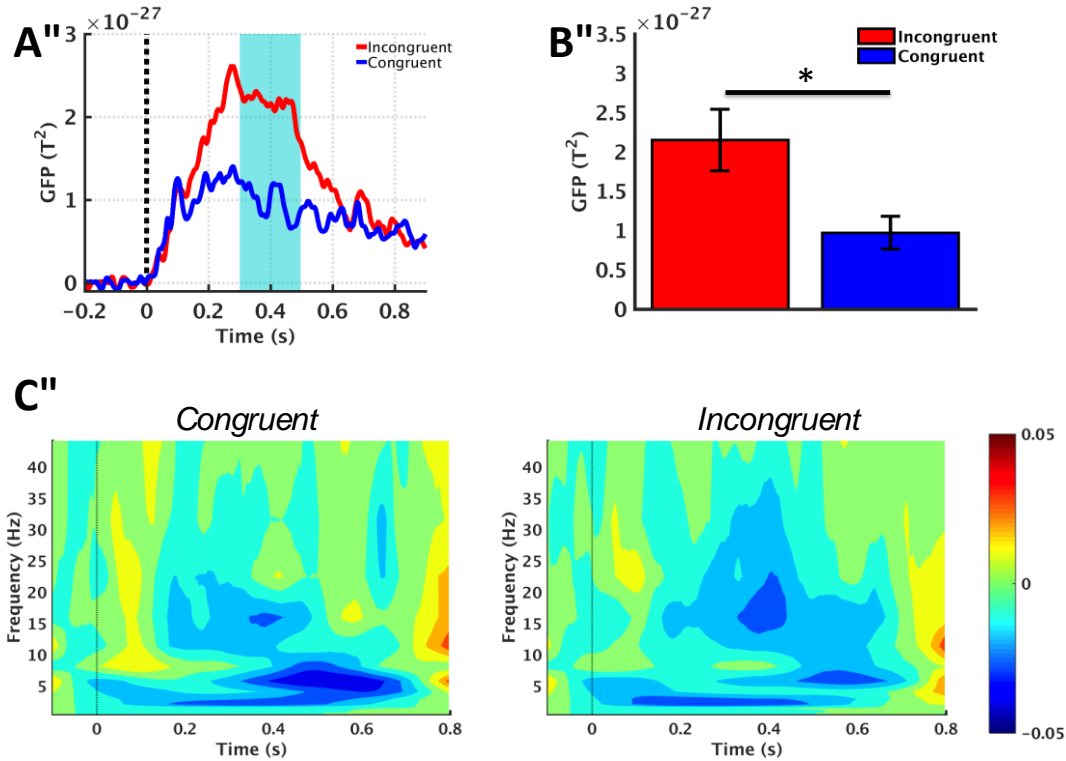
Figure 4.2.   Sensor-level MEG results showing differential processing in incongruent compared to congruent condition.
A) Grand-averaged GFP demonstrating increased power for incongruent relative to congruent condition. Shaded region denotes window of interest (300-500ms). B) Mean GFP averaged across the time window specified in part A, calculated for each subject and presented as mean ± SEM across subjects. *p<0.05.* C) Time-frequency wavelet spectral power averaged over all MEG channels. Colour bar represents log power values.

4.4.2. Temporal Effects in EEG

ERP waveforms exhibited greater negativity in the incongruent relative to congruent condition occurring within the 300-500ms interval, which was maximal at the Pz electrode (p<0.05, Figure 4.3A-C). The trained SVM classifier successfully distinguished between the congruent and incongruent conditions using denoised, trial-averaged, individual-level ERP waveforms with 88.89% accuracy, 88% sensitivity, and 90% specificity. All classification results were verified to be statistically significant through permutation analysis (p<0.05).
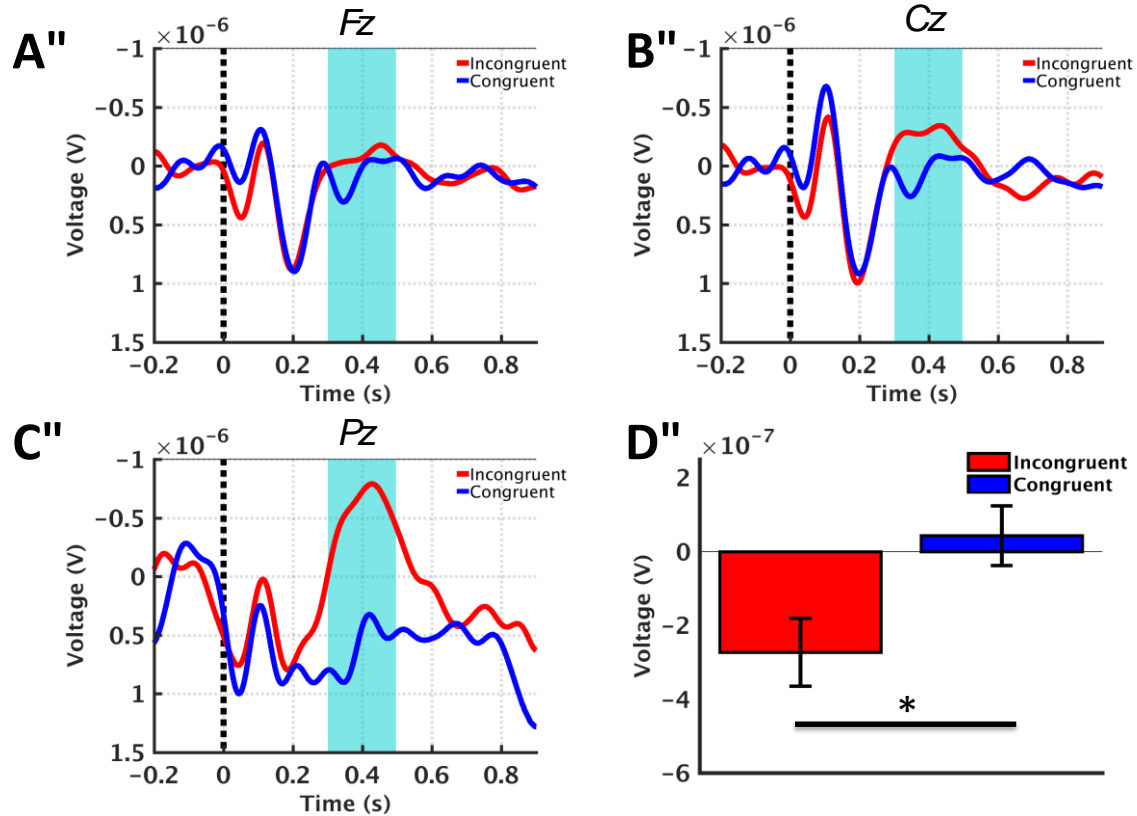
Figure 4.3. **ERP results demonstrating differential processing of semantic congruence and incongruence.**
A-C) Grand-averaged ERP waveforms at the Fz, Cz, and Pz electrode sites, respectively. Shaded regions denote windows of interest (300-500ms). D) Mean ERP amplitudes averaged over the windows of interest, calculated for each subject and presented as Mean ± SEM across subjects. *p<0.05.

4.4.3. Neuroanatomical Effects in MEG

Differential processing of incongruent words was source-localized to the inferior frontal, inferior parietal, and temporal regions (incongruent > congruent contrast, p<0.005, k=20). Key areas included left inferior, middle and superior temporal gyri (BA 20, 21 and 22) and regions encompassing both the anterior and posterior portions of the left inferior frontal gyrus (BA 45, 47). Additionally, areas of the right temporal and inferior frontal gyri were also activated. In comparison, no suprathreshold clusters were observed for the reverse contrast of congruent>incongruent (Figure 4.4 bottom panel).
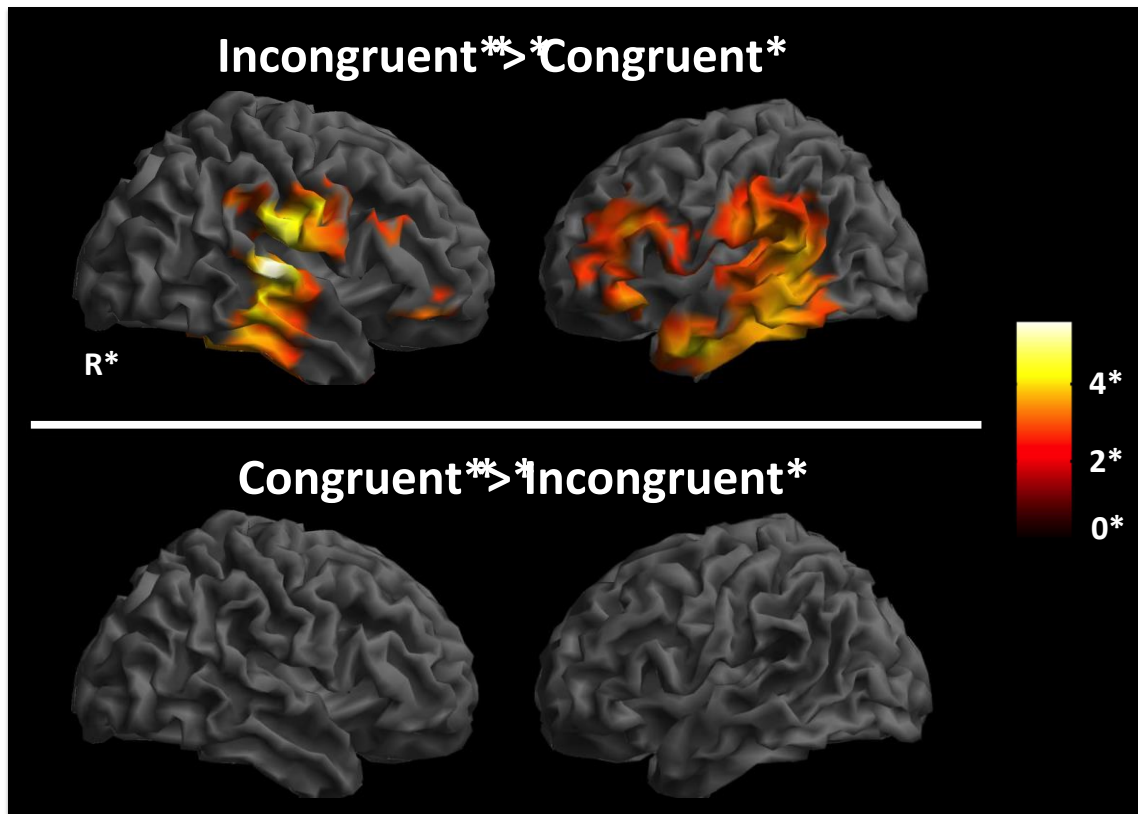
Figure 4.4.   Source localization results.
Top: Incongruent word processing activates a left-lateralized distributed region of cortex including temporal, inferior frontal and inferior parietal areas (incongruent > congruent contrast, *p<0.005unc.*). Bottom: No suprathreshold clusters were identified for the reverse contrast (congruent > incongruent). Color bar represents T-statistic values.

4.5. Discussion

4.5.1. Main Findings

This study employed MEG with concurrent EEG to investigate the temporal, spectral, and neuroanatomical characteristics of the rapidly elicited N400 response (rN400) generated through the brain vital sign framework. Using a compressed auditory stimulus sequence comprising both tones and prime-target word pairs, we demonstrated that the resulting rN400 response exhibited features consistent with characteristics previously reported for the N400 response in semantic language paradigms [68], [147]. In particular, we found that: 1) the sensor-level temporal characteristics showed rN400 ERP in the incongruent relative to congruent condition, peaking approximately 300-

500ms after stimulus presentation and with concomitant changes in GFP (Hypothesis 1); 2) a significant decrease in beta-band spectral power was observed during the same interval in the incongruent relative to congruent condition (Hypothesis 2); and 3) source localization analysis showed that rN400 processes activated cortical regions spanning the temporal, inferior frontal, and parietal regions known to be associated with the N400 response (Hypothesis 3). These main findings are summarized in Table 4.1.

Table 4.1.   Comparison of traditional and rapid N400 features.

Comparison of the features of interest between the N400 response elicited using traditional approaches and the rN400 response elicited under the rapid assessment brain vital sign framework. Effects are based on comparison of the incongruent condition with the congruent condition data. EEG-based features include peak amplitude (V), peak latency (ms), and scalp topography. MEG-based features include amplitude difference during the 300-500ms window (Δ300-500ms), spectral effects, and cortical activations. Cong. = congruent condition; incong. = incongruent condition; IFG = inferior frontal gyrus; TL = temporal lobe (superior, middle and inferior temporal gyri); IPL = inferior parietal lobule. Only statistically significant features are shown. a Kutas et. al. 2011. b Lau et. al. 2008. c Halgreen et. al. 2002. d Maess et. al. 2006. e Wang et. al. 2012. f Helenius et. al. 2002.

Modality	Feature of Interest	Traditional Approach N400	Rapid Framework (rN400)
EEG	Peak amplitude (cong. vs. incong)	ERP: $|V_{incong}| > |V_{cong}|$ [a]	ERP: $|V_{incong}| > |V_{cong}|$
	Peak latency (ms)	$\sim$400ms[a]	420ms
	Scalp topography	Centro-parietal maxima [b]	Max at parietal (Pz)
MEG	Amplitude difference (cong. vs. incong)	$\Delta_{300\text{-}500ms}$ [c,d]	$\Delta_{300\text{-}500ms}$
	Spectral effects	$\Downarrow$ beta-band power [e]	$\Downarrow$ beta-band power
	Cortical activation	$\Uparrow$ IFG, TL, IPL [c,d,f]	$\Uparrow$ IFG, TL, IPL

4.5.2. Hypothesis 1: Temporal Effects

The sensor-level temporal effects showed a robust rN400 ERP for processing the incongruent relative to the congruent words (Figure 4.3), consistent with previous findings based on sentences and semantic prime-target word pairs within auditory and visual modalities [68]. The response in the present study was observed to be maximal at the parietal (Pz) electrode location, also consistent with prior works suggesting a centro-parietal scalp distribution for the N400 ERP [139]. Importantly, these findings were also supported by our concurrent results using MEG which measures the magnetic counterpart of the rN400 ERP. Results showed that sensor-level GFP exhibited increased activity in the incongruent relative to congruent condition, peaking at similar

latencies relative to rN400 ERP (Figure 4.2A, B). It is important to note that polarity differences between the two modalities may be accounted for given that GFP is a power measure and is thus always non-negative, whereas ERP can be either positive or negative.

While the present study targeted the semantic processing effect indexed by the N400 and accordingly focused on the 300-500ms window of interest to be concordant with previous literature [147], [162], other temporal differences between the two conditions were also present at earlier latencies within the ERP/ERF traces. These effects may be related to processes in support of semantic language comprehension such as phonological matching [167], letter-string processing [163] or detection of mismatch based on predicted input [168]. These earlier effects may be further explored in future studies.

4.5.3. Hypothesis 2: Spectral Effects

Time-frequency results demonstrated a significant decrease in beta band power in the incongruent condition relative to the congruent (Figure 4.2C). These spectral changes occurred over the same time interval as the rN400 response, and provide further confirmatory evidence of the processing differences between the two conditions. A previous MEG study reported similar beta-band power reductions, and source-localized this effect to the left inferior frontal gyrus and temporal regions, with the authors postulating that the observed N400 effects may have represented a dynamic communication link between these regions [149]. Additionally, beta band power suppression has also previously been associated with increased level of cortical processing across a diverse range of experimental paradigms, such as motor movement [169], working memory [170] and information retrieval [171]. In light of these findings, the reduction in beta band power observed in the current study may be interpreted as a potential reflection of increased processing for the incongruent relative to congruent conditions within the relevant brain regions. It should also be noted that, although reduced power is visually observed for the theta frequency band in the current study, this effect was not statistically significant.

4.5.4. Hypothesis 3: Neuroanatomical Effects

Our results showed left-lateralized activations in the temporal cortices (BA 20, 21, 22) as well as inferior frontal gyri (BA 44, 45) (Figure 4.4 upper panel). This is in agreement with prior works using fMRI and EEG, confirming the left temporal lobe as the largest source of the N400 effect, with a smaller contribution from the right temporal areas [150]. In addition, other EEG based works have identified contributions from the left perisylvian cortex [141], and bilateral inferior frontal gyri [151]. MEG based source localization has largely confirmed these findings, and suggested contributions from cortical areas including the left superior and middle temporal gyri as well as the inferior parietal and frontal areas [152], [162]. The converging neuroimaging results and theoretical models [139], [172], [173] have led to increasing consensus that semantic language processing is supported by a left lateralized network of brain regions [139], [153], [162]. Our results are consistent with these previous findings, as more left-lateralized activations were observed in both the temporal and inferior frontal regions. In addition to the left hemisphere activity, the right hemisphere activations observed in the current study were also in line with other studies using auditory stimuli [174].

The lack of suprathreshold clusters in the congruent > incongruent contrast (Figure 3.4 lower panel) is also consistent with previous literature. MEG studies of N400 have shown largely overlapping areas of activation in both congruent and incongruent conditions, with greater extent of activations in the incongruent condition due to increased demands associated with incongruent stimulus [153]. Similarly, fMRI results showed increased hemodynamic activity for the incongruent condition compared to congruent [150]. Together, these hemodynamic and electromagnetic results support our findings regarding lack of suprathreshold clusters in the congruent > incongruent contrast.

4.5.5. Clinical Implications

Beyond the extensive laboratory based evaluations of N400, clinical applications are increasingly utilizing the N400 response in a variety of patient populations. The N400 is being particularly studied in disorders of consciousness (DOC) as a potential marker of residual functional integrity as well as for tracking rehabilitation progress. Beukema and colleagues reported the importance of including N400 in assessments of DOC

patients [138], while Steppacher et. al. demonstrated the N400 as a crucial tool for assessing information processing abilities that are predictive of eventual recovery in DOC patients [71]. Similarly, the N400 response has also been utilized to track rehabilitation progress in traumatic brain injury [130] and for assessments of stroke patients [58]. Moreover, the N400 response has been found to be abnormal in Alzheimer's disease [175], and was identified as a promising marker in differentially identifying MCI patients who may transition to dementia [51]. These demonstrations in clinical populations, combined with the excellent reliability and stability of N400 effects [176] provide an impetus for clinical integration of this promising response. The present study makes N400 assessments clinically accessible by balancing the need for rapid assessments in clinical settings with the inherent desire for high quality data while retaining the key known features of the N400 response. Our results demonstrated that the rapidly elicited N400 response through the brain vital sign framework exhibit many of the similar characteristics compared to traditional N400 paradigms [68], [139], [177].

Additionally, the robust identification of the N400 effect at the individual level using automated expert-independent machine learning approaches provides additional support for clinical application of this rapid assessment technique. The 89% hit rate in the present study is quite comparable to previous reports – with prior machine learning based analysis reporting results in the 86-92% range [65], [159] and other analytical techniques also reporting observable N400 effects in similar proportions of healthy participants [138], [155].

4.5.6. Caveats

Despite the promising findings in this study, two main limitations should also be noted. As this is the first study characterizing the rapidly elicited rN400 response within the brain vital sign framework, the focus was on examining its spatiotemporal and neuroanatomical effects and comparing them with known features of the traditional N400 response. However, given the myriad of language- and non-language-based experimental paradigms in which the N400 response has previously been described, it is not feasible to compare the rN400 response to every other traditional paradigm in one study. Rather, the current study focused on comparisons with language-based paradigms, and utilized response features and characteristics that have been identified as commonalities across different studies in order to account for variable modalities and

86

experimental parameters (e.g. experimental condition, stimulus duration and type, inter-stimulus interval) [68], [139], [177]. Nonetheless, future studies may be conducted to examine more detailed comparisons between the brain vital sign rN400 response and traditional N400 responses. Additionally, as the first study of rN400 response, the current study utilized a distributed source modeling approach for source localization to be consistent with previous MEG studies of N400 [153], [162]. However, given the inherent limitations of this approach in biasing sources towards the cortical surface, future studies are needed to confirm these results using alternate source localization techniques such as spatial filtering using beamformer [121].

4.6. Conclusions

In this study, we investigated the spatiotemporal and neuroanatomical features of the N400 response as elicited by the rapid assessment brain vital signs framework. Using both MEG and EEG, our results showed that the rapidly elicited N400 response exhibits characteristics consistent with those reported in traditional semantic language-based N400 paradigms. These characteristics include temporal features showing maximal response within 300-500ms latency; topographic scalp distribution demonstrating maximal response at the posterior Pz electrode; spectral effects showing reduction in beta band power; and source localization to left-lateralized temporal and inferior frontal areas. With the increasing use of the N400 response in patient assessments for neurological conditions such as dementia and traumatic brain injury, the convergent M/EEG results of the current study provide further support for the possibility of translating the N400 response from research to clinical settings through a rapid assessment framework for evaluating cognitive functions.

4.7. Author Contributions

This study was conducted in collaboration with co-authors who contributed to data collection and some study design.

Chapter 5.   Study III: Developing New Technique and Neural Marker for Assessing Contextual Orientation

5.1. Abstract

Objective: The ability to orient with respect to the current context (e.g. current time or location) is crucial for daily functioning, and is used to measure overall cognitive health across many frontline clinical assessments. However, these tests are often hampered by their reliance on verbal probes (e.g. "What city are we in?") in evaluating orientation. Objective, physiology-based measures of orientation processing are needed, but no such measures are currently in existence. We report the initial development of potential brainwave-based markers of orientation processing as characterized using electroencephlography (EEG) and magnetoencephalography (MEG).

Approach: An auditory stimulus sequence embedded with words corresponding to *orientation-relevant* (i.e. related to the 'here and now') and *orientation-irrelevant* (i.e. unrelated to the current context) conditions was used to elicit orientation processing responses. EEG/MEG data, in concert with clinical assessments, were collected from 29 healthy adults. Analysis at sensor and source levels identified and characterized neural signals related to orientation processing.

Results: *Orientation-irrelevant* stimuli elicited increased negative amplitude in EEG-derived event-related potential (ERP) waveforms during the 390-570ms window (p<0.05), with cortical activations across the left frontal, temporal, and parietal regions. These effects are consistent with the well-known N400 response to semantic incongruence. In contrast, ERP responses to *orientation-relevant* stimuli exhibited increased positive amplitude during the same interval (p<0.05), with activations across the bilateral temporal and parietal regions. Importantly, these differential responses were

robust at the individual level, with machine-learning classification showing high accuracy (89%), sensitivity (0.88) and specificity (0.90).

Significance: This is the first demonstration of a neurotechnology platform that elicits, captures, and evaluates electrophysiological markers of orientation processing. We demonstrate neural responses to orientation stimuli that are validated across EEG and MEG modalities and robust at the individual level. The extraction of physiology-based markers through this technique may enable improved objective brain functional evaluation in clinical applications.

Keywords: neurotechnology; orientation; MEG; ERP; neuroimaging; neural signal processing;

5.2. Introduction

The ability to understand the "here and now" and orient oneself to the current context is crucial to our day-to-day function. Studies investigating orientation ability have defined it operationally as the ability to orient in space, time and person with respect to the current context, such as knowing the current location and time [87]. This ability is often deemed a marker for overall cognitive health [178], and its evaluation is crucial to many frontline clinical decisions. In fact, orientation assessment is often among the first tests performed in cases of suspected brain dysfunction, such as dementia [83], concussion [88], and traumatic brain injury (TBI) [86]. Research has shown that orientation ability in TBI patients reflects their injury severity, is positively correlated with functional recovery, and even predicts cognitive outcomes months after injury [84], [179]. Similarly, orientation ability in Alzheimer's disease patients has been shown to be negatively correlated with disease progression [84], with reduction in orientation assessment scores signaling the presence of dementia in older adults [180]. Additionally, difficulty with orientation has also been shown to be a strong predictor of future cognitive decline in the elderly [181] .

Orientation assessments are a cornerstone of clinical management. Their significance can be seen in widely used clinical assessments such as the Mini Mental State Exam (MMSE) for cognitive decline and dementia, in which 33% of the total score is derived from orientation-related questions [82]. Orientation is currently assessed using

verbal probes such as "What month is it?" or "What city are we in?" (e.g. A&OX3[85]; MMSE). However, concerns have been raised about the potential limitations of such behavior-based assessments, including patient difficulties with motor movement and communication, as well as the lack of standardization among examiners [1], [2], [30]. More objective measures of orientation are thus needed that do not depend solely upon observations of behavior.

There are currently several objective clinical measures of health that have been widely adopted throughout the healthcare system, such as blood pressure and pulse oxygenation. These commonly used health metrics generally exhibit four key features: 1) They provide relatively direct measures of physiology rather than relying upon questionnaires, 2) they do not require active responses from the test subject, 3) they can be rapidly evaluated, and 4) they produce results that can be readily interpreted by non-experts. In light of this, any proposed objective measures of orientation processing should also incorporate these features in order to maximize their clinical utility.

Such objective, physiology-based measures are increasingly being developed at the intersection of neuroscience and biomedical engineering. Our group recently reported the *brain vital sign* framework, which is an integrated hardware and software platform for rapidly evaluating brain functional status in the sensory, attention, and language domains [159], [182]. Based on 20+ years of research on event-related potentials (ERPs) derived from electroencephalography (EEG), the brain vital sign framework provides a fully automated, 5-minute evaluation of well-established brain responses across these domains, then quantifies these responses with respect to normative bounds to produce easy-to-interpret output scores [159]. We previously demonstrated the brain vital sign framework in healthy adults across a broad age range, and successfully identified key ERP indicators corresponding to the processing of sensation ((N100 ERP, [61]), attention (P300 ERP,[62]) and language (N400 ERP,[63]) at the individual level – along with confirmation of aging-related changes [159]. Nonetheless, although the brain vital sign framework successfully meets many of the requirements listed as an objective, physiology-based measure of several key aspects of brain functional status, the platform does not provide any information about orientation processing. In light of the crucial need to incorporate salient clinical features into existing experimental task structures for maximizing translational capacity [19], the current study

investigated the potential for incorporating an ERP-based measure of orientation processing into the existing brain vital signs framework.

To elicit contextual orientation processes, *orientation-relevant* and *orientation-irrelevant* words were added into the existing *brain vital signs* auditory stimulus sequence (Figure 5.1A). O*rientation-relevant* words comprised those directly related to the current context in space, time, or situation (e.g. current city, day of the week, season), while *orientation-irrelevant* words were not directly relevant to the current context (e.g. jigsaw, bread, table). Brain responses to the two different types of stimuli could then be compared to evaluate potential differences in orientation processing. It is important to note that the stimulus sequence does not explicitly "prime" the participant with contextual information prior to testing; rather, this information is embedded within the *orientation-relevant* stimuli as implicit contextual cues. In other words, the focus of the current study was to evaluate the brain's "inherent" awareness of its surroundings as it processes information related to the current time, place, or situation.

To our knowledge, this is the first study to investigate neurophysiological correlates related to implicit contextual orientation, and no direct comparisons with prior literature are possible as a result. Nonetheless, we speculate that the contextual orientation processes may be related to detection of "alignment" or congruence between a particular stimulus and a given context. In particular, previous studies examining the comparison of concrete stimulus features (e.g. pitch, colour) to an established context have shown that new stimuli which are not consistent with the established pattern elicit a "mismatch negativity" response [57], [183]. On the other hand, studies using language-based stimuli have shown that a range of semantic stimuli (such as words and sentences) that are not congruent in meaning with the expected input generate an N400 ERP response [68], [184]. Since the current study utilizes language-based stimuli to elicit contextual orientation responses, it is likely that the neural processes in detection of language-based contextual meaning may fall within the framework of the known N400 response.

The N400 response comprises a negative-going deflection in the ERP waveform which tends to be maximal around 400ms post-stimulus, and is generally associated with the detection of incongruence in meaning [68]. Originally reported using semantic language paradigms in which the negative deflection was observed in the incongruent

condition waveform relative to congruent [63], N400-like responses have since been demonstrated across numerous domains including language processing, semantic memory, and recognition memory. Sample experimental paradigms have included viewing of videos that lack meaning [185], incorrect solutions to math problems [186], unfamiliar vs. familiar faces [187], and viewing incorrect action sequences [69]. Additionally, N400-like responses have also been shown to index world knowledge, as studies have demonstrated these responses using statements that violated factual information known to be true (e.g. statement "the Dutch trains are *white* in color" when the color of the trains are yellow) [188]. Collectively, the current evidence suggests that the N400 family of responses index neural processes associated with high-level incongruence detection. These processes take into account associative and semantic relations, knowledge of the world, as well as other factors to establish meaning of a given stimulus within a context, and the magnitude of the response is modulated by the relative fit of the corresponding stimuli within the context [68], [147]. Accordingly, we anticipate that the *orientation-relevant* words in the current study may be considered more "consistent" with the current world knowledge compared to *orientation-irrelevant* words. As such, we anticipate that the *orientation-irrelevant* words would elicit an N400-like response.

In this study, we conducted two experiments to elicit, capture and evaluate orientation processing related markers using the novel *brain vital signs* platform. The first experiment investigated the potential to identify potential neurophysiological markers of orientation processing using portable EEG which is capable of point-of-care deployment in real-world clinical/bedside evaluations. Additionally, to characterize and validate the functional neuroanatomical correlates of the identified orientation response, another experiment was conducted using magnetoencephalography (MEG) which has superior spatial resolution compared to EEG[46], [164]. We hypothesized that: 1) *orientation-irrelevant* stimuli would elicit an N400-like response, manifesting as an increased ERP negativity occurring approximately 400ms post stimulus onset along with increased cortical activations in brain regions consistent with those of the N400 response; and 2) *orientation-relevant* neural responses would be significantly different from that of the *orientation-irrelevant* in both temporal and spatial response features*.

5.3. Methods

5.3.1. Auditory stimulus sequence

The brain vital sign framework employs a novel auditory stimulus sequence with interlaced tones and words to elicit brain responses corresponding to auditory sensation, attention, language processing and contextual orientation in approximately 5 minutes. The sequence comprises 60 blocks of 5 seconds each, with each block containing 5 tones followed by 2 words that represent a prime-target word pair (Figure 5.1). Orientation-related responses were derived by conditionally averaging trials corresponding to the prime words. Orientation relevant words (e.g. name of current month, 50%) and orientation irrelevant words (e.g. bread, 50%) were utilized to capture the orientation-related differential processing. The two groups of words were not statistically different in word frequency, length, and concreteness [189], [190]. Thirty trials each of orientation relevant and orientation irrelevant stimuli were elicited by the stimulus sequence. Spoken words were recorded in a male voice and normalized for root-mean-square (RMS) volume using Audacity software.
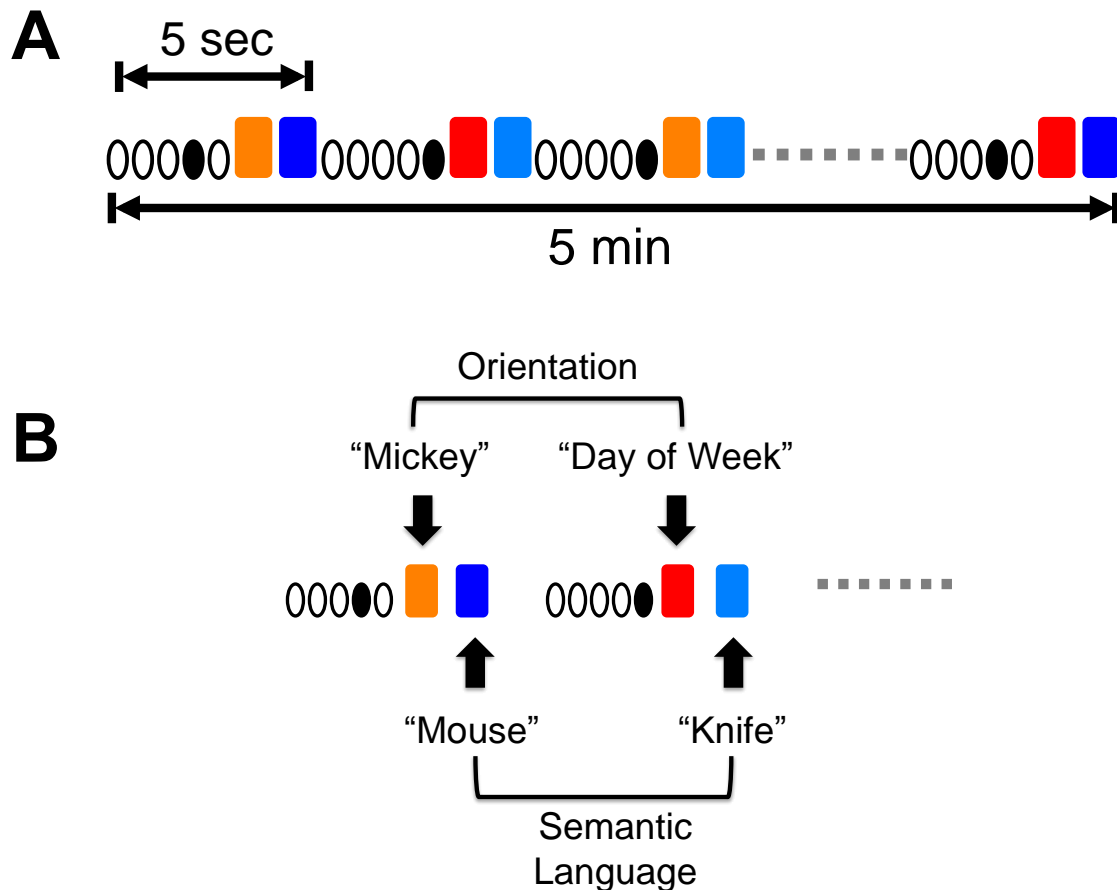
Figure 5.1.   Schematic illustration of stimulus sequence.
A) Five-second blocks are repeated 60 times over approximately 5 minutes. Each block begins with 5 tones for sensory and attention indicators (ovals, empty = standard, filled = deviant), followed by 2 words representing a prime-target pair (rectangles). Orientation-related responses are derived from prime words (red=orientation-relevant, orange = orientation-irrelevant). Language indicators are derived from target words (light blue=incongruent, dark blue=congruent). **B**) Illustrative stimuli showing two of the sixty blocks, with examples of stimuli used for generating orientation processing and language processing related markers. Prime words related to the present context/situation (orientation-relevant, red) were contrasted with words unrelated to the present context (orientation-irrelevant, orange) to generate the orientation processing markers. Target words were either semantically related (dark blue) or unrelated (light blue) to the preceding prime, and were used to generate semantic language markers.

5.3.2. Experiment I

Participant Details

Twelve participants ranging in age from 20-82 (age 43.61 ± 20.15, 7 females), fluent in English with no hearing issues, were enrolled in Experiment I. The research ethics boards at Simon Fraser University and Fraser Health Authority approved the

study with all participants providing written informed consent. Participants were screened for history of neurological problems and psychoactive medications.

Data Collection

Experiment I focused on identifying and capturing the orientation response using a technology platform which is capable of point-of-care deployment in a real-world setting (i.e. portable hardware, reduced electrode array, easy and fast setup procedures, and rapid testing). The *brain vital signs* framework was chosen as the technology platform as it has been previously demonstrated to meet these requirements[159]. Specifically, EEG was recorded using 8-channel portable g.Nautilus acquisition system (g.tec Engineering, Austria) with 0-250Hz built-in hardware filter, 500Hz sampling rate, and a portable computing platform. EEG was recorded from electrodes along the midline scalp sites (Fz, Cz, Pz), with 4 additional electrodes providing ground (forehead), reference for common mode rejection (right ear lobe) and eye movement monitoring (electroocculogram, EOG; supra-orbital ridge and outer canthus of left eye). Signal amplification, conditioning and digitization was undertaken near the electrode site and then transmitted over a bluetooth link to the computing platform. A custom-designed USB-to-TTL converter subsystem was utilized to generate time-stamping signals from the computing platform for recording stimulus presentation events. These TTL pulses were concurrently recorded with the EEG data by the amplifier and later used for generating ERPs. Contrary to conventional techniques, and in line with prior *brain vital signs* work[159], the scans were undertaken with minimal skin/site preparation (<5minutes), with the skin-electrode impedances maintained at <30kOhms. Auditory stimuli were delivered binaurally through Etymotic ER4 insert earphones, and participants were asked to pay attention to the stimuli while maintaining fixation on a cross located 2.0m away (black cross on white background). Data collection took place in a well-lit, non-magnetically shielded room to ensure consistency with real-life situations.

Each participant underwent neuropsychological screening using MMSE and Montreal Cognitive Assessment (MoCA, [83]), along with three runs of EEG/ERP data collections. MMSE examines five areas of cognition including orientation, with scores below 23 (out of 30) indicative of cognitive impairment. Similarly, MoCA also assesses

several high-level cognitive functions including orientation, with scores below 26 (out of 30) indicating impairment.

Data Analysis

Automated ERP processing was performed using a series of steps comprising a notch filter at 60Hz (5Hz bandwidth), 4th order Butterworth filters (1-20Hz passband), segmentation (-100 to 900ms relative to stimulus presentation), baseline correction (-100 to 0ms), and conditional averaging [48], [81]. The signal-to-noise ratio was further optimized by jittering the stimulus presentation timing as well as extensive artifact removal procedures [81]. To remove contamination due to ocular artifact arising from blinks and eye movements, a regression-based approach was utilized in line with previous work using the *brain vital signs* framework [159]. This process involved first computing a signal propagation factor that delineates the spatial propagation of ocular signals in the frontal-posterior direction, then applying the propagation factor to subtract the ocular contamination signals from each scalp EEG channel. The correction procedure for each trial is as follows:

$$\tilde{y}_{i,j} = y_{i,j} - k \cdot x_{i,j}$$

where $\tilde{y}_{i,j}$ is the corrected EEG signal in the i-th trial and j-th channel, $y_{i,j}$ is the corresponding raw EEG, $x_{i,j}$ the raw EOG, and k the propagation factor. For each channel, the propagation factor is computed by first averaging across all trials for each condition to derive the event-related potential (ERP), then subtracting the ERP signal from each trial in both EEG and EOG data to derive the residual background signal. The propagation factor for each trial and channel is then derived by computing the correlation coefficient between the residual background signal in EEG and EOG as follows:

$$k_{i,j} = \text{corr}\left(\frac{y_{i,j} - \bar{y}_j}{x_{i,j} - \bar{x}_j}\right)$$

where $k_{i,j}$ is the propagation factor for the i-th trial and j-th channel, $y_{i,j}$ denotes the raw EEG signal in the i-th trial and j-th channel, $x_{i,j}$ the corresponding raw EOG signal, and $\bar{y}_j$ and $\bar{x}_j$ represent the trial-averaged ERP signals for the j-th channel in EEG and EOG traces, respectively.

Following conditional averaging across trials to derive event-related potentials (ERPs), the ERP waveforms were subjected to statistical evaluation using a bootstrapping approach [109]. Briefly, this involved first computing the t-statistic at each time point between the orientation-relevant and orientation-irrelevant conditions of the ERP waveforms across all participants, then extracting the size of the maximum suprathreshold cluster. The data were then permuted over all subjects and conditions, and randomly divided into two groups. T-tests were performed at each time point following the permutations, and size of the maximum suprathrehold cluster determined. This process was repeated 1000 times to create a resampling distribution of suprathreshold cluster sizes, and the statistical probability was derived by comparing the true cluster size with those of the resampling distribution. This procedure was applied to the Cz channel using data within the 0.5-20Hz frequency range to be consistent with previous work [159]. Results were deemed statistically significant if p<0.05.

To further confirm the reliability of the orientation-related responses at the individual-level, machine-learning classification using support vector machine (SVM) was also employed to differentiate between the *orientation-relevant* and *orientation-irrelevant* conditions [110]. To achieve the best results, single-session trial-averaged data from all three electrode sites (i.e. Fz, Cz, Pz) were used as inputs to the SVM with a radial kernel in accordance with previous work [15]. A two-category classifier was first trained using 90% of the available data, then applied to the remaining 10% to assess classification accuracy. This process was repeated 10 times in a 10-fold cross-validation approach to ensure that the classifier is trained and tested on all available data. The proportion of correctly classified results relative to the total number of classifications was used as the accuracy metric. True positive, false positive, sensitivity and specificity measures were also derived from the confusion matrix. Additionally, bootstrapping statistics were performed to verify the statistical significance of the observed SVM classification results [132]. Briefly, the training data were first randomly relabeled according to *orientation-relevant* and *orientation-irrelevant* conditions, and the classifier was retrained using the relabeled data. The new classifier was then used to evaluate the test data to obtain a new classification accuracy. This process was repeated 1000 times with randomized condition labels each time, and the resulting test accuracies were used to generate a null distribution of SVM classifications. The true classification accuracy was then assessed relative to this null distribution to compute the statistical probability of

achieving a better classification accuracy using randomized distributions of conditions. Classification results were deemed to be statistically significant if p<0.05.

5.3.3. Experiment II

Participant Details

Seventeen right-handed healthy adults participated in Experiment II (23.6 ± 2.4 years, 10 males). None reported history of neurological problems or psychoactive medication. All individuals were fluent in English with normal hearing, and were undergraduate or graduate students. Research ethics boards at Fraser Health Authority and Simon Fraser University approved the study, and all participants provided written informed consent.

Data Collection

Data were collected using 151-channel CTF MEG system (MEG International Services Limited, Canada) inside a magnetically shielded room. Additionally, to enable comparison between the portable EEG results from Experiment I, concurrent EEG data were also collected using the same electrode configuration (i.e. Fz, Cz, Pz midline electrode sites). Data were collected while participants listened to two sessions of the auditory *brain vital signs* stimulus paradigm while lying in the supine position. MEG sampling frequency was 1200Hz, with axial gradiometers (5cm baseline) and synthetic 3rd order gradients for noise cancellation. Scalp EEG used three Ag/AgCl electrodes at the Fz, Dz, and Pz locations, with impedances kept below 5kOhms. Four additional electrode channels were utilized, including reference (left mastoid), ground (forehead), horizontal EOG (outer canthus of left eye), and vertical EOG (supra-oribtal ridge of left eye). Three head position indicator coils (HPI, placed at nasion as well as left and right pre-auricular points) were used to monitor head movements throughout the collection. To facilitate alignment of coordinate systems between the participant's head and the MEG scanner, a Polhemus electromagnetic digitization system (Polhemus Incorporated, USA) was utilized to record the head shape for each participant using at least 500 points, as well as the 3-dimensional location of the HPI coils and EEG/EOG electrodes [191]. Binaural auditory stimuli were presented to the participants through insert earphones, and they were instructed to pay attention to the stimuli while maintaining

visual fixation on a cross displayed on the overhead screen (white cross on black background).

Data Analysis

Raw data were first visually inspected, and artifactual channels were removed. Data were then down-sampled to 300Hz, notch filtered to remove signal from the HPI coils and power line noise along with its harmonics (60Hz, 120Hz, 180Hz), and subsequently band-pass filtered to 0.1-100Hz with a 4th order Butterworth filter.

MEG analysis

Following visual inspection, data from 2 of the 17 participants were excluded from subsequent analyses due to noise contamination. Independent component analysis (ICA) was performed using Infomax in EEGLAB [160], and components corresponding to ocular, cardiac, muscular and other sources were identified and removed based on well-established stereotypical features across the temporal, spatial and spectral domains [104], [160]. ICA is a blind source separation technique, and primarily aims to resolve the observed activity into a set of estimated independent source activities as described below:

$$s(t) = W \cdot x(t)$$

where **x**(t) is the set of observed signals (dimensions *sensor* × *time*), **s**(t) is the estimated source signals (dimensions *component* × *time*), and W is the weight or un-mixing matrix to transform between the two spaces. In the present study, the infomax technique was employed for estimating the un-mixing matrix through a maximum likelihood approach [192]. In this approach, the un-mixing matrix W is estimated in an iterative fashion by following the natural gradient adjustment with learning rate μ:

$$\Delta W = \mu \left(I - 2 \tanh(x)\, x^T \right) W$$

Sensor-level analysis

The spatial variance measure global field power (GFP) was used to evaluate the demeaned signal power across all channels [161], enabling the simultaneous

assessment of time course activity across all sensors while accounting for possible differences in head positioning among individuals [193]. GFP was computed for each condition and time point as follows:

$$power = \sqrt{\frac{\sum_{i=1}^{N}(v_i - \overline{v})^2}{N}}$$

where, v_i denotes the magnetic field measured in channel i, $\overline{v}$ the mean signal across all sensors, and N the total number of channels. Similar to the ERP analysis described earlier, a bootstrapping approach was utilized to compare GFP waveforms between the *orientation-relevant* and *orientation-irrelevant* conditions across the entire epoch, This procedure was also applied to data within the 0.5-20Hz frequency range to maintain consistency across modalities.

To determine whether any observed responses were due to sensory-related differences between the *orientation-relevant* and *orientation-irrelevant* conditions, additional analyses were also performed using an alternate time window. This alternate interval was chosen to be 90-130ms to be consistent with sensory processing [194], and the mean GFP signal was computed within this window for each subject and condition. Values were then compared at the group level using paired t-test.

Further analysis was also conducted to determine whether observed effects were specific to orientation-related processing (i.e. *orientation-relevant* vs. *orientation-irrelevant*) and were absent for alternate stimulus categorizations. Trial-level data for all participants were randomly distributed into *orientation-relevant* and *orientation-irrelevant* groups, and the GFP were compared using a bootstrapping approach similar to earlier procedures. Results were deemed statistically significant if p<0.05 after 1000 randomized permutations.

Source-level analysis

Source localization analysis was performed using SPM8 (Wellcome Trust Centre for Neuroimaging, UK, [195]) to identify cortical generators of the orientation-related

responses. Forward and inverse modeling procedures were undertaken in accordance with previously published work [164], [196]. Given this was the first investigation of orientation processing, the minimum norm estimates (MNE) approach was employed for inverse modeling as it requires few assumptions about the characteristics of the underlying data and therefore better reflects the amount of the information present [120]. Specifically, the source localization was achieved through the solution to the following:

$$\hat{x} = argmin_x \{\|x\|^2 + \lambda \|y - Fx\|^2\}$$

where, **F** is the lead field matrix calculated during forward modeling, **y** is the observed sensor data, λ is a regularization term or cost function calculated based on the signal-to-noise ratio of the data, and **x** is the estimated source activity. Group constrains were applied during inversion to ensure reliability across participants [165]. Source reconstruction was based on trial-averaged data for the 0.5-20Hz frequency band and -200 to 900ms time window relative to stimulus onset. To generate images of source activity for each participant, source estimates were averaged over predefined time windows (-100 to -20ms for *baseline* and 390-470ms for *active*) and frequency ranges (0.5-20Hz), projected to a 3D source space, and smoothed using a Gaussian kernel (8mm half-width full-maximum). Statistical analysis was performed using general linear model (GLM) with two-way analysis of variance (ANOVA), with time (i.e *baseline* vs *active*) and stimulus type (i.e. *orientation-relevant* vs *orientation-irrelevant*) as factors [166].

EEG analysis

EEG concurrently collected with the MEG was processed in the same manner as described previously. The only difference was in the technique for ocular artifact removal, which followed an adaptive filtering approach in line with previous literature using the same hardware platform[182]. In particular, adaptive filtering involves first selecting the recorded EOG channels as reference inputs, then processing the reference inputs using a finite impulse response filter (length = 3) before subtracting from the EEG channels using a recursive least squares algorithm (forget factor λ = 0.9999) to account

for the quasi-stationarity of the signal [103]. Statistical significance between the orientation-relevant and orientation-irrelevant condition ERPs was assessed using bootstrapping statistics as described earlier.

5.4. Results

5.4.1. Neuropsychological and orientation assessments

The MMSE/MoCA scores along with the orientation sub-scale score for the Experiment I participants are shown in Table 5.1. All participants obtained full scores (30/30) on their overall MMSE with perfect scores on the orientation sub-scale for both MMSE and MoCA assessments. The overall MoCA score was slightly lower but still within healthy range (29.65±0.3).

Table 5.1.   Participant characteristics and cognitive assessment scores

Education (years)	18.05 ± 3.75
MMSE (/30)	30
MMSE Orientation sub-scale (/10)	10
MoCA (/30)	29.65 ± 0.3
MoCA Orientation sub-scale (/6)	6
Sex (M:F)	1:1.4

5.4.2. ERP responses

Results from both Experiment I (portable EEG) and Experiment II (EEG concurrent with MEG) showed ERP waveform morphology with increased negative amplitude in the *orientation-irrelevant* condition compared to *orientation-relevant*, occurring approximately 300-600ms post-stimulus (Figure 5.2 A,B). This differential response was confirmed through bootstrapping statistics, which demonstrated that the windows of significant difference between the two conditions were 410-500ms and 390-570ms for Experiments I and II, respectively. Given the entirely overlapping nature of these windows, further statistical comparisons were conducted using the larger interval as a common window of interest across both experiments. Results showed that ERP amplitudes were significantly difference between the two conditions across both experiments (p<0.05, Figure 5.2C). Importantly, the pattern of increased ERP negativity

in the *orientation-irrelevant* compared to *orientation-relevant* condition was consistent at both group and individual levels.

The trained SVM classifier successfully distinguished between the ERP responses for *orientation-relevant* vs. *orientation-irrelevant* at the individual level, with high accuracy (88.89%), sensitivity (0.875), and specificity (0.903). True positive rate was high (0.875), while false positive rate was low (0.097). Crucially, these classification results were verified to be statistically significant through permutation analysis ($p<0.05$).
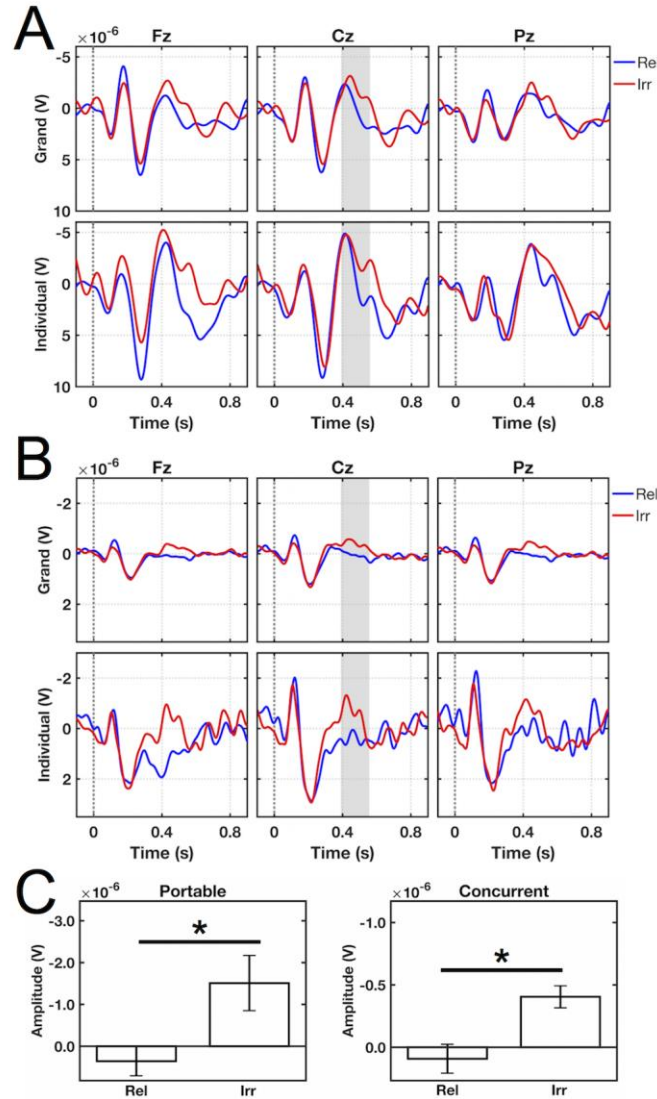
Figure 5.2.   ERP waveforms demonstrating differential orientation-related processing.
A) ERPs from Experiment I, collected using portable EEG system. **B)** ERPs from Experiment II, collected using EEG concurrent with MEG. Both grand-averaged and representative individual waveforms are shown for each experiment. Shaded regions denote windows of interest (390-570ms) for statistical comparison. **C)** Mean ERP amplitudes within the highlighted windows of interest, computed for each individual and presented as mean ± SEM across participants. *$p<0.05$ across conditions. *Rel = orientation-relevant, Irr = orientation-irrelevant.*

5.4.3. MEG sensor-level results

Consistent with ERP results, the differential processing between *orientation-relevant* and *orientation-irrelevant* conditions was also reflected in the MEG sensor-level

GFP (p<0.05, Supplementary Materials). Bootstrapping statistics identified the window of significant difference between conditions to be 390-470ms, also in agreement with the window of interest shown in ERP results. In contrast, the control time interval for sensory processing did not demonstrate differential responses between the two conditions (p=0.11). Additionally, robustness of the orientation-related response against alternate word categorizations was also confirmed using permutation-based statistics (p<0.05).

5.4.4. MEG source results

Source localization analysis showed that, relative to pre-stimulus baseline, processing of *orientation-irrelevant* stimuli activated the left-lateralized inferior frontal, temporal and parietal cortices (Figure 5.3A). On the other hand, *orientation-relevant* stimuli elicited activity in the bilateral parietal cortex, the superior, middle, and inferior temporal gyri, as well as the left-lateralized temporal pole and perirhinal cortex (Figure 5.3B).
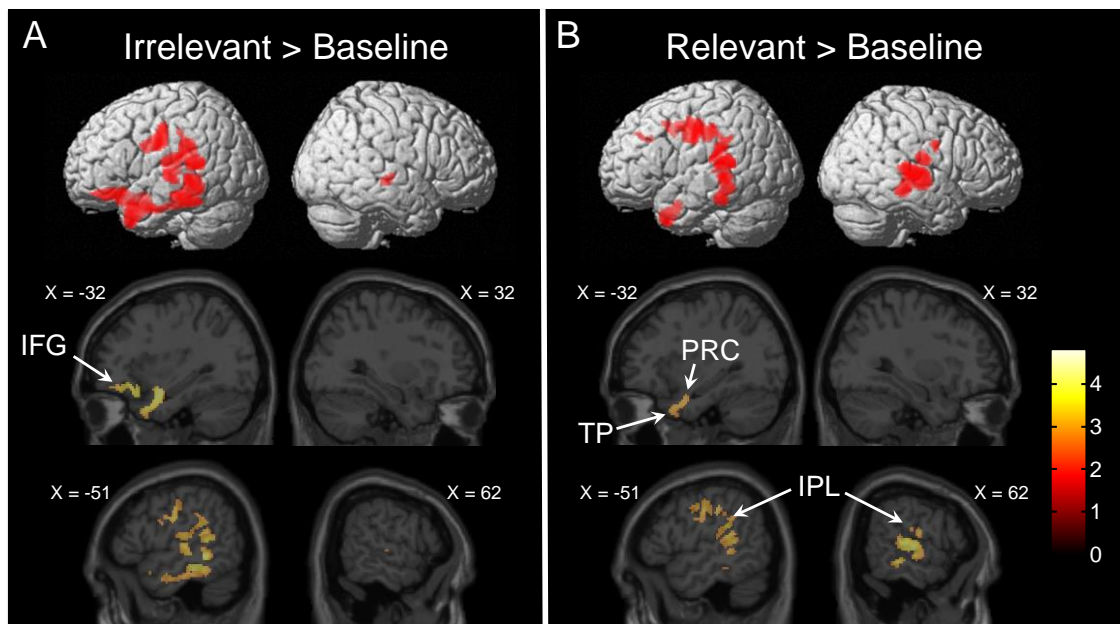
Figure 5.3.   Source localization results
Results shown for p<0.005 *unc.,* k=20**. A)** *Orientation-irrelevant* stimuli activated the left inferior frontal, temporal and parietal cortices (irrelevant > baseline contrast). **B)** *Orientation-relevant* stimuli activated the bilateral parietal and temporal areas, along with left temporal pole and perirhinal cortex (relevant > baseline contrast). *IFG = inferior frontal gyrus, PRC = perirhinal cortex, TP = temporal pole, IPL = inferior parietal lobule.* Color bar in the sagittal views represents T-statistic values. Coordinates in MNI space.

Additional contrasts were also performed to examine differences in cortical activations related to the orientation-related stimuli. Results showed that processing of *orientation-irrelevant* stimuli led to increased activity in the left posterior middle temporal gyrus (pMTG) relative to that of the *orientation-irrelevant*, while the reverse comparison showed no suprathreshold activations (Figure 5.4).
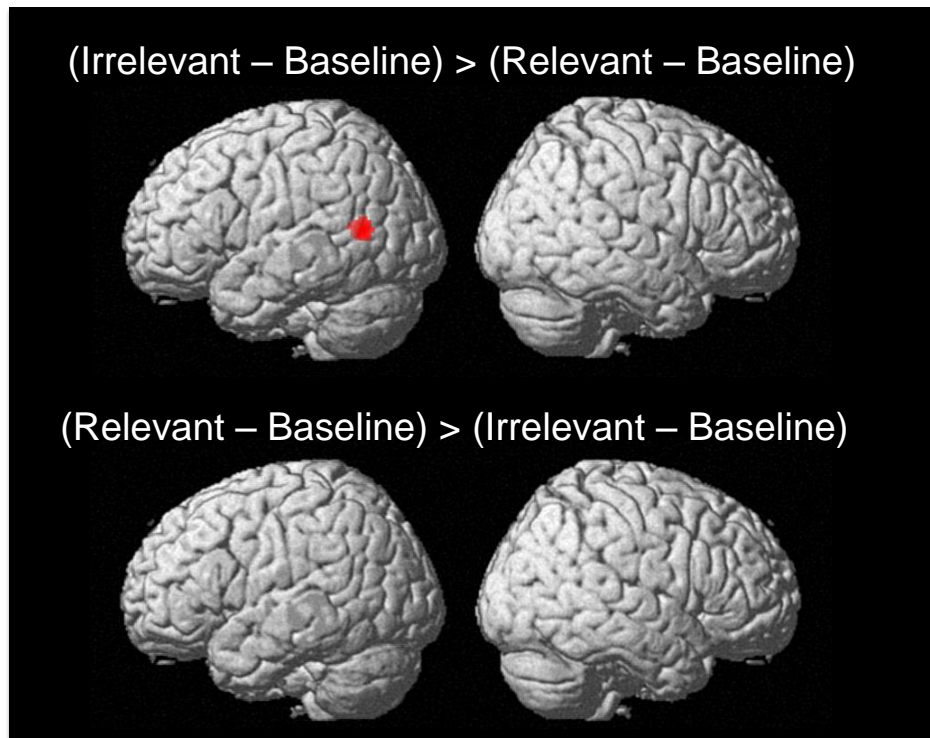
Figure 5.4.   Differential cortical activations in processing orientation-related stimuli
Result shown for p<0.005 *unc.*, k=20**.** *Top:* Increased activation of posterior middle temporal gyrus (pMTG) was observed for processing of *orientation-irrelevant* compared to *orientation-relevant* stimuli. *Bottom:* Processing of *orientation-relevant* compared to *orientation-irrelevant* stimuli did not show any suprathreshold clusters.

5.5. Discussion

5.5.1. Main Findings

The current study investigated neurophysiological correlates of orientation processing in order to identify an objective, physiology-based measure of orientation-related responses that could be readily integrated within the brain vital sign framework. Towards this end, we utilized an auditory stimulus sequence containing embedded words that were either *orientation-relevant* or *orientation-irrelevant* with equal probability. The *orientation-relevant* words presented information consistent with the current context (e.g. current month, year, city, country, season), while the *orientation-irrelevant* words did not relate to the current context (e.g. jigsaw, tuna). Our results demonstrate that the *orientation-irrelevant* stimuli elicited an N400-like response compared to the *orientation-relevant* stimuli, as evidenced by increased negative ERP amplitude occurring approximately 400ms after stimulus presentation, with cortical activations in the left temporal, inferior frontal and parietal regions (confirmation of Hypothesis 1). In comparison, responses to the *orientation-relevant* stimuli showed more positive amplitude in the ERP waveform, with significantly different response characteristics in both time course activity as well as neuroanatomical correlates (confirmation of Hypothesis 2).

5.5.2. Hypothesis 1: N400-like response for *orientation-irrelevant* stimuli

To investigate potential electrophysiological responses to orientation-related stimuli using EEG, we conducted two separate experiments. The first employed a portable EEG system with 3 midline scalp electrodes (Fz, Cz, Pz), while the second experiment utilized the same electrode channels but with simultaneous MEG for source localization. Results from both experiments showed that the ERP responses to *orientation-irrelevant* stimuli exhibited greater negative amplitude compared to the *orientation-relevant* stimuli, peaking at approximately 430ms post-stimulus (Figure 5.2 A,B). These findings are consistent with the well-known N400 response to semantically incongruent stimuli, in which the incongruent condition waveform exhibits similar

amplitude and timing characteristics [63], [139]. Additionally, source localization analysis revealed that processing of *orientation-irrelevant* stimuli activated largely left-lateralized brain regions across the inferior frontal, temporal, and parietal cortices (Figure 5.3A). These findings are also consistent with the cortical activation patterns for N400 response reported in previous studies, which demonstrated similar left-lateralized activity for the semantically incongruent condition [141], [153], [162], [197], [198]. It is important to note that these effects were not due to potential differences in sensory processing, as comparisons during the sensory processing window did not show any differences between the two conditions.

The N400-like response to inconsistent or unexpected stimuli is believed to represent the brain's processing of incoming information within the context of an established knowledge schema [68], [147]. This response has been demonstrated across a diverse range of experimental paradigms, with stimuli including incorrect solutions to math problems [186], nonsensical videos [185], and sentences with semantically incorrect words [139], [184]. Although most studies have elicited the N400 response using semantic knowledge violations, a recent report by Hagoort et al. suggested that the N400-like response might also be elicited when a given stimulus is semantically correct but violates known world knowledge [188]. Using the well-known fact that the Dutch trains were both crowded and yellow in color, Hagoort et al. demonstrated that N400-like responses were elicited not only when sentence stimuli contained an explicit violation of meaning (i.e. "*Dutch trains are sour and crowded*"), but also when semantically correct sentences violated the known world knowledge regarding the trains (i.e. "*Dutch trains are <u>white</u> and crowded*"). The authors postulated that the N400-like response may thus represent the brain's evaluation of incoming information within the context of the existing knowledge schema, with both explicit violations (i.e. linguistic error) and implicit falsehoods (i.e. incorrect color of the trains) producing the N400-like effect [188]. These findings are in line with observations in the current study, in that the N400-like response to *orientation-irrelevant* stimuli may represent the brain's evaluation of words within the context of the implicit world knowledge regarding the current situation or context. Thus the *orientation-relevant* stimuli would constitute the 'correct' or 'factual' information, while the *orientation-irrelevant* stimuli represented violations of this implicit context.

While the ERP waveforms generally exhibited a similar pattern across both experiments, differences were observed in response amplitudes as well as variance across individuals. This may be due to differences in experimental parameters for the two sub-studies, as Experiment I was conducted as a proof-of-concept evaluation of potential orientation-related responses, and thus employed a portable EEG system with a relatively small sample size (n=12). Additionally, as the orientation measure was intended to be integrated within the brain vital sign framework, the study sample included participants across a broad age range (i.e. 19-82 years) to demonstrate effect across the lifespan, potentially contributing to larger variance in observed response in this experiment [67], [199], [200]. In contrast, Experiment II was designed to facilitate assessment of orientation response characteristics, and involved EEG with simultaneous MEG for improved source localization. This study was conducted in a larger sample (n=15) with a relatively uniform participant age distribution (19-29 years) to enable more focal evaluation of response features while reducing potential variance across individuals. The different EEG hardware platform in the two experiments also led to differences in reference electrode location (right ear lobe for portable EEG vs. left mastoid for concurrent EEG), which may have contributed to differential response amplitudes [201]. Nonetheless, it is important to note that these differences in amplitude or variance between the two experiments did not alter the overall pattern of orientation-related responses observed across these experiments, and that the N400-like response to *orientation-irrelevant* stimuli persisted despite changes in EEG hardware platform, reference scheme, or participant characteristics. This lends further support to the validity of our findings regarding orientation-related processing.

5.5.3. Hypothesis 2: Response to *orientation-relevant* stimuli distinct from *orientation-irrelevant*

ERP results in both experiments showed that processing of *orientation-relevant* stimuli led to more positive amplitude compared to the *orientation-irrelevant* condition during the 300-600ms window (Figure 5.2), with similar differential processing also reflected in the corresponding GFP results for MEG (Supplementary Materials). These findings are consistent with previous research demonstrating late positive ERP amplitudes in response to stimuli that were both highly meaningful and familiar,

compared to stimuli that were familiar but less meaningful as well as those that were unfamiliar [202]. Similar positivity in ERP amplitudes have also been reported for encountering concepts that evoked knowledge of 'who, what, where, why and when' [203], processing task-relevant stimuli [204], and recognition of familiar objects [205]. In light of these findings, the current study's observation of late positive ERP amplitude to *orientation-relevant* stimuli may represent the assessment of incoming information within the context of existing world knowledge. In other words, words that pertain to the "here and now" may evoke neural processes for the evaluation of 'familiarity' in the incoming stimulus. In contrast, words that are unrelated to the present context would not evoke this evaluation of 'familiarity'. Nonetheless, these interpretations remain speculative given the available evidence, and more studies need to be conducted to further elucidate this phenomenon.

Further to ERP results, source localization analysis revealed that *orientation-relevant* stimuli activated regions of the bilateral temporal and parietal cortices as well as the left temporal pole and perirhinal cortex (Figure 5.3B). These results are consistent with previous morphometric, metabolic and neuroimaging studies that pointed to crucial roles for the temporal, rhinal, as well as parietal regions in orientation processing [84], [206]. Additionally, the fact that the right temporal and parietal activations were observed only in the *orientation-relevant* conditions and were absent in the *orientation-irrelevant* condition is also in line with previous reports demonstrating the link between right hemisphere dysfunction and difficulties in orientation processing [207]. Crucially, other research has reported that patients with right middle cerebral artery infarction exhibited disorientation and confusional states [208], which also helps to corroborate the current findings given that this artery supports blood perfusion to many of the areas activated by the *orientation-relevant* stimuli in our study [208]–[210].

The *orientation-relevant* stimuli in our study were designed to represent the current context in both temporal (i.e. time of day) and spatial (i.e. physical location) domains. As such, we anticipated that the neural processes elicited by these stimuli might also represent cortical evaluation of these types of information. Interestingly, the pattern of cortical activations observed for *orientation-relevant* stimuli do agree with previous studies investigating processing of temporal and spatial information. For instance, the right temporal, parietal and frontal areas have previously been implicated in spatial and temporal awareness [211], [212], while the right inferior parietal lobule and

superior temporal gyri have been associated with spatial processing [213]. Additionally, studies have shown that patients with spatial neglect often also have cortical damage in the superior temporal regions [214], while other studies pointed to the key role of the right inferior parietal lobule and frontal regions in processing of time-related information [215]. Together, these previous results help to corroborate our findings that the *orientation-relevant* stimuli activated brain regions associated with processing of temporal and spatial information.

Further to examining task-related activations in each stimulus condition, we also performed additional contrasts to evaluate differential activity between the two conditions. Results showed that the left pMTG regions exhibited increased activation in the *orientation-irrelevant* compared to *orientation-relevant* condition, while the reverse contrast did not produce any suprathreshold activations (Figure 5.4). The activation of pMTG in *irrelevant > relevant* contrast is also consistent with the activity of this region in the *irrelevant > baseline* contrast (Figure 5.3A), and is consistent with previous studies demonstrating the involvement of this region in tasks requiring high levels of conceptual or representation processing [216]. For instance, this area is known to be engaged when incoming stimuli do not agree with the expected input – such as the N400-like response [217]. In the current study, since *orientation-relevant* words were related to the current context while the *orientation-irrelevant* words were not, we speculate that the former may be more consistent with the 'expected input' given the current 'known world knowledge' regarding the current context compared to the latter. As such, the activation of the left pMTG region in processing *orientation-irrelevant* stimuli may represent 'additional efforts' made by the brain in order to 'fit' the incoming stimulus with the concurrent context or existing knowledge schema [217]. Nonetheless, this interpretation remains highly speculative, and further studies need to be conducted to better elucidate the neurocognitive mechanisms underlying *orientation-relevant* processing.

5.5.4. Orientation-related responses robust at the individual level

To ensure future clinical applicability, the responses to *orientation-relevant* and *orientation-irrelevant* stimuli were explored at the individual level. Machine-learning classification using SVM demonstrated that observed orientation related responses were

robust at the individual level, with high accuracy (88.89%), sensitivity (0.875), and specificity (0.903). These results further confirm the validity of the observed orientation responses, and were also consistent with the SVM-based classification outcomes for well-established N400 ERP markers elicited using semantic language violations [65], [159], [182]. These findings were also concordant with results of the behavior-based neuropsychological assessment as all participants earned full scores demonstrating complete knowledge of their present situation. Classification analysis was performed with 10-fold cross-validation, further improving the generalizability of our results [218].

5.5.5. Caveats and Future Work

Our results demonstrated excellent agreement between MEG and EEG findings, providing a promising initial demonstration of potential easy-to-use markers related to orientation processing. However, certain caveats should be noted. First, the current work is the first demonstration of potential electrophysiological markers of orientation processing, and the effects still need to be validated in a clinical sample to ensure clinical applicability. As such, ongoing activities in our lab are exploring potential changes in these markers within several clinical populations such as TBI and dementia patients. In addition, while this study utilized a sample size comparable to other studies of cognitive ERPs along with established best practices [219], future studies are needed to validate these results using larger samples of participants. Moreover, as the cortical sources for the orientation response were localized to lateral rather than medial regions in the brain, the midline sites of Fz, Cz, and Pz used in the current study may not have captured the maximal response. Nonetheless, these electrode positions enabled the effective initial demonstration of this response as a valid marker at the individual level, and future studies will investigate alternative electrode configurations that better capture this response. Similarly, as SVM classification performance is dependent on training sets, the relatively small sample size in the current study may have impacted the robustness of this approach. Nonetheless, as this is the first investigation of neurophysiological effects in orientation processing, the use of SVM classification enabled the initial demonstration of statistical differences at the individual level in line with prior studies[65], [110], [182]. Further studies are needed to validate the SVM outcomes using larger samples. Finally, as the first study of orientation processing, the

112

current study utilized a MNE-based source localization technique since it requires few assumptions about cortical source characteristics [120]. However, since this approach has limitations in biasing towards sources that are closer to the cortical surface, further studies are needed to validate the source localizations results using alternate approaches such as spatial filtering with beamformer [121].

5.6. Conclusion

The current study demonstrated a new technique to elicit, capture, and evaluate brain electrophysiological responses to orientation processing. The results showed increased negative ERP amplitude to *orientation-irrelevant* stimuli in line with the N400-like response, while *orientation-relevant* processing exhibited late positive ERP amplitude. These differential responses were confirmed across both MEG and EEG, and validated against alternate effects such as potential sensory processing differences as well as differential word classifications. Importantly, responses were also robust at the individual level as confirmed using SVM-based machine learning classification. The findings in the current study suggest that an N400-like ERP response to *orientation-irrelevant* stimuli may represent a potential electrophysiological signature of orientation processing. With the widespread use of orientation in frontline clinical assessments, these findings provide promising initial evidence to for the potential to create a rapid, point-of-care enabled, objective measure of orientation processing that may augment existing clinical assessments.

5.7. Supplementary Material

5.7.1. MEG Global Field Power Results
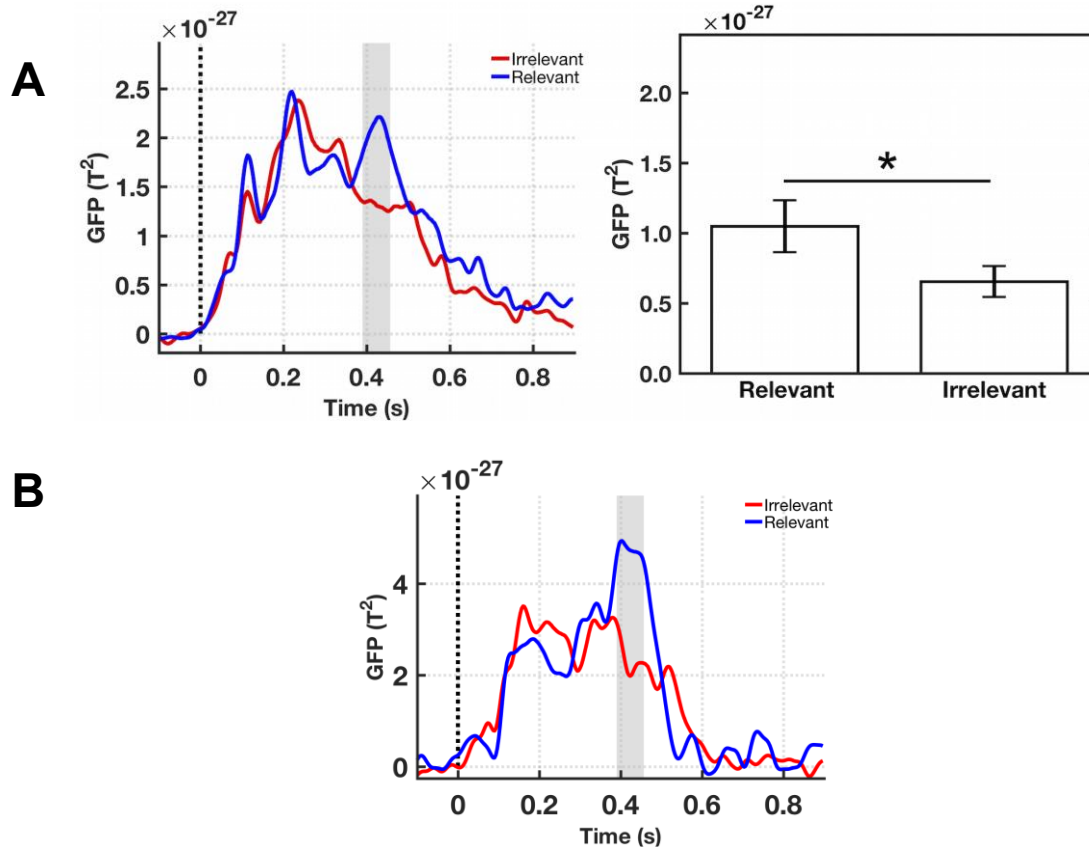
Figure 5.5.   MEG sensor-level global field power (GFP) results showing differential processing for orientation-relevant (Relevant) and orientation-irrelevant (Irrelevant) conditions.
A) *Left:* Group-level GFP waveforms. Shaded region denotes window significant difference between the two conditions determined using bootstrapping statistics (as described in Methods). *Right:* Mean GFP value for each condition within the shaded window, calculated for each individual and presented as mean ± SEM across individuals. *$p<0.05$. **B**) Individual-level GFP waveform for a representative participant. Shaded region denotes the same window of interest shown for group-level results.

5.7.2. Developing Stimulation Technique for Capturing Orientation Responses

As discussed in 3.7.3, the initial versions (version 1, 2 and 3) of the stimulus sequence entailed 120 word pairs, half of which were dedicated to semantic processing (i.e. semantically related or semantically unrelated word pairs for generating language processing neural markers), while the other half were word pairs for assessing

orientation processing by way of comparison of word pairs that were either correct with respect to the current situation (e.g. 'Today' 'Monday' if testing was being undertaken on a Monday, 50%) or incorrect with respect to the current situation (e.g. 'Today' 'Friday' if testing was being undertaken on a Monday, 50%).

A

Today → Monday *Correct*

Today → Friday *Incorrect*

Bread → Butter *Congruent*

Bread → Quack *Incongruent*
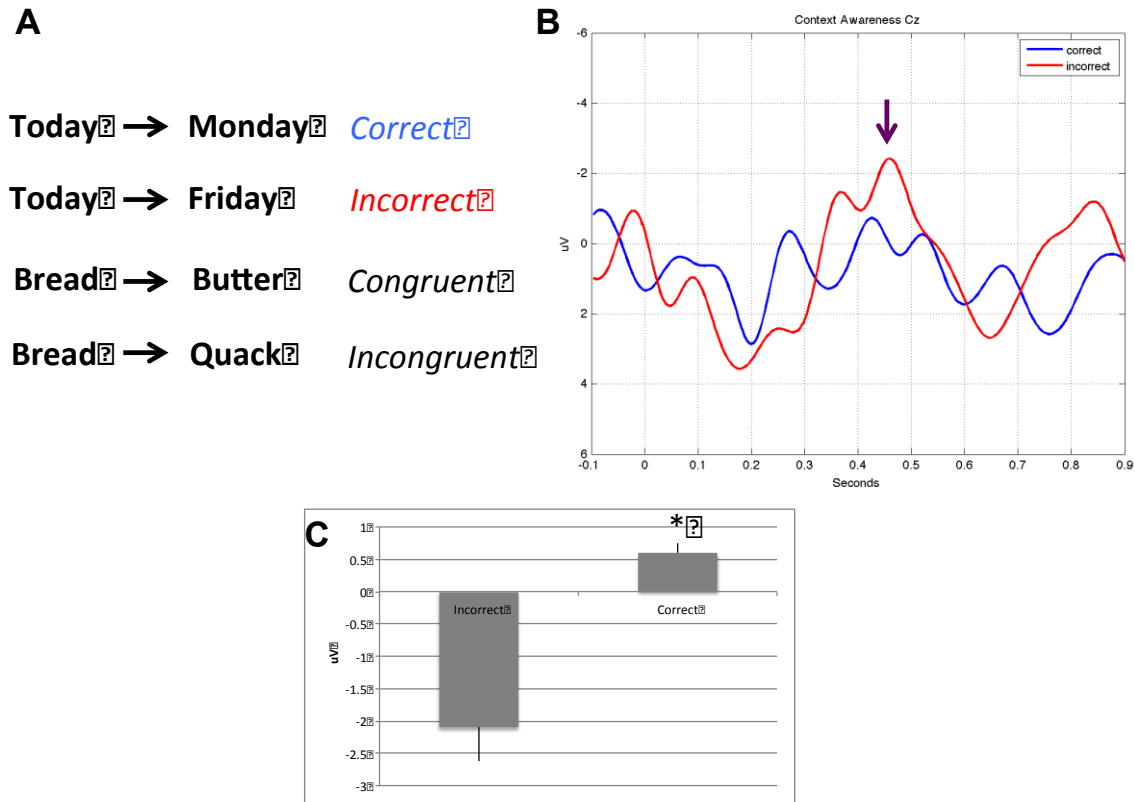
Figure 5.6.   Original Stimulus Sequence for Orientation Processing Assessment
A) Sample stimulus for eliciting orientation (correct/ incorrect) and language (congruent/ incongruent) processing. Black arrow indicates direction of relational content used for subsequent extraction of ERPs of interest. Correct refers to stimuli related to the present context/situation whereas incorrect refers to stimuli unrelated to the current situation/context. Example shown for when testing is undertaken on a Monday. **B)** Group averaged ERP showing responses corresponding to stimulus related to current situation/context (correct) and unrelated to current context/situation (incorrect). Purple arrow indicates ERP response of interest showing differential processing of correct and incorrect stimulus, peaking at 450ms post-stimulus presentation. Time zero represents moment of stimulus delivery/presentation. **C)** Quantitative measures of responses to two types of stimuli, shown as mean ± SEM across group of 6 participants within the 300-500ms time interval post-stimulus presentation. *p<0.05 across conditions.

While this stimulus sequence was successful in eliciting the expected orientation related responses as shown in Figure 5.6, the need for explicit priming of the participant with information (e.g. 'Today') ultimately limited the overall timing of the stimulus sequence (and therefore testing) to 10 minutes. In order to further shorten the sequence, a key innovation was introduced by way of multiplexing the role of the first word in the

115

word pair to both serve as a priming word for the language processing contrast and also to itself be a target stimulus for orientation processing. While this removed the explicit priming of the participants to the orientation stimuli, it also ensured a stimulus sequence that was only 5 minutes long (involving 60 word pairs rather than 120). As shown in 5.3.1, this innovation was successful in capturing orientation processing related neural markers while balancing the need for a shorter stimulus sequence.

5.8. Author Contributions

This study was conducted in collaboration with co-authors who contributed to data collection and some study design.

Chapter 6.   Study IV: Maximizing Signal Capture for Rapid and Low-Density POC Operations

Content of this chapter under consideration for publication as: Ghosh Hajra S, et.al. (2019). Enhancing event related response measurability using dynamic SNR-weighted signal augmentation: simulation and experimental demonstrations. *IEEE Transactions on Biomedical Engineering.* (Revisions requested)

6.1. Abstract

Objective: Electroencephalography (EEG) derived event-related potentials (ERPs) are promising for diagnosis and prognostication in brain diseases, but have traditionally had signal-to-noise ratio (SNR) challenges. This study aims to develop and evaluate a method using multi-channel data fusion to improve the measurability of ERPs. *Methods:* Per-channel ERP waveforms were combined, weighted by their relative SNR, to create a channel pool. Signals from this and an existing pooling technique, and un-pooled individual electrodes were subjected to statistical analysis of the sensation (N100), attention (P300) and language processing (N400) ERPs within the *brain vital signs* paradigm from 37 healthy participants. A Cohen's *d*-like statistic was used to measure effect size for each ERP derived from pooling schemes and un-pooled electrodes. Similar analysis using simulated data was also undertaken as "ground truth" assessment of the impact of pooling techniques. The impact of channel pooling on the ability of machine-learning classifiers to distinguish among ERP condition waveforms was also assessed through comparisons of accuracy. *Results:* In both Monte-Carlo simulation and experimental data, the results show that the new pooling technique improves the measurability of neural responses compared to un-pooled electrodes and an existing channel pooling technique ($p<0.001$). Improvements in machine-learning classification were observed for the N400 ERP ($p<0.01$), but not for the N100/P300 ERPs. *Conclusion:* The results suggest that the new technique improves measurability of neural responses relative to existing techniques. *Significance:* The current technique may enable the application of ERP techniques in rapid testing (low trial numbers) scenarios and allow for assessments in real-world (low SNR) environments.

6.2. Introduction

In recent years, there has been increasing interest in utilizing non-invasive brain imaging technologies to provide objective, physiology-based measurements of brain function. These physiology-based measures help to augment existing behaviour-based assessments that have been shown to be highly subjective and error-prone [14], [28], [47]. Among the available neuroimaging options, electroencephalography (EEG) is particularly advantageous due to its low cost and portability compared to larger, fixed-infrastructure systems such as magnetic resonance imaging (MRI) and magnetoencephalography (MEG) [81], [220]. Moreover, EEG-derived measures such as event-related potentials (ERPs) have been shown to be capable of indexing numerous aspects of brain function, spanning both low-level sensory processes and high-level cognitive responses[48], [107]. In fact, both our group and others have previously demonstrated the significant utility of ERPs in capturing age-related changes in brain function[159], [200], and also cognitive changes in injury, disease, and recovery[71], [75], [221], [222].

ERP assessments in both research and clinical settings rely on comparing the brain's responses to different types of stimuli (Figure 6.1A). Responses of interest are known as ERP components, the magnitudes of which are typically measured by first identifying the particular features of interest in the waveform (e.g. peak of specific polarity within an expected time interval[131]), then contrasting the signal amplitudes between different experimental conditions (i.e. type of stimuli). Thus, the goal of many ERP experiments is to increase the measurability of an effect of the experimental manipulation. This measurability, often quantified through effect size (ES) measures, can be improved by either increasing the difference between the means of the experimental conditions, or by decreasing the variance of that difference. Increasing the difference among the means is generally considered infeasible and so reduction of variance is commonly pursued through various signal-processing approaches[223]. One of the key technical challenges in ERP application and a major contributor to the variance, is the fact that the neural responses of interest are orders of magnitude smaller than background EEG signals (i.e. very low signal-to-noise ratio)[224], [225]. To overcome

this challenge, traditional ERP experiments enhance the signal-to-noise ratio (SNR) of the response (and reduce variance) by averaging the signal over a large number of repeated trials (Figure 6.1B). As the response of interest is time-locked with stimulus onset while the background EEG signals are uncorrelated with the stimulus, trial-averaging in this manner enables the effective removal of background EEG signals while retaining and enhancing the neural response of interest[48], [226]. Nonetheless, a significant drawback to this approach is the lengthy experimental time necessary for obtaining a large number of trials. Moreover, the use of this strategy is further constrained by practical considerations in ERP methodology, such as habituation, participant compliance or fatigue, as well as clinical challenges such as rapidly changing attention and awareness levels in patients [158].
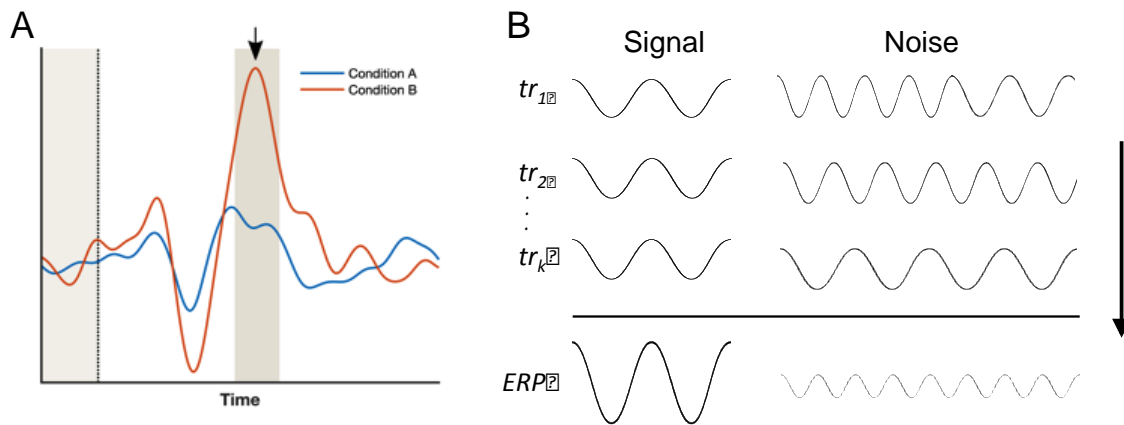
Figure 6.1.   Sample ERP waveforms illustrating experimental methodology and ERP trial averaging process.
(A) Brain responses to specific stimuli are measured by contrasting a target experimental condition (Condition B, orange) with a control condition (Condition A, blue). Black arrow indicates the response peak of interest, or ERP component. Black dotted line denotes moment in time when stimulus is presented. ERP component are typically evaluated by quantifying amplitude differences between the two conditions over an interval of interest spanning the peak (dark shaded region). Additional comparisons are also made with the signals during a pre-stimulus baseline interval (light shaded region). **(B)** ERP waveforms are generated through conditional averaging of several trials ("tr"), each of consists of a signal and a noise component. This process relies on the event related neurophysiological signal of interest ("Signal") having the same morphology and latency in each trial in contrast to the noise components ("Noise") being uncorrelated from trial to trial. Under this assumption, the ERP component, while not easily distinguishable from noise at the trial level, becomes distinguishable from the residual noise when k trials are averaged together as the signal-to-noise increases by a factor of $\sqrt{k}$.

Since ERP experiments generally utilize multi-channel electrode arrays that cover the scalp, another common approach for further enhancing ERP signals is by averaging over several adjacent electrodes within an area[223]. As EEG signals are

generated by the propagation of electric fields through the brain and other tissues of the head, electrodes within the same region of the head can be expected to capture similar brain activity[225]. Thus, pooling together data from several electrodes enables the effective total number of trials to be further increased (with corresponding decrease in variance) without lengthening the experimental time. However, given that the relative amounts of signal and noise content in individual channels are likely to vary depending on factors such as their respective scalp-electrode impedances[227], pooling together several channels without accounting for these differences may lead to inaccuracies in the captured ERP signal. Indeed, there have been reports of the blurring of the ERP effects following channel pooling resulting in attenuation rather than improvement of statistical measures of differences among experimental conditions [228].

To address these challenges and improve ERP measurement, a new technique is needed that can retain the good features of channel pooling and enhance ERP signals but without introducing inaccuracies due to cross-channel signal quality variation. Here, we present a new approach using dynamic SNR-weighted signal capture (dSNRw) that enables the pooling of multiple channels while dynamically accommodating potential differences in signal quality for each electrode. Specifically, our technique first quantifies the relative signal-to-noise content of each channel and condition, then uses this information to inform ERP response measurement. The current study validates the dSNRw approach using both simulated ground-truth data and 64-channel EEG data collected on healthy adults. Our results show that the dSNRw technique improves ES measurements for multiple ERP components that index sensory, attention, and language processing responses. This technique represents a significant improvement compared to traditional channel-pooling approaches for ERP measurement, and will crucially enable continued applications of ERP technology in both clinical and research domains.

6.3. Methods

6.3.1. Participants

Thirty-seven healthy individuals (34 ±12years, 16 females) volunteered for the study. All were fluent in English, had normal hearing, and normal or corrected-to-normal vision. None had history of neurological disease or psychoactive medications. The study was approved by the Research Ethics Boards at Simon Fraser University and Fraser

Health Authority, and all participants provided written informed consent prior to data acquisition.

6.3.2. Stimulus Paradigms

ERP experimental paradigm used auditory stimulation from the *brain vital signs* framework, which enables the elicitation and evaluation of a spectrum of ERP brain responses in about 5 minutes [229]. This paradigm utilizes a series of interlaced auditory tones and spoken words to elicit a variety of ERP components spanning auditory sensation (N100 ERP,[61]), attention (P300 ERP, [62]), and language processing (N400 ERP, [63]). This framework has been validated in numerous studies across multiple imaging modalities including MEG as well as both low- and high-density EEG [182], and has recently also been expanded to the visual modality [107]. Details of the stimulus sequences have been presented elsewhere [229], [230]. Briefly, the tones were 250 ms in duration and comprised two types of sounds: a more frequently occurring *standard* tone (740 Hz, 75 dB, 80% occurrence), and a less frequently occurring *deviant* tone (1047 Hz, 100 dB, 20% occurrence). The words were presented in pairs across two equally likely experimental conditions: the *congruent* condition consisted of two words that were congruent in meaning (e.g. 'Bread' 'Butter', 50% occurrence), and an *incongruent* condition in which the words did not agree in meaning (e.g. 'Bread' 'Quack', 50% occurrence). The N100 (sensation) and P300 (attention) ERP components were derived by comparing the *standard* and *deviant* response waveforms, while the N400 component was derived by contrasting waveforms between the *congruent* and *incongruent* conditions.

6.3.3. Data Acquisition

EEG data were collected using a 64-channel system with active Ag/Ag-Cl electrodes (BrainAmp 64-channel with actiCap) in a dedicated EEG room with consistent conditions such as lighting levels. Skin-electrode impedances were maintained below 20kOhms, and binaural auditory stimulation was provided to the participants via insert earphones (ER4), while they maintained visual fixation on a cross displayed on a screen 75cm away. Stimulus delivery and time stamping signals were controlled by Presentation software (Neurobehavioral Systems Inc.), and EEG data (with concurrent

time stamping signal recording) were recorded using BrainVision Recorder software (Brain Products GmbH).

6.3.4. Data Pre-processing and ERP generation

Raw EEG data were first visually inspected, and artifactual channels were removed. Data were then notch-filtered to remove power line noise (60Hz), band-pass filtered (0.1-50Hz), and automatic artifact rejection was applied using a gradient analysis approach with 10 μV/ms as threshold. Thereafter, independent component analysis (ICA, [164], [196]) was employed to select and remove artefacts corresponding to ocular, muscular, cardiac and other sources based on previously established criteria [104]. For each channel, the ICA-cleaned data were then low-pass filtered to 20 Hz, segmented (-100 to 900ms epochs relative to stimulus onset), baseline corrected (-100 to 0ms), and conditionally averaged to generate the ERPs using established procedures [47], [48].

6.3.5. Multi-Channel Data Fusion

Once ERPs were generated for each channel as outlined above, data from channels were pooled together in two different approaches – 1) using the traditional channel pooling technique and 2) using the new dSNRw technique. The channels selected for pooling were dependent on the ERP of interest due to the spatial distribution differences among the N100, P300 and N400 ERP responses [107]. Specifically, data from Fz and Cz electrode sites were pooled for the N100 and P300 ERPs since these responses are maximal at fronto-central sites, whereas data from the Cz and Pz electrodes were pooled for N400 as it is maximal at centro-parietal sites [182].

Traditional channel pooling Technique

The commonly accepted technique for channel pooling entails signal augmentation through the process of time-point by time-point averaging across the channels being pooled for each stimulus/experimental condition, described mathematically in (1).

$$C_{pooled}(s,t) = \sum_{n=1}^{N} \frac{1}{N} C_n(s,t) \tag{1}$$

where, C_{pooled} is the combined signal from each channel C_n for stimulus type *s* and all time *t* within an epoch/trial, and N is the total number of channels pooled.

Each channel being pooled has a signal and a noise component. Generally, the channels being pooled are in close proximity to each other, and due to the volume conduction process underlying the generation of EEG signals, the distribution of values of the signal being recorded in each of them can be regarded as similar. In contrast, the noise component remaining after signal processing depends on various instrumentation and physiological factors, and therefore may be different among the channels. The impact of the traditional channel pooling process on the noise factor can be analytically modelled as a mixture of Gaussian distributions as shown in (2).

$$f(x) = \sum_{i=1..n} w_i \, N_i(\mu_i, \sigma_i) \tag{2}$$

where, f(x) is the probability density function (PDF) of the channel created from the pooling/mixture, N_n is the PDF of the individual channel noise with mean µ and standard deviation σ, w_n is the weighting factor (=1/n), n is the number of channels being pooled.

From (2), it follows that any moment *k* can be calculated as shown in (3), and the variance (2nd moment) of the mixture/pool can be calculated as shown in (4).

$$\mu^{(k)} = \sum_n w_n \, \mu_n^{(k)} \tag{3}$$

$$Var(f) = \sum_n w_n \, \sigma_n^2 + \sum_n w_n (\mu_n^{(1)})^2 + \left(\sum_n w_n \, \mu_n^{(1)} \right)^2 \tag{4}$$

where, $\mu^{(k)}$ is the kth moment of f, and $\mu_n^{(k)}$ is the kth moment of N_n. Var (f) is the variance of the mixture of the pooled electrodes/channels.

Using Jensen's inequality, the variance of the mixture can be stated as the mixture of the variances plus a term to account for the dispersion of the means. With the filtering and baseline correction steps in ERP generation, the noise distributions of the component channels in the pool can be considered to be zero-mean Gaussians and so (4) can be further simplified to be the weighted mix of the underlying variances.

In the simplest case of pooling of two electrodes/channels, A and B, each with noise components that are zero-mean and variances σ_A and σ_B respectively using the traditional channel pooling (i.e. w=0.5), the variance of the mixture/pool based on (4) can

123

be written as Var (A+B) =(0.5) $\sigma_A{}^2$ + (0.5) $\sigma_B{}^2$. If the component channel noise variances are equal, the variance of the noise component of the mixture/pool remains the same and the measurability of the ERP effect improves due to the impact of trial averaging process mentioned previously. However, if the two variances are unequal (e.g. $\sigma_B = 2$ σ_A), the variance of the pool actually becomes larger than the original variance of each channel thereby increasing the impact of the noise and potentially obscuring the ERP effect. While the example here utilized the simplest case of pooling two channels, the same challenges exist when multiple channels are part of the pooling as well. However, weighting the constituent channels of the pool differently based on the relative amounts of noise, rather than a constant weighting as applied in the traditional channel pooling technique, can mitigate the negative impact of the mismatched variances.

Dynamic SNR-Weighted (dSNRw) Technique

To account for variation in signal quality across different electrodes, the dSNRw technique first quantifies the relative contribution of the signal of interest compared to noise for each channel. In line with previous work [231], the pre-stimulus interval is considered to not contain significant stimulus/event related neural response and therefore is used as surrogate of the amount of noise remaining after signal-processing steps have been undertaken to minimize the contamination. Since the signal of interest (ERP amplitude) is generally evaluated within a time interval of interest post stimulus presentation, SNR is commonly defined as shown in (5).

$$\text{SNR} = \frac{\overline{y_{tw}}}{\sigma_{M,b}} \qquad\qquad (5)$$

where, $\overline{y_{tw}}$ is the mean amplitude of the ERP waveform within a time interval of interest (*tw*, e.g. 250-500ms for P300), and $\sigma_{M,b}$ is the standard error of the waveform within the pre-stimulus baseline internal.

Once the SNR for each channel has been evaluated, the dSNRw technique performs a weighted combination of signals from the constituent channels depending on relative noise contributions as shown in (6).

$$C_{dSNRw}(s,t) = \sum_{n=1}^{N} w_n C_n(s,t) \qquad\qquad (6)$$

where, C_{dSNRw} is the combined signal from each channel C_n for stimulus type *s* and all time *t* within an epoch/trial combined using the dSNRw technique, w_n is calculated as the ratio of the SNR of the channel divided by the sum of the SNR values of all channels in the pool (i.e. $SNR_n/(SNR_1+SNR_2+...+SNR_N)$) and N is the total number of channels pooled.

6.3.6. Assessing Impact of Channel Pooling on Feature-based ERP measurability

As highlighted previously, the goal of most ERP experiments is to assess the brain's response to a stimulus condition of interest and contrast it with a control condition. Thus, maximising the separation among the waveforms for the experimental and control conditions within specific time windows of interest (corresponding to the ERP peak as shown in Figure 6.1) is key to enhancing the detection of the ERP effect and can be quantified using effect size (ES) measurements as shown in (7).

$$ES_i = \frac{|\hat{X}_{iB}(t_W) - \hat{X}_{iC}(t_W)|}{\sigma(t_W)} \qquad (7)$$

where, X_{iB} and X_{iC} are means of conditions 1 and 2 respectively (e.g. deviant and standard stimuli for P300, congruent and incongruent stimuli for N400) and σ is the pooled standard deviation, both measured within time intervals of interest t_W (e.g. 80-180ms for N100, 250-550ms for P300, 300-600ms for N400).

The impact of the two channel pooling techniques (traditional and dSNRw) was assessed with both simulated and experimental data, using ES as the comparison metric. The simulated data were used as "ground truth" to assess the impact of variable noise levels in the channels being pooled using the two channel pooling techniques, and the real-world experimental data were then utilized to confirm the findings across ERPs ranging from sensation (N100) to attention (P300) to higher-level cognition (N400).

Assessing performance with Monte-Carlo simulation

Synthetic data, created by combining template ERP waveforms with simulated noise vectors, was used to assess the impact of the channel pooling techniques on the

measurability of ERPs in situations of equal and unequal noise among the channels being pooled. Data from healthy participants tested using the *brain vital signs* framework, as described in [107], [159], were utilized to generate template ERPs corresponding to P300 and N400 ERP responses. Specifically, this entailed grand-averaging the neuronal responses at the Cz electrode site to standard and deviant stimuli (for P300), and congruent and incongruent stimuli (for N400) to create pairs of template waveforms. Using an additive model of ERP generation[232], the template ERP waveforms were combined with simulated noise, modelled as background EEG, as shown in Figure 6.2(A) to create channels of simulated ERP data.

	Traditional Pooling	dSNRw Pooling
Equal Noise	Pooling: $(y_1 + y_2)/2$ Noise: $\mathrm{pwr}(\eta_1) = \mathrm{pwr}(\eta_2)$	Pooling: $(w1*y1 + w2*y2)/2$ Noise: $\mathrm{pwr}(\eta_1) = \mathrm{pwr}(\eta_2)$
Unequal Noise	Pooling: $(y_1 + y_2)/2$ Noise: $\mathrm{pwr}(\eta_1) \neq \mathrm{pwr}(\eta_2)$	Pooling: $(w1*y1 + w2*y2)/2$ Noise: $\mathrm{pwr}(\eta_1) \neq \mathrm{pwr}(\eta_2)$
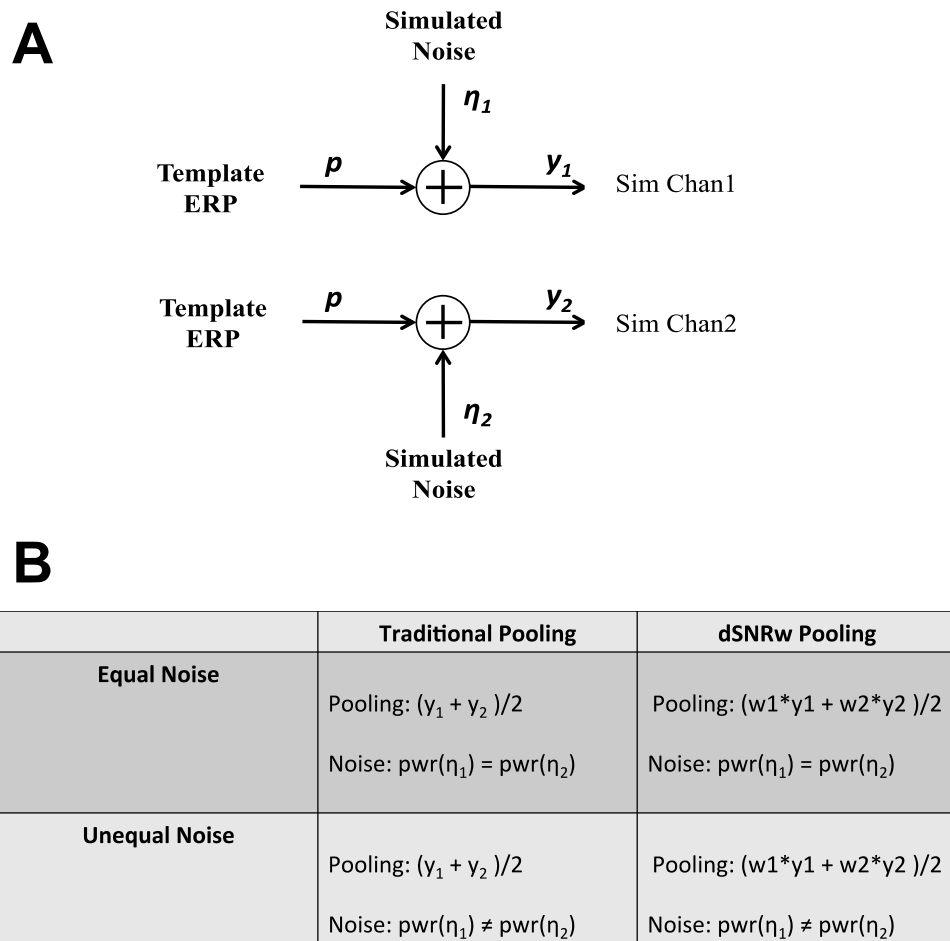
Figure 6.2.   Overview of simulation process
(A) Template ERP waveforms generated from healthy participants were combined with simulated noise signals to create channels of simulated ERP data. **(B)** Simulated channels of data were generated under two scenarios – 1) with the power of the noise being equal in both simulated channels, and 2) power of the noise being unequal in the two simulated channels. Data from both scenarios were combined using the traditional channel pooling and the dSNRw techniques.

Previous work has demonstrated that background EEG can be modeled as a 3rd-order auto-regressive (AR) process, with coefficients estimated by the Burg method [233], [234]. This is modeled as described in (8), where η(t) is the auto-regressive process and r(t) is Gaussian white noise driving the system, and parameters $(\alpha_1, \alpha_2, \alpha_3)$ are as described in previous work [234].

$$\eta(t) = \alpha_1(t-1) + \alpha_2(t-2) + \alpha_3(t-3) + r(t) \quad (8)$$

For each of P300 and N400 ERP, the template ERP waveforms (example shown in Figure 6.3(A)) were combined with 30 AR models to generate 30 simulated "trials" as shown in Figure 6.3(B). These simulated trials were then averaged together to generate simulated ERPs for one "participant" (Figure 6.3(C)); with the process repeated 100 times to generate simulated ERPs for one simulated channel for 100 simulated "participants". The entire process was then repeated for the second simulated channel using the same template ERPs, first with equal power of the additive noise as the first channel, and then with different power of the additive noise compared to the first channel. As shown in Figure 6.2(B), data from the two simulated channels were combined using both the traditional channel pooling and the proposed dSNRw technique.

The effect size, defined in (7), of the resultant ERP following the channel pooling was used as a metric to assess the impact of the two pooling techniques under both equal and unequal noise power of the two channels. Specifically, this entailed selecting a subset of simulated participants (out of the 100 simulated participants), for each selected participant calculating the effect size within a time interval of interest across the pairs of waveforms/conditions combined using both the traditional and the dSNRw techniques. The time interval of interest for ES calculations were 250-550ms post-stimulus presentation for P300, and 300-600ms for N400, in line with prior literature [65], [107]. This process was repeated 1000 times, with 10 simulated participants selected in each repetition for the calculations. Paired t-tests were utilized to compare the outcomes of the two channel pooling techniques for both equal and unequal noise level scenarios, with p<0.001 considered to be significant.
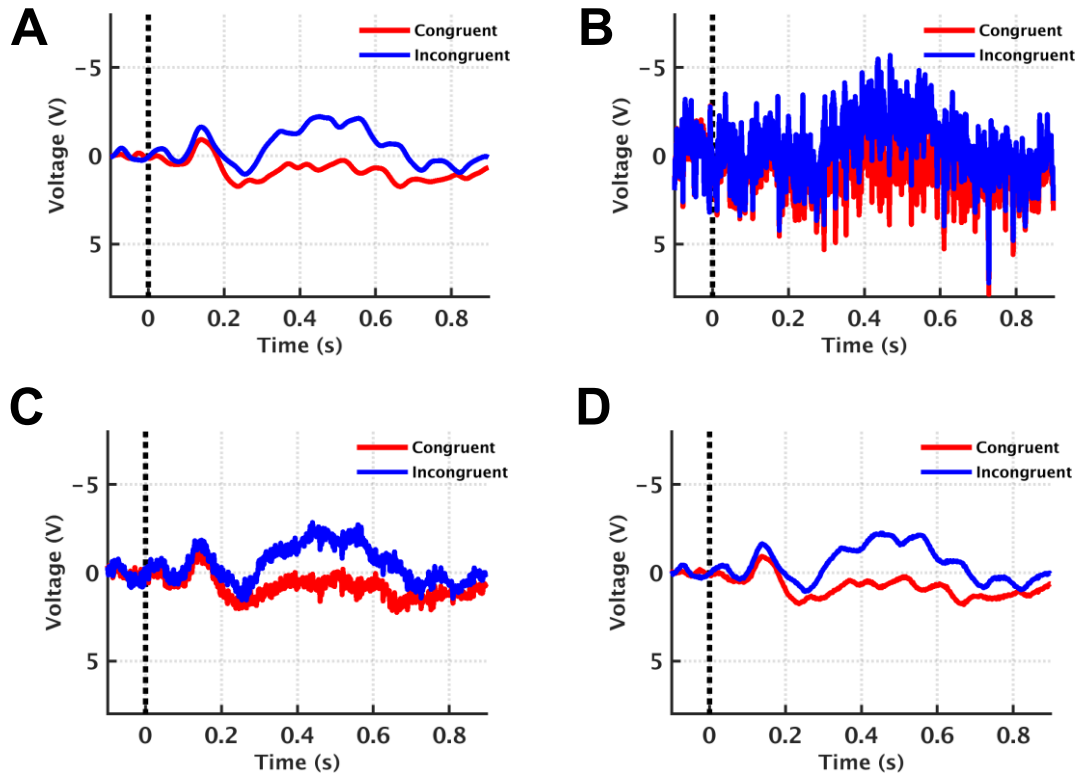
Figure 6.3.   Sample waveforms of real and simulated N400 ERP.
(A) Grand averaged ERP from experimentally derived results from healthy participants used as template ERP in the data generation process. **(B)** Sample simulated single trial generated by combination of template ERP shown in (A) with an auto-regressive process. **(C)** Sample simulated participant level waveforms derived by conditional signal averaging of 30 simulated single-trials like that shown in (B). **(D)** Group-level grand averaged ERP waveforms of 100 simulated participants derived by averaging simulated participant-level waveforms.

Assessing performance with experimental data

Following the generation of ERPs for each channel as described in 6.3.4, channel-level data were pooled using both the traditional and the dSNRw techniques as detailed in section 6.3.5. Specifically, due to the fronto-central distribution commonly observed for N100 and P300 ERP components, data from the Fz and Cz electrode sites were pooled together, whereas due to the centro-parietal maxima of N400 data from the Cz and Pz sites were combined for N400 ERP. The effect size of the ERP data generated by pooling channels using traditional and dSNRw techniques were compared to each other and to the individual electrode with the largest effect size. Statistical

analysis utilized a bootstrapping approach using sub-selection of participants from the available data pool to compare single channel ERP effect sizes and the two combinatorial techniques. Specifically, this entailed selecting a subset of 10 participants, and calculating the effect size as defined in (7) for each of the individual channels as well as the pooled channel formed using each of the traditional and dSNRw channel pooling techniques. This process was repeated 1000 times, and the calculated effect size measures across the two pooling approaches as well as single-channel ERP measures were assessed with 1-way ANOVA (with Huynh-Feldt corrections for violation of sphericity assessed with Mauchly's test) to identify omnibus effects of the combination approach, and paired t-tests with Bonferroni correction for multiple comparisons for post-hoc analysis of significant effects.

6.3.7. Assessing Impact of Channel Pooling on Feature-free ERP Assessment

Assessments of ERPs generally focus on specific features of interest such as peaks and troughs of waveforms that signify ERP components, which are considered to index specific cognitive functions. Additionally, however, feature-free assessments are also being undertaken. Such assessments generally apply machine learning based techniques to the entire ERP waveform rather than focusing on specific waveform features. While feature-free assessments enable confirmation of the absence or presence of differences among the pairs of ERP waveforms, feature-based assessments are the focus of most ERP experiments since they enable assessments of specific cognitive functions. Perhaps a good example of this is a recent study employing ERPs from the *brain vital signs* framework in concussion assessment. The study demonstrated that while waveform differences among the pairs of conditions (e.g. standard and deviant stimulus conditions) were present in all participants, specific ERP features (e.g. amplitude of attentional P300) distinguished participants with concussion [222]. Nonetheless, as shown in Figure 6.4, in addition to assessing the impact of the channel pooling on specific waveform features (as detailed in section 6.3.6), the impact of channel pooling techniques on feature-free machine learning based analysis was also undertaken.
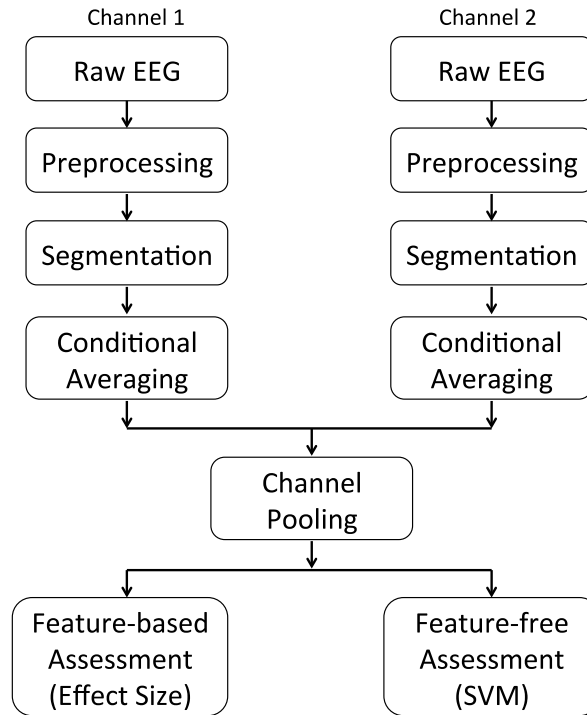
Figure 6.4. **Flowchart of data analysis and assessment of channel pooling techniques.**
Each EEG channel was processed using semi-automated commonly accepted techniques including removal of artifactual data channels, re-referencing, filtering, segmentation and conditional averaging to generate ERPs. Once per-channel ERPs were generated, data from two channels were combined to create pooled channel using both the traditional and the dSNRw techniques. ERPs in the pooled channels generated with the two pooling techniques were compared to each other as well as to single electrode ERPs by assessing the impact on specific features of interest (measured using effect size calculated across paired ERP waveforms) and the impact on the overall waveform (assessed via accuracy of support vector machine classifications).

Specifically, using previously demonstrated techniques[65], [159], [230] support vector machines (SVM) were trained as two-category classifiers to distinguish between the stimulus conditions within the ERP experiment (i.e., between standard and deviant condition waveforms for N100/P300 and between congruent and incongruent waveforms for N400). Three SVM classifiers with radial kernels were utilized with inputs of either ERP data from two of the three electrodes (Fz and Cz for N100/P300, Cz and Pz for N400), or the signals generated by pooling the two electrodes using the traditional approach, or the signals obtained by combining electrodes with the dSNRw technique. For each input data feature type, ninety percent of the available data was used to train the classifier and the remaining ten percent was used to assess the accuracy of

classification. Within a 10-fold cross validation framework, this process was repeated 10 times to ensure that the classifier was trained and tested on all available data. The total number of correct classifications relative to the total number of classifications provided the accuracy number. The above process was repeated 100 times to generate a distribution of the accuracy numbers. The results from three SVMs with the different input types (channel data, pooled data with traditional approach, and pooled data using the dSNRw technique) were compared using paired t-tests with Bonferroni correction for multiple comparisons.

6.4. Results

6.4.1. Feature-based analysis with simulation data

Simulated channel-level ERP data were generated by combining simulated noise vectors with template ERP waveforms corresponding to standard and deviant stimulus conditions for P300 and congruent and incongruent stimulus conditions for N400. Such simulated channel level ERP waveforms were combined using both traditional and dSNRw techniques, and effect size measurements were undertaken within specified time windows across the pairs of waveforms. Effect size measurements on simulation data showed that the dSNRw combinatorial technique better captures the difference among the ERP waveform pairs compared to traditional channel pooling (Figure 6.5). The differential impact of the two pooling techniques is prominent when the channels being combined had varying background noise levels ($p<0.001$), but no significant differences are observed when the same level of noise is present in the channels being pooled. In fact, the effect size measures for the equal noise scenario are highly correlated across the two combination approaches (simulated P300: $r=0.8996$, $p<0.001$; simulated N400: $r=0.8792$, $p<0.001$).
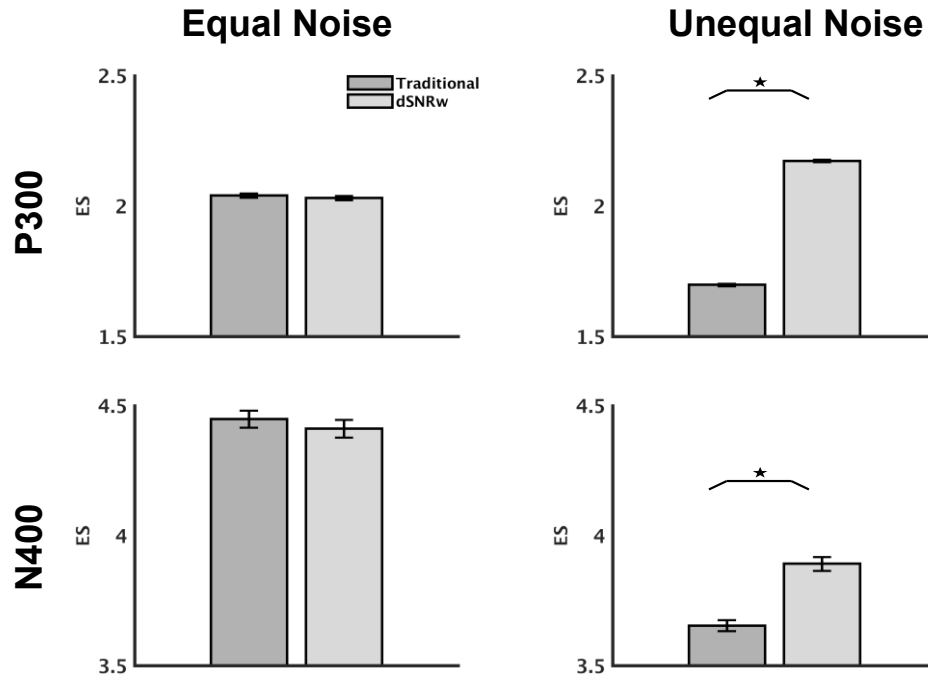
Figure 6.5.   Effect size measurements for simulated P300 and N400 ERPs with varying noise levels for channels being combined.
Effect sizes (ES) were calculated within Monte-Carlo analysis framework with 1000 repetitions and selection of subset of simulated participant in each repetition and calculating the ES across the two conditions of interest for each ERP. Results are shown across 1000 repetitions as mean ± SEM. The dSNRw signal combinatorial approach outperforms the traditional channel pooling technique in the presence of unequal noise levels in the channels being pooled for both simulated P300 and N400 ERPs. No significant differences among the techniques were observed for the situation of equal noise levels in the channels being pooled. *p<0.001.

6.4.2. Feature-based analysis with experimental data

ERP waveforms corresponding to the standard and deviant conditions from the Fz and Cz sites were combined using both the traditional and the dSNRw techniques, and the effect size corresponding to N100 and P300 ERP components were calculated. For N400, waveforms corresponding to the congruent and incongruent condition from the Cz and Pz sites were combined in a similar fashion and effect size measurements were undertaken. In addition to comparing the ES of ERPs in the pooled channel derived from traditional and dSNRw channel pooling techniques, the ES of the individual channel ERPs were also assessed and the larger of the two channel ES values were used as a baseline against which the impact of the channel pooling techniques were measured as a percentage change.

In line with results from simulation data, the dSNRw approach also improved the measurability of ERPs corresponding to sensation (N100), attention (P300) and language processing (N400) in experimental data (quantified by effect size) as shown in Figure 6.6(left panel). The percentage change in the effect size measurements derived from the dSNRw and the traditional channel pooling approaches compared to the effect size of the largest single channel ERP results are also shown in Figure 6.6(right panel). Statistical analysis demonstrated a significant effect of combination technique for N100 $[F(1.4,1376.6)=80.7, p<0.001]$, P300 $[F(1.2,1204.0)=497.8, p<0.001]$ and N400 $[F(1.5,1531.2)=31.9, p<0.001]$. Post-hoc testing demonstrated that the dSNRw technique produced higher ES measurements compared to the traditional channel pooling, as well as the electrode with the largest effect size measurement ($p<0.001$, Bonferroni corrected). The improved measurability of the ERPs is further confirmed in Figure 6.6 (right panel) demonstrating the significant improvement in percentage increase of effect size measurements relative to the electrode with the largest effect size ($p<0.001$).
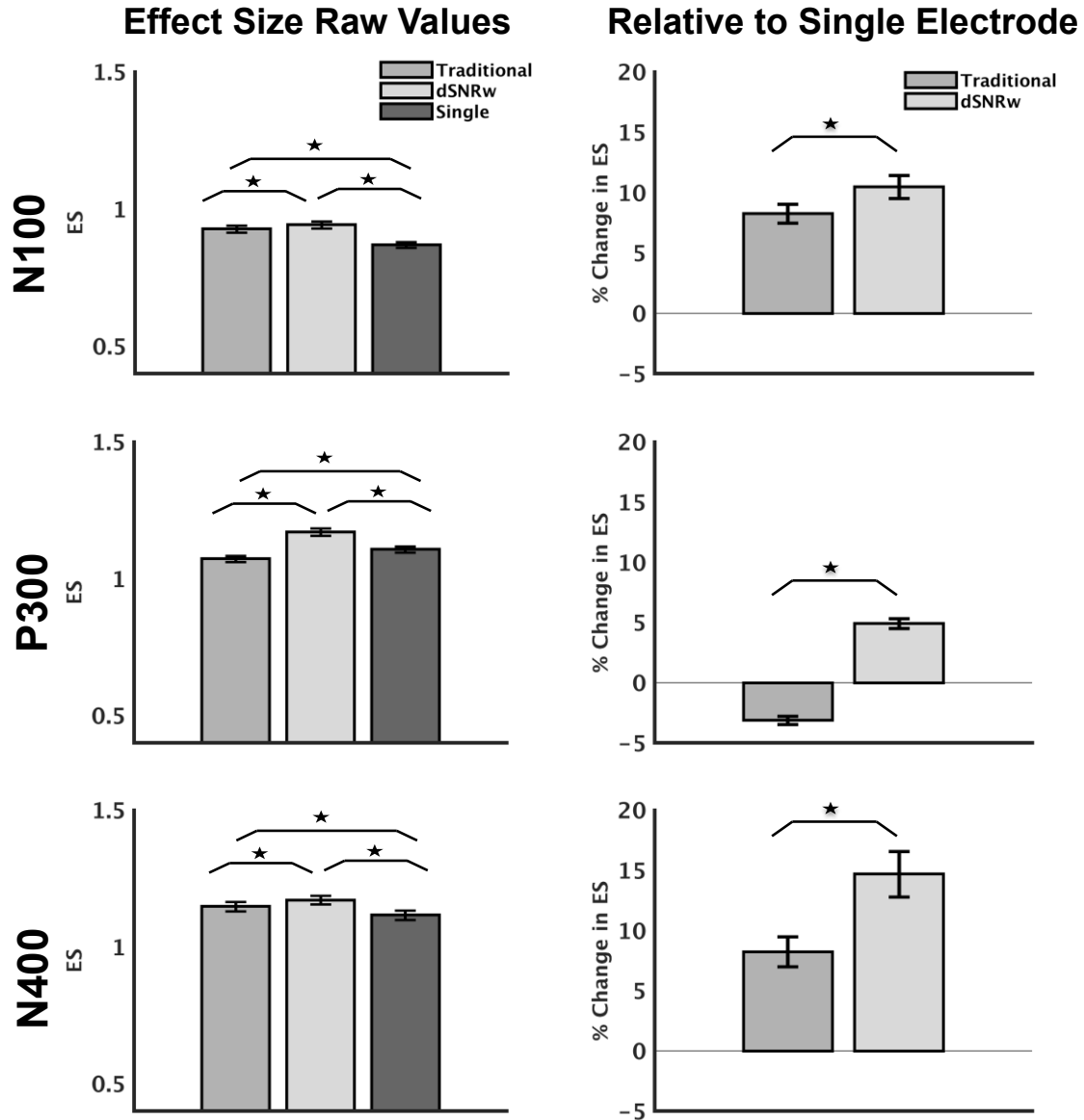
Figure 6.6.   Effect size measurements for experimental N100, P300 and N400 ERPs.

ES measurements from all 1000 repetitions shown as mean ± SEM. Left: ES measurements for all three ERPs are shown at midline electrodes. Right: The relative percentage change in ES for each of the two combinatorial approaches relative to the electrode with the largest ES are shown. All pair-wise comparisons were found to be significant at p<0.001 with Bonferroni correction for multiple comparisons. Traditional: conventional channel pooling approach, dSNRw: dSNRw channel pooling technique, Single: electrode with the largest effect size measurement.

6.4.3. Feature-free analysis

Further to assessments of the impact of channel pooling on specific ERP features through effect size measurements, the impact of channel pooling on feature-free machine learning based analysis were also undertaken. In particular, three machine learning classifiers were trained and tested using un-pooled ERP channel data, pooled signals using traditional channel pooling and pooled signals generated by the dSNRw combinatorial technique as inputs respectively. As shown in Table 6.1, the ERP waveforms generated using dSNRw pooling produced significantly better classification accuracies compared to traditional channel pooling and un-pooled ERP waveforms for the congruent/incongruent waveform discrimination potentially reflecting the N400 response (p<0.01, Bonferroni corrected). For the standard and deviant waveform discrimination, which embed the N100/P300 responses, classification accuracies obtained when using the un-pooled electrode ERP waveforms as input features, as well as the two channel pooling techniques were found to not differ significantly (p=0.07).

Table 6.1.   Support Vector Machine classification results.

Classification accuracies across all permutations shown as mean ± SEM. *p<0.01 across three SVMs (corrected for multiple comparisons).

	N100/P300 [%]	N400 [%]
Individual-channel ERP	95.08 ± 0.61	69.71 ± 1.92
Traditional Pooling	94.96 ± 0.56	65.43 ± 1.93
dSNRw Pooling	95.01 ± 0.67	76.43 ± 1.39 *

6.5.   Discussions

6.5.1. Main Findings

In this paper, we developed and validated a novel signal augmentation technique (dSNRw) that combines data from multiple electrodes/channels while accounting for the relative contributions of signal and noise within each channel. Our results indicate that the dSNRw technique generates waveforms that enable improved measurability of ERP features compared to waveforms generated from traditional channel pooling and individual channels. These results were confirmed using both "ground truth" simulated data and experimental data for ERPs spanning the entire information processing

spectrum from low-level auditory sensation (N100) to attention (P300) to high-level language processing (N400). Furthermore, in addition to improving the measurability of specific ERP features, the dSNRw technique also improved the classification accuracy of SVM classifiers when discriminating between congruent and incongruent stimulus condition waveforms (which contain the N400 response), but not when discriminating between the standard and deviant stimulus condition waveforms (which contain the N100/P300 response).

6.5.2. Feature-based analysis using simulated data

Typical models of EEG generation assume the brain tissue to be resistive, and therefore volume conduction mediated by a propagation vector with minimal capacitive effects is considered to give rise to the scalp-recorded potentials [225]. Within the context of ERP studies, the task-relevant ERPs are considered *signals* and all non-phase locked neural activity as well as interfering non-neural artifacts are considered *noise*, with the superposition of the two recorded at the electrodes [235]. The amount of signal and the amount of noise recorded at each electrode can therefore vary, with empirical studies with ERPs having previously demonstrated the impact of various external factors such as skin-electrode impedance on the signal-to-noise ratio [224], [227]. In the present study, the results demonstrate that when equal background noise is present in the channels being combined, both traditional channel pooling as well as the dSNRw technique perform equally (Figure 6.5 *left panel*). However, in the more realistic scenario of unequal noise levels, the proposed SNR-weighted combinatorial technique far outperforms the traditional channel pooling approach for both the attention (P300) and language processing (N400) neural markers (Figure 6.5 *right panel*).

6.5.3. Feature-based analysis using experimental data

Following the successful demonstration of the proposed technique using simulated data, the same technique was applied to real world experimental data collected using the *brain vital signs* framework [159] capturing neural responses corresponding to sensation (N100), attention (P300) and language processing (N400). Improvements in the measurement of ERP responses were observed for all three neural markers using the dSNRw technique relative to the single electrode/channel with the best effect size as well as the traditional channel pooling technique (Figure 6.6).

For the P300 response, the traditional channel pooling technique resulted in a reduction of effect size, and may be reflective of prior reports suggesting the blurring of amplitude effects due to channel pooling [223], [228]. In contrast, the application of the dSNRw technique resulted in an increase in measurability of the P300 response. Similarly, the dSNRw technique resulted in an almost doubling of ES of the N400 response (~8% improvement with traditional pooling vs. ~15% improvement with dSNRw technique). For N100 ERP, the improvements were not as dramatic (~8% for traditional vs. ~10% for dSNRw technique), and may be reflective of the inherent robustness of the N100 ERP [65].

Since ERPs are generated as conditionally signal averaged neural responses to pairs of stimuli (e.g. standard and deviant tone stimuli for P300) [47], [48], increases in measurement/effect size implies a reduction of the variance of the difference among the two pairs of waveforms for the conditions, resulting in more successful capture of neural responses. Most state-of-the-art ERP-based assessments currently rely upon the averaging of hundreds of trials [65], [75], often resulting in long testing times, with 30-90minutes being routine. However, as highlighted in previous work, most commonly used clinical assessments are pervasive in part due to their rapid assessment capabilities [81], and improved ES provides the possibility of reducing the number of trials (and therefore test time) necessary to capture reliable neural signatures thereby enabling more widespread clinical applications of ERP-based techniques.

6.5.4. Feature-free analysis using experimental data

While assessments of specific ERP components (i.e., peaks and troughs of the ERP waveform) remain the gold standard for all ERP experiments, certain ERP studies are also incorporating feature-free assessment of the entire waveform in order to provide an estimate of the ability of an unbiased, expert-independent machine learning classifier to distinguish waveforms corresponding to experimental and control conditions [65], [110]. Accordingly, in the present study, in addition to assessing the impact of channel pooling on specific ERP features, we also undertook assessments to determine the impact of channel pooling on feature-free machine learning based analysis of the entire waveform.

Specifically, three 2-class SVM classifiers were created, each with either the data from the two individual electrodes, or pooled data from traditional channel pooling or pooled data from dSNRw pooling. The waveforms generated with the dSNRw combinatorial approach resulted in significantly higher classification accuracies relative to traditional channel pooling and single-electrode waveform inputs when discriminating the congruent and incongruent stimulus conditions reflecting the N400 ERP (p<0.01). In contrast, when classifying the standard and deviant stimulus condition waveforms reflecting the N100/P300 ERPs, classification accuracies obtained for un-pooled electrode-level ERPs as well as the two pooling techniques did not differ significantly (p=0.07). At first, this may seem inconsistent with the results obtained using the effect size measurements. However, as articulated in previously published work[65], the difference among the classification and effect size results may be explained by the fact that the entire waveform is utilized as the input feature for SVM classification (in line with prior work [65]) whereas the effect size measurements are conducted on an *a-priori* specified time interval of interest corresponding to the ERP component.

The extremely high (>95%) classification accuracy for standard and deviant condition waveforms from un-pooled individual channel-level data are consistent with previous reports [65], [159]. For classification of the congruent and incongruent waveforms, the waveforms generated with dSNRw combination provided significantly better classification accuracy compared to individual channel-level waveforms (from Cz and Pz sites) and pooled data from traditional channel pooling. However, the reported mean accuracy of 76.43% is still lower than those reported when utilizing un-pooled channel-level waveforms from three (Fz, Cz and Pz) sites commonly employed for brain vital signs measurements; with previous studies reporting classification accuracies as high as 90% [65], [182]. Taken together, these results may represent the ability of the SVM classifiers to utilize the spatial distribution/variance information embedded within the channel-level waveforms. We acknowledge the speculative nature of this statement, but the results suggest that it may be more appropriate to utilize the un-pooled channel-level waveforms from the three electrodes as input without any channel combination for achieving the best classification accuracies for the N400 ERP response.

6.5.5. Caveats and Future Directions

While the results of the current study are promising for the initial validation of the dSNRw technique of signal augmentation, certain limitations of the study should be noted. First, in this study the midline electrodes (Fz, Cz and Pz) were studied as candidate electrodes for pooling for easy integration into the existing *brain vital signs* framework. Future work should focus on replicating these results using other electrode/channel montages which may be necessary for other applications (e.g. in and around the ears [236], [237]). Similarly, as an initial starting point, the results of the dSNRw combinatorial technique were compared to traditional channel pooling and single-electrode waveforms only within this study. However, this does not reflect an exhaustive comparative analysis with all signal combinatorial techniques (e.g. singular value decomposition or deep-learning based approaches are possible alternatives) and future work may be undertaken for more extensive comparisons. Finally, while this study utilized a sample size and best practises recommended for ERP studies [137], the results should be further verified using larger and/or distinct participant populations (e.g. patients).

6.5.6. Study Implications

All ERP experiments are focussed on eliciting and assessing specific ERP features that are embedded within background EEG and other unrelated neural, physiological, instrumentation and environmental noise, which are often orders of magnitude larger than the ERP features of interest [47], [48]. Signal conditioning and processing techniques such as differential amplification, filtering, trial averaging and channel pooling enable the isolation of the ERP features of interest by enhancing the contribution of the ERP features ('signal') and/or minimizing the impact of the unrelated artifactual noise [225]. However, techniques such as channel pooling were developed in the era when all ERP experiments were undertaken within pristine laboratory environments and EEG instrumentation mandated strict operating conditions (e.g. <5kOhm skin-electrode impedances). In recent years, there has been a resurgence of interest in ERPs, with experiments often undertaken outside laboratory environments (e.g. patient bedside [220], [221]) and modern EEG equipment now enable operations in less strict conditions (e.g. <30kOhm skin-electrode impedance with active electrodes [159]). Accordingly, while the relative signal and noise contributions may have been

similar across channels when experiments were undertaken within pristine environments and with lower impedances, that may no longer be the case when operating in more realistic environments and with higher skin-electrode impedances [227]. Our dSNRw technique thereby brings the channel pooling approach into the modern era by explicitly assessing the SNR of the channels being pooled and enabling dynamic combinations in order to retain the maximum signal contributions and minimizing the noise influences.

6.6. Conclusions

In this study, we developed and evaluated a novel signal augmentation technique based on dynamically combining multi-sensor data through SNR-weighting (dSNRw). Results from Monte-Carlo based simulations demonstrate the superiority of the dSNRw technique compared to the traditional channel combination approach in the realistic scenario of uneven noise levels among the channels being pooled. Real world experimental data on healthy individuals using *brain vital signs* targeting the sensation (N100), attention (P300), and language processing (N400) neural markers further confirms the importance of the dSNRw technique in improving the measurability of the ERP features of interest. While most ERP experiments focus on assessing feature-based analysis of specific ERPs, the results suggest that, if instead feature-free machine-learning based approaches to simply identify absence/presence of differences among waveforms (without regard for specific ERP features) are desired, then it may be more prudent to use un-pooled channel-level data. With the increasing use of ERP-based techniques, such as *brain vital signs*, for monitoring across various brain diseases and disorders including traumatic brain injury and dementia, the improvements in measurability afforded by the dSNRw technique further optimize the translation of EEG capabilities from research settings into clinical applications.

6.7. Supplementary Materials

6.7.1. Assessing dSNRw Technique at Mastoid Electrodes

Within the above mentioned study, midline electrode/sensor sites (Fz, Cz and Pz) were utilized, in line with existing brain vital signs work, to assess the impact of the

dSNRw technique on ERP effects of interest. However, in recent years, there has been an increase in interest in obtaining ERP-based metrics from in or around the ears as it provides an easy access point for application of EEG sensors. Indeed, several groups have created specialized sensors/equipment for recording EEG and ERP from these alternate sites [236]–[238]. In order to further assess the robustness of the dSNRw approach, the technique was also applied to combining data from sensors located near the ears (i.e., at mastoid locations). Specifically, data from T7 and T9 sensors were combined using the traditional and the dSNRw technique (same specific methods as described in Methods above), and compared using paired t-tests for assessing the impact on recording N100, P300 and N400 ERPs.
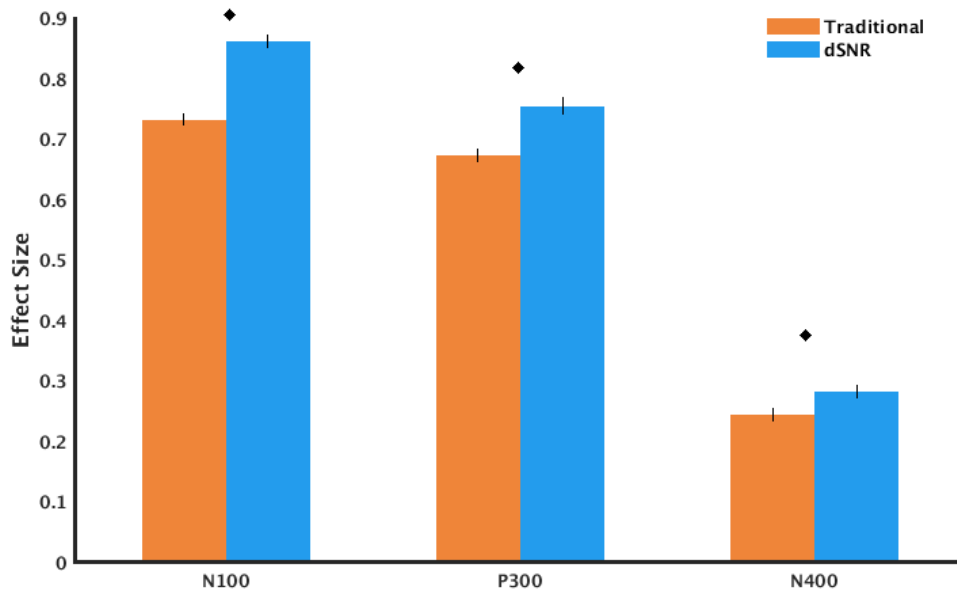
Figure 6.7.   Comparison of Traditional and dSNRw pooling techniques at mastoid locations

The dSNRw technique captures significantly better ERP effects of interest compared to the traditional channel pooling technique across all three (N100, P300 and N400) ERP components. For each ERP component, values shown for 1000 permutations of effect size calculations as mean ± std. error. Diamond signifies p<0.05 across pooling techniques.

While the general pattern of dSNRw outperforming traditional pooling holds for all three ERPs, the absolute effect size values are lower for N400 which may be a reflection of the source of the N400 (left temporal lobe largest contributor) being close to the

recording (T7, TP7) and reference (TP9) electrodes within this specific measurement scheme.

6.7.2. Assessing dSNRw Technique as Function of Distance to Reference Electrode

EEG is measured in reference to an electrode, and as mentioned in 6.7.1 often the relative location of the recording and reference electrodes can impact the amount of signal and noise captured. Accordingly, a sub-analysis was undertaken to assess the dSNRw technique by varying the distance of the electrodes being pooled from the reference electrode (specifically TP9). As shown in Figure 6.8, since P300 is a frontally concentrated response, electrode pairs were pooled starting from the outer periphery towards the midline in the left frontal quadrant (e.g. F5+FC5, F3+FC3 etc.); whereas for N400 as a posteriorly maximal response, electrodes in the left posterior quadrant were pooled starting from the periphery and moving towards the midline (e.g. CP5+C5, CP3+C3 etc.). The results indicate that as expected, the effect size increases with distance from the reference electrode, and furthermore dSNRw technique significantly improves the ERP effects capture in all instances (Figure 6.8).
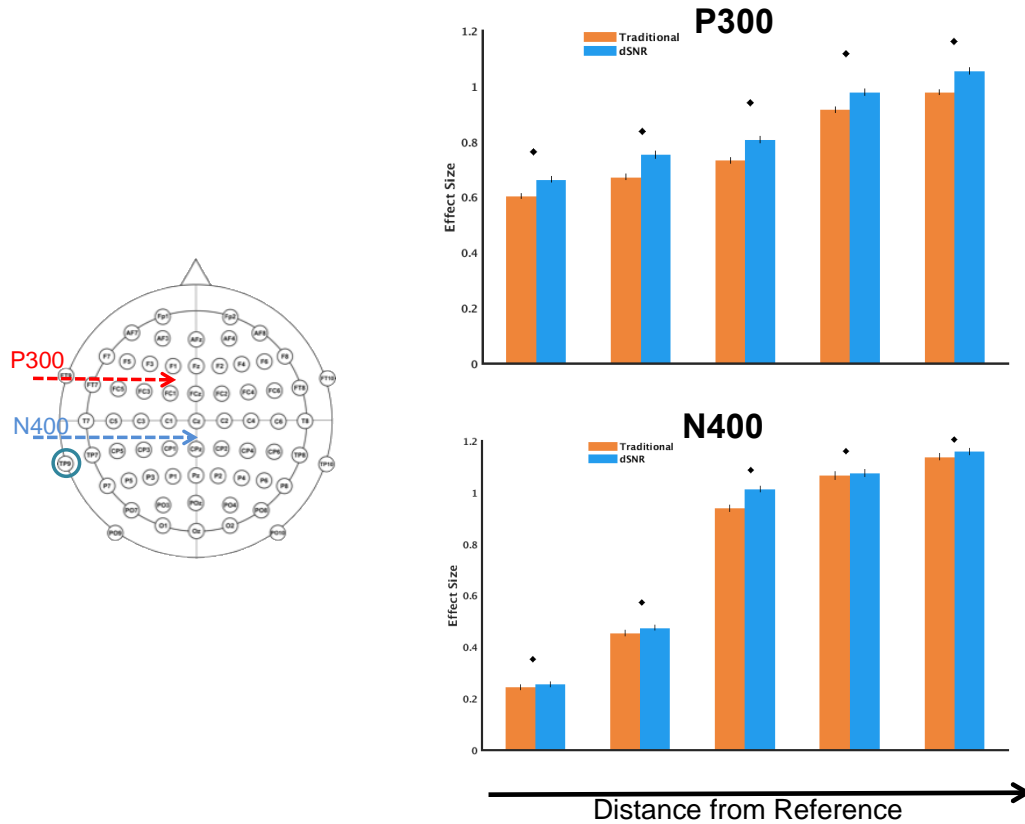
Figure 6.8. Comparison of Tradiitonal and dSNRw pooling as function of distance to reference electrode

Reference electrode located at TP9 (cyan circle). Pooling of pairs of electrodes undertaken along the left frontal quadrant (for P300 ERP) and left posterior quadrant (for N400 ERP), moving from periphery to the midline. Effect size increased with distance from reference electrode and dSNRw outperformed traditional pooling in all instances. Values shown as mean ± std. error for 1000 permutations of effect size calculations, and diamond signifies p<0.05 across pooling techniques.

6.7.3. Assessing dSNRw and Traditional pooling with Differential Pool Size

In order to assess the impact of the underlying pool size (i.e. number of constituent electrodes/sensors), increasing number of channels were pooled in the vicinity of the Fz electrode (Fz+FCz, Fz+FCz+F1, Fz+FCz+F1+F2 and Fz+FCz+F1+F2+AFz) using both the traditional and the dSNRw techniques. Comparisons were made among the two pooling techniques for each of the pool sizes, and as shown in Figure 6.9, increasing pool size leads to increased effect size. This finding is as expected and in line with prior studies where channel pooling was applied, as increasing pool size reduces the variance [223]. Importantly, for every pool size, dSNRw technique significantly improved the ERP effect captured.
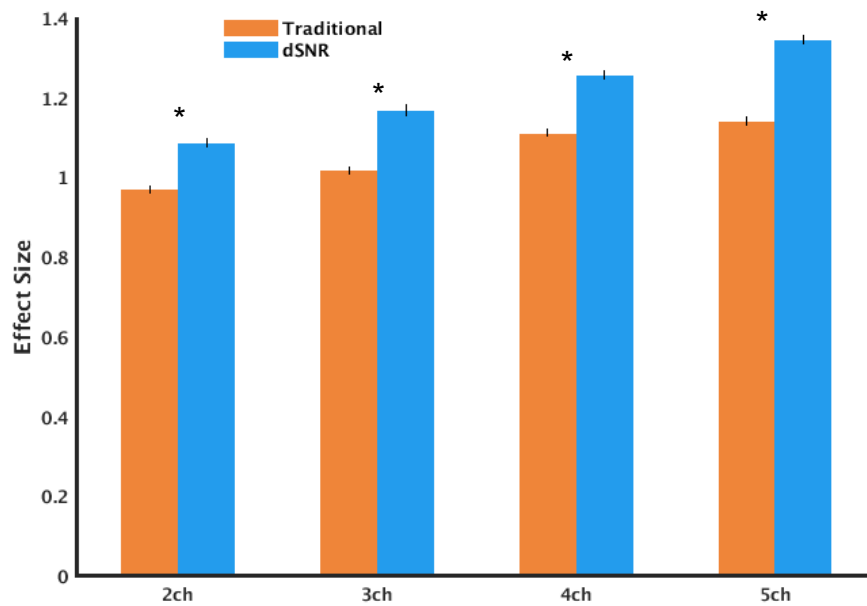
Figure 6.9. **Comparison of Traditional and dSNRw Pooling Techniques with Increasing Pool Size**

Results of traditional and dSNRw pooling for varying number of channels/electrodes, ranging from 2 channels (2ch) to 5 channels (5ch). Values shown are mean ± std. error of 1000 permutations of P300 effect size calculations. *$p<0.05$ across pooling techniques for each pool size.

6.8. Author Contributions

This study was conducted in collaboration with co-authors who contributed to the data collection and some study design.

Chapter 7.   Discussion

7.1. Summary of Key Findings & Scientific Contributions

The overall objective of this research program was to create a vital sign-like measure for the brain through portable, rapid, non-invasive, physiology-based assessment of brain functions ranging from low-level sensory processing to high-level cognitive functions such as orientation, and producing outputs indexed by normative values that are reflective of level of brain function. To meet this overall objective, a series of studies were undertaken with specific sub-goals: 1) create methods and apparatus for portable, rapid, automated physiology-based assessment of a spectrum of brain functions encompassing sensation, attention and language processing; 2) confirm the scientific validity of the measurements developed in the first study; 3) create a novel brain assessment method to enable neurophysiological assessment of orientation function that has hereto not been possible; and 4) devise a signal processing technique for ensuring maximization of neural signal capture with the methods developed above.

The primary contribution of the first study was the successful demonstration that a platform could be developed for portable, non-invasive, physiology-based assessments of a variety of brain functions, and that a normative-referenced score/output could be created for transforming complex neuroimaging data into easy-to-understand metrics. Importantly, this was the very first demonstration of an integrated portable EEG hardware and software platform for assessing the brain's sensation, attention and language processing capabilities with an automated rapid (5-minute) test, and this study also provided the very first evidence of capturing aging-related changes in neural function using such a rapid test. The second study focused on assessing the characteristics and confirming the scientific validity of the highly novel experimental paradigm used within the first study. Specifically, the key contribution of the second study was to demonstrate using MEG and concurrent EEG that the neural marker generated by the rapid assessment technique was consistent in the time, frequency, and spatial domains and had similar neuroanatomical features to the neural markers studied in traditional laboratory settings. As any potential brain function assessment should capture and evaluate the highest levels of cognitive function, in the third study, a new technique for brain function assessment was developed to access knowledge of the

145

current situation/context (i.e., orientation) as it is widely utilized in the clinic with well-established diagnostic and prognostic capabilities, but for which no neurophysiological marker was available until now. Indeed, this study not only developed a brand new neural marker of orientation enabling objective assessments of this crucial brain function but importantly also advanced our knowledge of how the brain processes information related to the present context or situation. Lastly, the fourth study focussed on enabling the developed solutions to better operate in 'real world' settings. Specifically, the neural markers of interest suffer from low SNR, in that they are microvolt signals embedded within background signals that are often orders of magnitude larger, and are particularly vulnerable when deployed in realistic settings (i.e. outside well controlled laboratory environments). The last study demonstrates a new signal processing technique for boosting the capture of the effects of interest, with both simulation and experimental data confirming the suitability of this technique for maximizing the capture of neural responses of interest.

Together these studies help overcome the clinical challenge of creating more objective physiology-based assessments through direct measurements of the brain, advance our scientific knowledge of critical high-level brain functions and their characteristics, and create technological innovations for enabling rapid, standardized and automated brain assessments at point-of-care.

7.2. Towards Improved Brain Function Assessment

The primary clinical gap is the lack of easily accessible, objective, physiology-based assessments of the brain. As discussed in Chapter 1, most current clinical assessments rely on subjective observations of behaviour as a surrogate measure for brain function, and this introduces several confounds that limit their efficacy and even leads to high misdiagnosis rates [1], [130]. Consequently, this research aims to improve the assessment of brain function by developing physiology-based direct measures of the brain that do not rely on overt behavioural responses to be generated by the person being evaluated. To ensure maximum clinical translation capacity, this research aimed to develop a new brain imaging approach that closely mimics characteristics of existing widely used objective measures of health in the clinic – i.e. vital signs.

Existing vital signs such as blood pressure, heart rate and body temperature share several key characteristics: 1) they are direct physiology-based measurements rather than relying on questionnaires or other behaviour-based assessments; 2) use non-invasive techniques with possibility of repeated measurements; 3) they provide measurements that reflect the functions of the target organ/body system; 4) they require no response from the person being evaluated; 5) they can be easily and rapidly administered; and 6) they produce easy-to-understand scores/outputs indexed by normative means that can be easily interpreted by non-experts.

By meeting all of the above-mentioned requirements, the work presented within this thesis helps create a vital sign like metric for the brain. As highlighted in Chapter 3, the choice of EEG with its non-invasive measurement properties [47], high portability [14], low cost (estimated at $1-3USD per use compared to $800USD for fMRI [239]), and direct electric assessment of underlying brain neurophysiology with excellent temporal resolution [48], [225], enables brain vital signs to meet its goal of providing physiology-based, non-invasive measurements that can be repeatedly assessed. As mentioned previously, existing vital signs provide measurements reflective of key functions of the organ without the need for overt responses from the individual. Since the brain is a multi-faceted organ, any potential brain vital sign necessarily needs to provide a profile of various brain functions, and in fact previous work in this area has repeatedly highlighted the need for multidimensional assessments of the brain [65], [76]. EEG-derived ERPs were chosen for the development of brain vital signs as they are able to assess a variety of brain functions at the millisecond level without requiring an overt response from the individual [48] and because they embody excellent measurement characteristics such as good test-retest reliability and excellent internal consistency [52], [53], [176], [240]. While several ERP-based markers have previously been reported in literature [48], for the initial development (Chapter 3), the specific target ERPs (N100, P300, N400) were chosen as they enable assessment of cognitive domains ranging from sensation to attention to language processing without any overt response from the individual, can be robustly elicited in healthy individuals, and have been extensively studied under varying experimental conditions [182] – indeed the ERP literature itself highly recommends the use of these ERP measures [241]. In addition to their recommended use in healthy individuals, these ERPs have also long been evaluated within clinical populations [50], [58], [59], [156] with well-established changes reflective of clinical state (e.g. N400

amplitude reflecting severity of language impairment due to stroke-induced aphasia [70]), and thereby they represent excellent candidates for monitoring potential brain dysfunction.

However, the existing repertoire of neurophysiology based ERP measures of cognitive functions had one key gap in that no assessments of the key cognitive function of orientation were available. Orientation is widely used for assessments in major brain trauma, concussions, and dementia as well as for general cognitive assessment [82], [85], [86], [88]. Indeed, it is considered an index of overall brain health [85]. In spite of its high clinical salience, no neurophysiological techniques for assessing this crucial function were available. To address this shortcoming and ensure that the newly created brain vital signs platform is able to provide information about the highest levels of cognitive functions, a major undertaking of the present research was to develop such a neural marker for orientation processing as described in Chapter 5. Further to developing a brand new marker of a key brain function, this work also significantly advanced our knowledge of brain processing. Specifically, the results indicate that the brain not only distinguishes between stimuli that are related to the present situation/context and those that are not, but more importantly when the stimulus is related to the present situation it activates a cascade of brain networks for processing the stimulus within space, time and person domains [230]. These results may thus provide the initial neuroimaging evidence for the long hypothesized theories of orientation, specifically in that it may be dependent on processing of relationships in space, time and person with respect to the self [84], [87].

While the above-mentioned advances fulfilled many of the desired characteristics of a potential brain vital sign (e.g. non-invasive, physiology-based, assessment without response, and measurements reflective of key functions), in order to meet the need for rapid assessment, innovations in the way the brain is stimulated were required. Within this research (as detailed in Chapter 3 and Chapter 5) a 5-minute assessment was created to stimulate the brain and capture neural responses across sensation, attention, language processing and orientation domains, which represents a significant improvement over traditional laboratory-based ERP assessments which require hours of testing [65], and even clinically oriented ERP assessments which are routinely 30-90minutes in length [71], [75], [79]. While at first glance, this order of magnitude reduction in testing time may raise concerns for some readers with respect to the

integrity of the assessment and if it truly captures the neural responses of interest, such concerns should be alleviated due to the following reasons: 1) the lowest number of trials/repetitions used to generate ERPs within the current paradigm is 30, which is in line with other works that have suggested the possibility of generating ERP responses with minimum 30 trials provided appropriate choice of ERP markers and signal processing techniques are made [241]; 2) the assessment time of 5 minutes was chosen not only to meet the rapid testing requirement of vital signs but also because prior empirical evidence has shown that 5-minute assessment blocks for ERP experiments are well tolerated by individuals and provides a good balance between shorter times potentially not generating enough trial numbers, and longer times introducing fatigue and non-compliance resulting in signal degradation [239]; and most importantly 3) as detailed in Chapter 4, when assessed using multimodal neuroimaging techniques the neural response elicited by the current paradigm shared the same temporal, spatial, spectral and neuroanatomic features as the principal characteristics of the target neural marker derived from decades of research in traditional laboratory settings [182].

Related to the above point, valid ERP markers are generated through averaging of several trials/repetitions as individual responses generally have very low SNR, and the averaging process helps to boost the SNR and make the neural response discernable [48]. While increasing numbers of trials improve the SNR [223], this also increases the overall test times, making this approach of simply adding more trials impractical for use within brain vital signs. Accordingly, to boost the captured signal quality without increasing testing time, as detailed in Chapter 6, a new signal processing technique was developed to pool data from multiple sensors by weighting them by their respective inherent SNR. This pooling approach showed promise when applied to experimental data collected from human participants, significantly boosting the captured effects of interest and thereby potentially safeguarding the quality of the data in high-noise situations or enabling a further reduction in the number of trials (and therefore test time) necessary to generate a valid ERP response.

The innovations discussed so far successfully meet all the desired characteristics of brain vital signs, except for the need for easy-to-understand outputs that are referenced to normative values. This is a crucial need since the lack of standardized values was cited as a major impediment to the clinical use of ERP-based measures by practising clinicians [80]. To meet this challenge, as described in Chapter 3, a

transformation was introduced to translate raw ERP values into normative-referenced measures, creating a normative comparison framework similar to existing vital signs. Since this transformation would eventually be required to track clinically salient information, the initial assessment focussed on its ability to track a biologically salient phenomenon. Specifically, the impact of aging was assessed using this normative-referenced metric and it successfully identified aging-related neural changes, which were in line with those reported previously using laboratory-based ERP studies [67], [133]. Importantly, consistent with previous literature reporting differences in ERP measures without changes in behavioural measures (e.g. reaction time) in aging [67], the present research also found aging-related changes in the normative-referenced measures but not in behaviour-based neuropsychological assessments undertaken concomitantly [159].

7.3. Extensions of Current Thesis Research

The success of this research program towards developing a brain vital signs framework has in turn enabled an array of complimentary research. One prominent example is the recent work where brain vital signs were deployed to our partners at Mayo Clinic in order to assess impacts of concussion. This study provided an initial demonstration of the ability of brain vital signs to be applied to "true" point-of-care (POC) settings (in this case, a hockey arena). But more importantly, it also demonstrated the possibilities of establishing new science that were made possible only through the development of brain vital signs. Specifically, novel findings of the impacts of concussion on attentional and language processing markers were found that have previously not been reported, and this may be related to the newly developed ability to test individuals soon after an injury made possible by brain vital signs [222], [242]. Additionally, this study also provided an ideal testing ground for the normative-referenced measures, and these measures successfully tracked individual performance longitudinally and captured brain dysfunction when a concussion occurred [242].

Yet another study was the work undertaken towards the development of a visual analogue of the auditory brain vital signs described within this thesis. As part of the development of the visual brain vital signs, a key analysis was the comparison among the visual and auditory domain ERPs. While significant differences were observed among the ERPs from the two sensory modalities when comparing the raw ERP

amplitude and latency values, the normative-referenced metric showed no significant differences between the two modalities [107]. Indeed, this points to one of the key advantages of the normative standardized metric developed within the current thesis, in that it helps remove systematic differences and correctly demonstrates that the underlying brain phenomenon are similar across sensory modalities in spite of an apparent difference in the ERP-based measurements that are secondary to the latent common modality-independent processing effects.

Indeed, the success of this work can also been seen by the commercialization of brain vital signs – with the commercially available device measuring brain vital signs having recently received Health Canada approval as a medical device. This in turn may significantly further enable the demonstrations of brain vital signs in more real-world point-of-care settings such as clinics, hospitals and assisted living facilities.

7.4. Limitations

The limitations of each individual study are listed within the respective chapters. A limitation of the overall research described within this thesis is the reliance on auditory stimulation to elicit the neural markers of interest. If assessments of brain function are called for in situation of compromised hearing (e.g. assessments of older adults with aging-related hearing loss, or cases of mild traumatic brain injury with blast induced hearing loss as a comorbidity), the auditory stimulus based brain vital signs framework may be rendered less effective. However, to a large extent, the subsequent development of the visual version of brain vital signs has ameliorated this issue by providing an alternate access pathway [107]. Additionally, the results reported within this thesis should thus be further verified with additional EEG devices as well in order to further expand the possible use scenarios. Lastly, while the results presented within this thesis with healthy individuals and the preliminary application to concussion assessment in related work are promising, additional research needs to be undertaken to confirm these findings in larger sample of healthy individuals and to apply brain vital signs in various clinical contexts to better ascertain the efficacy of brain vital signs measurements in improving the level of care.

7.5. Future Directions

In this research, significant progress has been made towards the development of potential vital signs for the brain. Further work needs to be undertaken to build upon this success.

A key area of further refinement is the normative-indexed score developed in this thesis. For the initial development and implementation, a database of 100 healthy individuals was used as the reference for indexing the ERP measures [159]. However, in order to move towards a more widespread deployment of brain vital signs, more research needs to be undertaken for creating age and disease specific databases of ERP values in order to improve the granularity of the normative-indexed score. Additionally, further work also needs to be undertaken to assess the impact of differing EEG platforms and/or collection environments. Indeed, on-going work is already being undertaken by partner organizations (e.g. Centre for Neurology Studies) on this front.

Similarly, as the brain vital signs includes an assessment of language processing as one of the key indicators of brain function, it is essential to also create non-English versions of the assessment in order to expand the potential target populations. Preliminary work has already been undertaken on this front. Given the large South Asian population in Surrey, the initial work on the development of non-English versions of brain vital signs focussed on developing a Hindi version of the assessment. In fact, initial results from healthy participants using both MEG and concurrent EEG show similar responses using the Hindi version of the test to those elicited by the English version of the test (unpublished results).

Many of the target ERP components within the brain vital signs framework are extremely well characterized, with established reliability (e.g. test-retest reliabilities of 0.85, 0.79 and 0.89 for N400, P300 and N100 amplitudes respectively [53], [176]; internal consistency of N100 is >0.9 whereas for P300 it is >0.8 [240]) and validity (e.g. convergent validity: N400 parameters are related to an individual's language proficiency [68]; predictive validity: N400 amplitude correlates with ability to learn new language [243]) characteristics. However, with the creation of a brand new neural marker (for orientation) within this thesis and its incorporation within brain vital signs, a future direction to be explored should be the assessment of both reliability (within-session and

longitudinal) and validity (internal, external, content etc.) characteristics of the brain vital signs paradigm as a complete set of ERP markers indexing a range of functions from the lowest (sensation) to the highest (orientation) levels.

Finally, explorations of the potential application of brain vital signs to non-clinical situations should also be undertaken. In addition to addressing the challenges commonly associated with clinical neurology (as highlighted within this thesis), brain vital signs may also play a key role in addressing the general need for improved brain function assessments for health and wellness applications. For example, assessments of the impact of workload on cognitive functions (e.g. for monitoring cognitive status in high acuity environments for pilots or astronauts) may be made possible with brain vital signs.

Chapter 8.   Conclusion

This research developed and demonstrated a brainwave-based technology platform that provides the first objective metric embodying the characteristics of vital signs for the brain which is portable, rapid, easy to use, and produces objective, standardized outputs that are easy to interpret. The brain vital signs technology evaluates a spectrum of brain functions spanning from the low-level sensation domains to high-level cognitive domains. The research also created a novel neurophysiological marker of contextual orientation, which represents the highest level integration functions that are key to frontline clinical assessments, but for which no objective measures have been possible until now. In addition, this research not only validates the brain vital sign outputs against established lab-based measures, but also demonstrates the critical ability of the brain vital signs platform to capture biological salient information about brain function changes that are currently undetectable using existing behaviour-based metrics. Finally, this research addresses the key technological challenge of developing advanced data analytic techniques to maximize signal capture in noisy environments typical of point-of-care settings. Together, this research addresses a key scientific, clinical, and technology gap that not only advances our understanding about brain function, but also has tremendous potential in improving clinical brain function assessments at the point of care.

References

[1] J. R. Gawryluk, R. C. D'Arcy, J. F. Connolly, and D. F. Weaver, "Improving the clinical assessment of consciousness with advances in electrophysiological and neuroimaging techniques," *BMC Neurol.*, vol. 10, p. 11, Jan. 2010.

[2] F. C. Reith, P. M. Brennan, A. I. Maas, and G. M. Teasdale, "Lack of Standardization in the Use of the Glasgow Coma Scale: Results of International Surveys," *J. Neurotrauma*, vol. 33, no. 1, pp. 89–94, Jan. 2016.

[3] V. L. Feigin *et al.*, "Global, regional, and national burden of neurological disorders during 1990–2015: a systematic analysis for the Global Burden of Disease Study 2015," *Lancet Neurol.*, vol. 16, no. 11, pp. 877–897, 2017.

[4] M. DiLuca and J. Olesen, "The cost of brain diseases: a burden or a challenge?," *Neuron*, vol. 82, no. 6, pp. 1205–1208, 2014.

[5] B. I. Canada, "Acquired Brain Injury (ABI) — The Basics," *Acquired Brain Injury (ABI) — The Basics*. [Online]. Available: https://www.braininjurycanada.ca/acquired-brain-injury/. [Accessed: 26-Aug-2019].

[6] D. P. Rao, S. McFaull, W. Thompson, and G. C. Jayaraman, "Trends in self-reported traumatic brain injury among Canadians, 2005-2014: a repeated cross-sectional analysis," *C. open*, vol. 5, no. 2, p. E301, 2017.

[7] B. I. Canada, "Brain Injury Can Happen to Anyone.," *Brain Injury Can Happen to Anyone.* .

[8] S. Signoretti, G. Lazzarino, B. Tavazzi, and R. Vagnozzi, "The pathophysiology of concussion," *Pm&r*, vol. 3, no. 10, pp. S359–S368, 2011.

[9] C. Madl *et al.*, "Improved outcome prediction in unconscious cardiac arrest survivors with sensory evoked potentials compared with clinical assessment," *Crit. Care Med.*, vol. 28, no. 3, pp. 721–726, 2000.

[10] C. Madl and M. Holzer, "Brain function after resuscitation from cardiac arrest," *Curr. Opin. Crit. Care*, vol. 10, no. 3, pp. 213–217, 2004.

[11] S. Jain, S. B. Dharap, and M. A. Gore, "Early prediction of outcome in very severe closed head injury," *Injury*, vol. 39, no. 5, pp. 598–603, 2008.

[12] D. Demetriades, E. Kuncir, G. C. Velmahos, P. Rhee, K. Alo, and L. S. Chan, "Outcome and prognostic factors in head injuries with an admission Glasgow Coma Scale score of 3," *Arch. Surg.*, vol. 139, no. 10, pp. 1066–1068, 2004.

[13] D. Bor, "Advances in the scientific investigation of consciousness," in *Brain

function and responsiveness in disorders of consciousness, Springer, 2016, pp. 13–24.

[14] J. T. Giacino, J. J. Fins, S. Laureys, and N. D. Schiff, "Disorders of consciousness after acquired brain injury: the state of the science," *Nat. Rev. Neurol.*, vol. 10, no. 2, pp. 99–114, 2014.

[15] F. Plum and J. B. Posner, *The diagnosis of stupor and coma*, vol. 19. Oxford University Press, USA, 1982.

[16] D. Bates, "The vegetative state and the Royal College of Physicians guidance," *Neuropsychol. Rehabil.*, vol. 15, no. 3–4, pp. 175–183, 2005.

[17] M.-A. Bruno, A. Vanhaudenhuyse, A. Thibaut, G. Moonen, and S. Laureys, "From unresponsive wakefulness to minimally conscious PLUS and functional locked-in syndromes: recent advances in our understanding of disorders of consciousness," *J. Neurol.*, vol. 258, no. 7, pp. 1373–1384, 2011.

[18] G. Bauer, F. Gerstenbrand, and E. Rumpl, "Varieties of the locked-in syndrome," *J. Neurol.*, vol. 221, no. 2, pp. 77–91, 1979.

[19] D. Larrivee, "Improving objective assessment in disorders of consciousness: An option for classification technology?," *Clin Sci Res Reports*, vol. 1, pp. 1–4, 2017.

[20] D. S. Gray and R. S. Burnham, "Preliminary outcome analysis of a long-term rehabilitation program for severe acquired brain injury," *Arch. Phys. Med. Rehabil.*, vol. 81, no. 11, pp. 1447–1456, 2000.

[21] S. Laureys, A. M. Owen, and N. D. Schiff, "Brain function in coma, vegetative state, and related disorders," *Lancet Neurol.*, vol. 3, no. 9, pp. 537–546, 2004.

[22] R. T. Seel *et al.*, "Assessment scales for disorders of consciousness: evidence-based recommendations for clinical practice and research," *Arch. Phys. Med. Rehabil.*, vol. 91, no. 12, pp. 1795–1813, 2010.

[23] G. Teasdale and B. Jennett, "Assessment of coma and impaired consciousness: a practical scale," *Lancet*, vol. 304, no. 7872, pp. 81–84, 1974.

[24] R. W. Rimel, B. Giordani, J. T. Barth, and J. A. Jane, "Moderate head injury: completing the clinical spectrum of brain trauma," *Neurosurgery*, vol. 11, no. 3, pp. 344–351, 1982.

[25] J. T. Giacino, K. Kalmar, and J. Whyte, "The JFK Coma Recovery Scale-Revised: measurement characteristics and diagnostic utility," *Arch. Phys. Med. Rehabil.*, vol. 85, no. 12, pp. 2020–2029, 2004.

[26] W. D. Gouvier, P. D. Blanton, K. K. LaPorte, and C. Nepomuceno, "Reliability and validity of the Disability Rating Scale and the Levels of Cognitive Functioning

Scale in monitoring recovery from severe head injury.," *Arch. Phys. Med. Rehabil.*, vol. 68, no. 2, pp. 94–97, 1987.

[27] A. Shiel, S. A. Horn, B. A. Wilson, M. J. Watson, M. J. Campbell, and D. L. McLellan, "The Wessex Head Injury Matrix (WHIM) main scale: a preliminary report on a scale to assess and monitor patient recovery after severe head injury," *Clin. Rehabil.*, vol. 14, no. 4, pp. 408–416, 2000.

[28] K. Andrews, L. Murphy, R. Munday, and C. Littlewood, "Misdiagnosis of the vegetative state: retrospective study in a rehabilitation unit," *BMJ*, vol. 313, no. 7048, pp. 13–16, Jul. 1996.

[29] N. L. Childs, W. N. Mercer, and H. W. Childs, "Accuracy of diagnosis of persistent vegetative state," *Neurology*, vol. 43, no. 8, p. 1465, 1993.

[30] C. Schnakers *et al.*, "Diagnostic accuracy of the vegetative and minimally conscious state: clinical consensus versus standardized neurobehavioral assessment," *BMC Neurol.*, vol. 9, p. 35, Jul. 2009.

[31] W. S. Van Erp, J. C. M. Lavrijsen, P. E. Vos, H. Bor, S. Laureys, and R. T. C. M. Koopmans, "The vegetative state: prevalence, misdiagnosis, and treatment limitations," *J. Am. Med. Dir. Assoc.*, vol. 16, no. 1, pp. 85-e9, 2015.

[32] N. D. Schiff, "Cognitive motor dissociation following severe brain injuries," *JAMA Neurol.*, vol. 72, no. 12, pp. 1413–1415, 2015.

[33] H. Gill-Thwaites, "Lotteries, loopholes and luck: misdiagnosis in the vegetative state patient," *Brain Inj.*, vol. 20, no. 13–14, pp. 1321–1328, 2006.

[34] B. L. Edlow, "Covert Consciousness: Searching for Volitional Brain Activity in the Unresponsive," *Curr. Biol.*, vol. 28, no. 23, pp. R1345–R1348, 2018.

[35] B. Lee and A. Newberg, "Neuroimaging in traumatic brain imaging," *NeuroRx*, vol. 2, no. 2, pp. 372–383, 2005.

[36] E. Tollard *et al.*, "Experience of diffusion tensor imaging and 1H spectroscopy for outcome prediction in severe traumatic brain injury: Preliminary results," *Crit. Care Med.*, vol. 37, no. 4, pp. 1448–1455, 2009.

[37] A. M. Owen, M. R. Coleman, M. Boly, M. H. Davis, S. Laureys, and J. D. Pickard, "Detecting awareness in the vegetative state," *Science (80-.).*, vol. 313, no. 5792, p. 1402, 2006.

[38] L. Naci, R. Cusack, M. Anello, and A. M. Owen, "A common neural code for similar conscious experiences in different individuals," *Proc. Natl. Acad. Sci.*, vol. 111, no. 39, pp. 14277–14282, 2014.

[39] M. Boly *et al.*, "Perception of pain in the minimally conscious state with PET

activation: an observational study," *Lancet Neurol.*, vol. 7, no. 11, pp. 1013–1020, 2008.

[40] R. P. Lystad and H. Pollard, "Functional neuroimaging: a brief overview and feasibility for use in chiropractic research," *J. Can. Chiropr. Assoc.*, vol. 53, no. 1, p. 59, 2009.

[41] B.-K. Min, M. J. Marzelli, and S.-S. Yoo, "Neuroimaging-based approaches in the brain–computer interface," *Trends Biotechnol.*, vol. 28, no. 11, pp. 552–560, 2010.

[42] M. Peterson, B. C. Eapen, M. Himmler, P. Galhotra, and D. Glazer, "Evolution of Care for the Veterans and Active Duty Service Members with Disorders of Consciousness," *Phys. Med. Rehabil. Clin.*, vol. 30, no. 1, pp. 29–41, 2019.

[43] S. Wannez, L. Heine, M. Thonnard, O. Gosseries, S. Laureys, and C. S. G. Collaborators, "The repetition of behavioral assessments in diagnosis of disorders of consciousness," *Ann. Neurol.*, vol. 81, no. 6, pp. 883–889, 2017.

[44] S. Ogawa, T.-M. Lee, A. R. Kay, and D. W. Tank, "Brain magnetic resonance imaging with contrast dependent on blood oxygenation," *Proc. Natl. Acad. Sci.*, vol. 87, no. 24, pp. 9868–9872, 1990.

[45] A. M. Kempny *et al.*, "Functional near infrared spectroscopy as a probe of brain function in people with prolonged disorders of consciousness," *NeuroImage Clin.*, vol. 12, pp. 312–319, 2016.

[46] M. J. Brookes *et al.*, "Measuring functional connectivity using MEG: Methodology and comparison with fcMRI," *Neuroimage*, vol. 56, no. 3, pp. 1082–1104, Jun. 2011.

[47] J. R. Gawryluk and R. C. N. D'Arcy, "Electroencephalography: basic concepts and brain applications," *Handb. Phys. Med. Biol.*, 2010.

[48] S. J. Luck, *An introduction to the event-related potential technique*. MIT press, 2014.

[49] R. Näätänen and T. Picton, "The N1 wave of the human electric and magnetic response to sound: a review and an analysis of the component structure," *Psychophysiology*, vol. 24, no. 4, pp. 375–425, 1987.

[50] M. Gaetz and D. M. Bernstein, "The current status of electrophysiologic procedures for the assessment of mild traumatic brain injury," *J. Head Trauma Rehabil.*, vol. 16, no. 4, pp. 386–405, Aug. 2001.

[51] J. M. Olichney, J. C. Yang, J. Taylor, and M. Kutas, "Cognitive event-related potentials: biomarkers of synaptic dysfunction across the stages of Alzheimer's disease," *J. Alzheimers. Dis.*, vol. 26 Suppl 3, pp. 215–228, 2011.

[52] L. M. Williams, E. Simms, C. R. Clark, R. H. Paul, D. Rowe, and E. Gordon, "The test-retest reliability of a standardized neurocognitive and neurophysiological test battery:'neuromarker,'" *Int. J. Neurosci.*, vol. 115, no. 12, pp. 1605–1630, 2005.

[53] S. M. Cassidy, I. H. Robertson, and R. G. O'Connell, "Retest reliability of event-related potentials: Evidence from a variety of paradigms," *Psychophysiology*, vol. 49, no. 5, pp. 659–664, 2012.

[54] S. P. Broglio, R. D. Moore, and C. H. Hillman, "A history of sport-related concussion on event-related brain potential correlates of cognition," *Int. J. Psychophysiol.*, vol. 82, no. 1, pp. 16–23, 2011.

[55] C.-T. Ip *et al.*, "Pre-intervention test-retest reliability of EEG and ERP over four recording intervals," *Int. J. Psychophysiol.*, vol. 134, pp. 30–43, 2018.

[56] V. J. M. Wijnen, G. J. M. Van Boxtel, H. J. Eilander, and B. De Gelder, "Mismatch negativity predicts recovery from the vegetative state," *Clin. Neurophysiol.*, vol. 118, no. 3, pp. 597–605, 2007.

[57] D. Morlet, P. Bouchet, and C. Fischer, "Mismatch negativity and N100 monitoring: potential clinical value and methodological advances," *Audiol. Neurootol.*, vol. 5, no. 3–4, pp. 198–206, 2000.

[58] R. C. N. D'Arcy *et al.*, "Electrophysiological assessment of language function following stroke," *Clin. Neurophysiol.*, vol. 114, no. 4, pp. 662–672, 2003.

[59] J. Daltrozzo *et al.*, "Cortical information processing in coma," *Cogn. Behav. Neurol.*, vol. 22, no. 1, pp. 53–62, Mar. 2009.

[60] M. F. A. U. Balconi, R. F. A. U. Arangio, and C. Guarnerio, "Disorders of Consciousness and N400 ERP Measures in Response to a Semantic Task," *J. Neuropsychiatry Clin. Neurosci.*, vol. 25, p. 237, 2013.

[61] P. A. Davis, "Effects of acoustic stimuli on the waking human brain," *J. Neurophysiol.*, vol. 2, no. 6, pp. 494–499, 1939.

[62] S. Sutton, P. Tueting, J. Zubin, and E. R. John, "Information delivery and the sensory evoked potential," *Science*, vol. 155, no. 3768, pp. 1436–1439, Mar. 1967.

[63] M. Kutas and S. A. Hillyard, "Reading senseless sentences: brain potentials reflect semantic incongruity," *Science*, vol. 207, no. 4427, pp. 203–205, Jan. 1980.

[64] B. A. Martin, K. L. Tremblay, and P. Korczak, "Speech evoked potentials: from the laboratory to the clinic," *Ear Hear.*, vol. 29, no. 3, pp. 285–313, 2008.

[65] L. Sculthorpe-Petley *et al.*, "A rapid event-related potential (ERP) method for

point-of-care evaluation of brain function: Development of the Halifax Consciousness Scanner," *J. Neurosci. Methods*, vol. 245, pp. 64–72, 2015.

[66] J. Polich, "Updating P300: an integrative theory of P3a and P3b," *Clin. Neurophysiol.*, vol. 118, no. 10, pp. 2128–2148, 2007.

[67] T. W. Picton, D. T. Stuss, S. C. Champagne, and R. F. Nelson, "The Effects of Age on Human Event-Related Potentials," *Psychophysiology*, vol. 21, no. 3, pp. 312–326, May 1984.

[68] M. Kutas and K. D. Federmeier, "Thirty years and counting: finding meaning in the N400 component of the event-related brain potential (ERP)," *Annu. Rev. Psychol.*, vol. 62, pp. 621–647, 2011.

[69] T. Sitnikova, P. J. Holcomb, K. A. Kiyonaga, and G. R. Kuperberg, "Two neurocognitive mechanisms of semantic integration during the comprehension of visual real-world events," *J. Cogn. Neurosci.*, vol. 20, no. 11, pp. 2037–2057, 2008.

[70] W. Kawohl, S. Bunse, K. Willmes, A. Hoffrogge, H. Buchner, and W. Huber, "Semantic Event-Related Potential Components Reflect Severity of Comprehension Deficits in Aphasia," *Neurorehabil. Neural Repair*, vol. 24, no. 3, pp. 282–289, 2010.

[71] I. Steppacher, S. Eickhoff, T. Jordanov, M. Kaps, W. Witzke, and J. Kissler, "N400 predicts recovery from disorders of consciousness," *Ann. Neurol.*, vol. 73, no. 5, pp. 594–602, 2013.

[72] O. Keren, S. Ben-Dror, M. J. Stern, G. Goldberg, and Z. Groswasser, "Event-related potentials as an index of cognitive function during recovery from severe closed head injury," *J. Head Trauma Rehabil.*, vol. 13, no. 3, pp. 15–30, Jun. 1998.

[73] K. R. Wilson, H. O'Rourke, L. A. Wozniak, E. Kostopoulos, Y. Marchand, and A. J. Newman, "Changes in N400 topography following intensive speech language therapy for individuals with aphasia," *Brain Lang.*, vol. 123, no. 2, pp. 94–103, 2012.

[74] J. F. Connolly, C. C. Mate-Kole, and B. M. Joyce, "Global aphasia: an innovative assessment approach," *Arch. Phys. Med. Rehabil.*, vol. 80, no. 10, pp. 1309–1315, Oct. 1999.

[75] J. D. Sitt *et al.*, "Large scale screening of neural signatures of consciousness in patients in a vegetative or minimally conscious state," *Brain*, vol. 137, no. 8, pp. 2258–2270, Aug. 2014.

[76] C. Sergent *et al.*, "Multidimensional cognitive evaluation of patients with disorders of consciousness using EEG: A proof of concept study," *NeuroImage Clin.*, 2016.

[77] H. L. Lew, M. Gray, and J. H. Poole, "Temporal stability of auditory event-related potentials in healthy individuals and patients with traumatic brain injury," *J. Clin. Neurophysiol.*, vol. 24, no. 5, pp. 392–397, 2007.

[78] M. A. Boudewyn, S. J. Luck, J. L. Farrens, and E. S. Kappenman, "How many trials does it take to get a significant ERP effect? It depends," *Psychophysiology*, vol. 55, no. 6, p. e13049, 2018.

[79] R. L. Mah and J. F. Connolly, "A framework for the extended monitoring of levels of cognitive function in unresponsive patients," *PLoS One*, vol. 13, no. 7, p. e0200793, 2018.

[80] N. André-Obadia *et al.*, "Recommendations for the use of electroencephalography and evoked potentials in comatose patients," *Neurophysiol. Clin.*, vol. 48, no. 3, pp. 143–169, 2018.

[81] R. C. N. D'Arcy, S. Ghosh Hajra, C. Liu, L. D. Sculthorpe, and D. F. Weaver, "Towards Brain First-Aid: A Diagnostic Device for Conscious Awareness," *Biomed. Eng. IEEE Trans.*, vol. 58, no. 3, pp. 750–754, 2011.

[82] M. F. Folstein, S. E. Folstein, and P. R. McHugh, "'Mini-mental state': a practical method for grading the cognitive state of patients for the clinician," *J. Psychiatr. Res.*, vol. 12, no. 3, pp. 189–198, 1975.

[83] Z. S. Nasreddine *et al.*, "The Montreal Cognitive Assessment, MoCA: a brief screening tool for mild cognitive impairment," *J. Am. Geriatr. Soc.*, vol. 53, no. 4, pp. 695–699, 2005.

[84] M. Peer, R. Salomon, I. Goldberg, O. Blanke, and S. Arzy, "Brain system for mental orientation in space, time, and person," *Proc. Natl. Acad. Sci.*, vol. 112, no. 35, pp. 11072–11077, 2015.

[85] J. F. Benge, S. Balsis, P. J. Massman, W. Havins, and R. S. Doody, "Beyond 'A&OX3': What temporal and spatial orientation questions tell clinicians about cognitive dysfunction in Alzheimer's disease," *Clin. Gerontol.*, vol. 34, no. 1, pp. 45–56, 2010.

[86] H. S. Levin, V. M. O'Donnel, and R. G. Grossman, "The Galveston Orientation and Amnesia Test: A Practical Scale to Assess Cognition after Head Injury.," *J. Nerv. Ment. Dis.*, vol. 167, no. 11, pp. 675–684, 1979.

[87] G. E. Berrios, "Orientation failures in medicine and psychiatry: discussion paper," *J. R. Soc. Med.*, vol. 76, no. 5, pp. 379–385, May 1983.

[88] K. M. Guskiewicz *et al.*, "Evidence-based approach to revising the SCAT2: introducing the SCAT3," *Br. J. Sports Med.*, vol. 47, no. 5, pp. 289–293, Apr. 2013.

[89] M. K. Islam, A. Rastegarnia, and Z. Yang, "Methods for artifact detection and removal from scalp EEG: A review," *Neurophysiol. Clin. Neurophysiol.*, vol. 46, no. 4–5, pp. 287–305, 2016.

[90] S. Baillet, J. C. Mosher, and R. M. Leahy, "Electromagnetic brain mapping," *IEEE Signal Process. Mag.*, vol. 18, no. 6, pp. 14–30, 2001.

[91] S. Murakami and Y. Okada, "Contributions of principal neocortical neurons to magnetoencephalography and electroencephalography signals," *J. Physiol.*, vol. 575, no. 3, pp. 925–936, 2006.

[92] S. Baillet, "Magnetoencephalography for brain electrophysiology and imaging," *Nat. Neurosci.*, vol. 20, no. 3, p. 327, 2017.

[93] I. Marinova and V. Mateev, "Electromagnetic field modeling in human tissue," *World Acad. Sci. Eng. Technol.*, vol. 64, pp. 298–303, 2010.

[94] D. Cheyne and J. Verba, "Biomagnetism," *Encycl. Med. devices Instrum.*, 2006.

[95] S. Taulu, J. Simola, J. Nenonen, and L. Parkkonen, "Novel noise reduction methods," in *Magnetoencephalography*, Springer, 2014, pp. 35–71.

[96] S. Krachunov and A. Casson, "3D printed dry EEG electrodes," *Sensors*, vol. 16, no. 10, p. 1635, 2016.

[97] J. G. Webster, *Medical instrumentation: application and design*. John Wiley & Sons, 2009.

[98] A. F. Jackson and D. J. Bolger, "The neurophysiological bases of EEG and EEG measurement: A review for the rest of us," *Psychophysiology*, vol. 51, no. 11, pp. 1061–1071, 2014.

[99] A. J. Ries, J. Touryan, J. Vettel, K. McDowell, and W. D. Hairston, "A comparison of electroencephalography signals acquired from conventional and mobile systems," *J. Neurosci. Neuroengineering*, vol. 3, no. 1, pp. 10–20, 2014.

[100] G. Bianchi and R. Sorrentino, *Electronic filter simulation & design*. McGraw Hill Professional, 2007.

[101] C. A. Joyce, I. F. Gorodnitsky, and M. Kutas, "Automatic removal of eye movement and blink artifacts from EEG data using blind component separation," *Psychophysiology*, vol. 41, no. 2, pp. 313–325, 2004.

[102] G. Gratton, M. G. . Coles, and E. Donchin, "A new method for off-line removal of ocular artifact," *Electroencephalogr. Clin. Neurophysiol.*, vol. 55, no. 4, pp. 468–484, Apr. 1983.

[103] P. He, G. Wilson, and C. Russell, "Removal of ocular artifacts from electro-

encephalogram by adaptive filtering," *Med. Biol. Eng. Comput.*, vol. 42, no. 3, pp. 407–412, 2004.

[104] T.-P. JUNG *et al.*, "Removing electroencephalographic artifacts by blind source separation," *Psychophysiology*, vol. 37, no. 2, pp. 163–178, 2000.

[105] A. Hyvärinen and E. Oja, "Independent component analysis: algorithms and applications," *Neural networks*, vol. 13, no. 4–5, pp. 411–430, 2000.

[106] D. Langlois, S. Chartier, and D. Gosselin, "An introduction to independent component analysis: InfoMax and FastICA algorithms," *Tutor. Quant. Methods Psychol.*, vol. 6, no. 1, pp. 31–38, 2010.

[107] G. M. Pawlowski *et al.*, "Brain Vital Signs: Expanding From the Auditory to Visual Modality," *Front. Neurosci.*, vol. 12, p. 968, 2019.

[108] V. Bostanov and B. Kotchoubey, "The t-CWT: a new ERP detection and quantification method based on the continuous wavelet transform and Student's t-statistics," *Clin. Neurophysiol.*, vol. 117, no. 12, pp. 2627–2644, 2006.

[109] E. Maris and R. Oostenveld, "Nonparametric statistical testing of EEG-and MEG-data," *J. Neurosci. Methods*, vol. 164, no. 1, pp. 177–190, 2007.

[110] H. Parvar, L. Sculthorpe-Petley, J. Satel, R. Boshra, R. C. N. D'Arcy, and T. P. Trappenberg, "Detection of event-related potentials in individual subjects using support vector machines," *Brain Informatics*, vol. 2, no. 1, pp. 1–12, 2014.

[111] G. Mountrakis, J. Im, and C. Ogole, "Support vector machines in remote sensing: A review," *ISPRS J. Photogramm. Remote Sens.*, vol. 66, no. 3, pp. 247–259, 2011.

[112] M. V. M. Yeo, X. Li, K. Shen, and E. P. V Wilder-Smith, "Can SVM be used for automatic EEG detection of drowsiness during car driving?," *Saf. Sci.*, vol. 47, no. 1, pp. 115–124, 2009.

[113] C. Bielza, G. Li, and P. Larranaga, "Multi-dimensional classification with Bayesian networks," *Int. J. Approx. Reason.*, vol. 52, no. 6, pp. 705–727, 2011.

[114] H. Park, "An introduction to logistic regression: from basic concepts to interpretation with particular attention to nursing domain," *J. Korean Acad. Nurs.*, vol. 43, no. 2, pp. 154–164, 2013.

[115] M. Hämäläinen, R. Hari, R. J. Ilmoniemi, J. Knuutila, and O. V Lounasmaa, "Magnetoencephalography—theory, instrumentation, and applications to noninvasive studies of the working human brain," *Rev. Mod. Phys.*, vol. 65, no. 2, p. 413, 1993.

[116] D. B. Geselowitz, "On bioelectric potentials in an inhomogeneous volume

conductor," *Biophys. J.*, vol. 7, no. 1, pp. 1–11, 1967.

[117] J. C. Mosher, R. M. Leahy, and P. S. Lewis, "EEG and MEG: forward solutions for inverse methods," *IEEE Trans. Biomed. Eng.*, vol. 46, no. 3, pp. 245–259, 1999.

[118] J. N. Reddy, *An introduction to the finite element method*, vol. 1221. McGraw-Hill New York, USA, 2004.

[119] A. M. Dale and M. I. Sereno, "Improved localizadon of cortical activity by combining EEG and MEG with MRI cortical surface reconstruction: a linear approach," *J. Cogn. Neurosci.*, vol. 5, no. 2, pp. 162–176, 1993.

[120] O. Hauk, "Keep it simple: a case for using classical minimum norm estimation in the analysis of EEG and MEG data," *Neuroimage*, vol. 21, no. 4, pp. 1612–1621, 2004.

[121] A. Hillebrand and G. R. Barnes, "Beamformer analysis of MEG data," *Int. Rev. Neurobiol.*, vol. 68, pp. 149–171, 2005.

[122] C. Tallon-Baudry and O. Bertrand, "Oscillatory gamma activity in humans and its role in object representation," *Trends Cogn. Sci.*, vol. 3, no. 4, pp. 151–162, 1999.

[123] J. Sinkkonen, H. Tiitinen, and R. Näätänen, "Gabor filters: an informative way for analysing event-related brain activity," *J. Neurosci. Methods*, vol. 56, no. 1, pp. 99–104, 1995.

[124] M. D. Lezak, *Neuropsychological assessment*. Oxford university press, 2004.

[125] J. F. Connolly and R. C. N. D'Arcy, "Innovations in neuropsychological assessment using event-related brain potentials," *Int. J. Psychophysiol.*, vol. 37, no. 1, pp. 31–47, 2000.

[126] J. F. Connolly, J. M. Byrne, and C. A. Dywan, "Assessing adult receptive vocabulary with event-related potentials: an investigation of cross-modal and cross-form priming," *J. Clin. Exp. Neuropsychol.*, vol. 17, no. 4, pp. 548–565, 1995.

[127] V. V Pravdich-Neminsky, "Experiments on the registration of the electrical phenomena of the mammalian brain," *Zbl.Physiol*, vol. 27, pp. 951–960, 1913.

[128] B. Kotchoubey *et al.*, "Information processing in severe disorders of consciousness: vegetative state and minimally conscious state," *Clin. Neurophysiol.*, vol. 116, no. 10, pp. 2441–2453, 2005.

[129] A. Vanhaudenhuyse, S. Laureys, and F. Perrin, "Cognitive event-related potentials in comatose and post-comatose states," *Neurocrit. Care*, vol. 8, no. 2, pp. 262–270, 2008.

[130] C. Fleck-Prediger *et al.*, "Clinical applications of the Halifax Consciousness Scanner: tracking recovery in a severely brain injured patient," *Int. Brain Org*, pp. 1–12, 2014.

[131] Y. Marchand, R. C. N. D'Arcy, and J. F. Connolly, "Linking neurophysiological and neuropsychological measures for aphasia assessment," *Clin. Neurophysiol.*, vol. 113, no. 11, pp. 1715–1722, 2002.

[132] P. Golland and B. Fischl, "Permutation tests for classification: towards statistical significance in image-based studies," *Inf. Process. Med. imaging*, pp. 330–341, 2003.

[133] E. R. Braverman and K. Blum, "P300 (latency) event-related potential: an accurate predictor of memory impairment," *Clin. EEG Neurosci.*, vol. 34, no. 3, pp. 124–139, 2003.

[134] T. Radüntz, "Signal quality evaluation of emerging EEG devices," *Front. Physiol.*, 2018.

[135] E. M. Buchanan, J. L. Holmes, M. L. Teasley, and K. A. Hutchison, "English semantic word-pair norms and a searchable Web portal for experimental stimulus creation," *Behav. Res. Methods*, vol. 45, no. 3, pp. 746–757, 2013.

[136] W. L. Taylor, "'Cloze procedure': a new tool for measuring readability," *Journal. Bull.*, vol. 30, no. 4, pp. 415–433, 1953.

[137] C. C. Duncan *et al.*, "Event-related potentials in clinical research: guidelines for eliciting, recording, and quantifying mismatch negativity, P300, and N400," *Clin. Neurophysiol.*, vol. 120, no. 11, pp. 1883–1908, Nov. 2009.

[138] S. Beukema *et al.*, "A hierarchy of event-related potential markers of auditory processing in disorders of consciousness," *NeuroImage Clin.*, vol. 12, pp. 359–371, 2016.

[139] E. F. Lau, C. Phillips, and D. Poeppel, "A cortical network for semantics:(de) constructing the N400," *Nat. Rev. Neurosci.*, vol. 9, no. 12, pp. 920–933, 2008.

[140] J. F. Connolly, N. A. Phillips, S. H. Stewart, and W. G. Brake, "Event-related potential sensitivity to acoustic and semantic properties of terminal words in sentences," *Brain Lang.*, vol. 43, no. 1, pp. 1–18, 1992.

[141] R. C. N. D'Arcy, J. F. Connolly, E. Service, C. S. Hawco, and M. E. Houlihan, "Separating phonological and semantic processing in auditory sentence processing: A high- resolution event- related brain potential study," *Hum. Brain Mapp.*, vol. 22, no. 1, pp. 40–51, 2004.

[142] R. C. N. D'Arcy, E. Service, J. F. Connolly, and C. S. Hawco, "The influence of increased working memory load on semantic neural systems: a high-resolution

event-related brain potential study," *Cogn. Brain Res.*, vol. 22, no. 2, pp. 177–191, 2005.

[143] P. J. Holcomb and H. J. Neville, "Auditory and visual semantic priming in lexical decision: A comparison using event-related brain potentials," *Lang. Cogn. Process.*, vol. 5, no. 4, pp. 281–312, 1990.

[144] H. J. Neville, D. L. Mills, and D. S. Lawson, "Fractionating language: different neural subsystems with different sensitive periods," *Cereb. cortex (New York, N.Y. 1991)*, vol. 2, no. 3, pp. 244–258, 1992.

[145] S. Bentin, G. McCarthy, and C. C. Wood, "Event-related potentials, lexical decision and semantic priming," *Electroencephalogr. Clin. Neurophysiol.*, vol. 60, no. 4, pp. 343–355, 1985.

[146] M. D. Rugg, "The Effects of Semantic Priming and Word Repetition on Event-Related Potentials," *Psychophysiology*, vol. 22, no. 6, pp. 642–647, 1985.

[147] M. Kutas and K. D. Federmeier, "Electrophysiology reveals semantic memory use in language comprehension," *Trends Cogn. Sci.*, vol. 4, no. 12, pp. 463–470, 2000.

[148] D. Roehm, I. Bornkessel-Schlesewsky, and M. Schlesewsky, "The internal structure of the N400: Frequency characteristics of a language related ERP component," 2007.

[149] L. Wang *et al.*, "Beta oscillations relate to the N400m during language comprehension," *Hum. Brain Mapp.*, vol. 33, no. 12, pp. 2898–2912, 2012.

[150] C. Van Petten and B. J. Luka, "Neural localization of semantic context effects in electromagnetic and hemodynamic studies," *Brain Lang.*, vol. 97, no. 3, pp. 279–293, 2006.

[151] H. Haan, J. Streb, S. Bien, and F. Rösler, "Individual cortical current density reconstructions of the semantic N400 effect: Using a generalized minimum norm model with different constraints (L1 and L2 norm)," *Hum. Brain Mapp.*, vol. 11, no. 3, pp. 178–192, 2000.

[152] P. Helenius, R. Salmelin, E. Service, J. F. Connolly, S. Leinonen, and H. Lyytinen, "Cortical activation during spoken-word segmentation in nonreading-impaired and dyslexic adults," *J. Neurosci.*, vol. 22, no. 7, pp. 2936–2944, Apr. 2002.

[153] B. Maess, C. S. Herrmann, A. Hahne, A. Nakamura, and A. D. Friederici, "Localizing the distributed language network responsible for the N400 measured by MEG during auditory sentence processing," *Brain Res.*, vol. 1096, no. 1, pp. 163–172, 2006.

[154] N. F. Dronkers, D. P. Wilkins, R. D. Van Valin, B. B. Redfern, and J. J. Jaeger,

"Lesion analysis of the brain areas involved in language comprehension," *Cognition*, vol. 92, no. 1, pp. 145–177, 2004.

[155] N. Neumann and B. Kotchoubey, "Assessment of cognitive functions in severely paralysed and severely brain-damaged patients: neuropsychological and electrophysiological methods," *Brain Res. Protoc.*, vol. 14, no. 1, pp. 25–36, 2004.

[156] J. M. Olichney *et al.*, "Patients with MCI and N400 or P600 abnormalities are at very high risk for conversion to dementia," *Neurology*, vol. 70, no. 19 Pt 2, pp. 1763–1770, May 2008.

[157] K. Wang, E. F. C. Cheung, Q. Gong, and R. C. K. Chan, "Semantic Processing Disturbance in Patients with Schizophrenia: A Meta-Analysis of the N400 Component," *PLoS One*, vol. 6, no. 10, p. e25435, Oct. 2011.

[158] J. T. Wang, G. B. Young, and J. F. Connolly, "Prognostic Value of Evoked Responses and Event-Related Brain Potentials in," *Can. J. Neurol. Sci.*, vol. 31, no. 04, pp. 438–450, 2004.

[159] S. Ghosh Hajra *et al.*, "Developing brain vital signs: Initial framework for monitoring brain function changes over time," *Front. Neurosci.*, vol. 10, 2016.

[160] A. Delorme and S. Makeig, "EEGLAB: an open source toolbox for analysis of single-trial EEG dynamics including independent component analysis," *J. Neurosci. Methods*, vol. 134, no. 1, pp. 9–21, 2004.

[161] W. Skrandies, "Global field power and topographic similarity," *Brain Topogr.*, vol. 3, no. 1, pp. 137–141, 1990.

[162] E. Halgren *et al.*, "N400-like magnetoencephalography responses modulated by semantic context, word frequency, and lexical class in sentences," *Neuroimage*, vol. 17, no. 3, pp. 1101–1116, 2002.

[163] L. Pylkkänen and A. Marantz, "Tracking the time course of word recognition with MEG," *Trends Cogn. Sci.*, vol. 7, no. 5, pp. 187–189, 2003.

[164] C. C. Liu, S. Ghosh Hajra, T. P. L. Cheung, X. Song, and R. C. N. D'Arcy, "Spontaneous Blinks Activate the Precuneus: Characterizing Blink-Related Oscillations Using Magnetoencephalography," *Front. Hum. Neurosci.*, vol. 11, p. 489, 2017.

[165] V. Litvak and K. Friston, "Electromagnetic source reconstruction for group studies," *Neuroimage*, vol. 42, no. 4, pp. 1490–1498, 2008.

[166] K. J. Friston, A. P. Holmes, K. J. Worsley, J. Poline, C. D. Frith, and R. S. J. Frackowiak, "Statistical parametric maps in functional imaging: a general linear approach," *Hum. Brain Mapp.*, vol. 2, no. 4, pp. 189–210, 1994.

[167] J. F. Connolly and N. A. Phillips, "Event-related potential components reflect phonological and semantic processing of the terminal word of spoken sentences," *J. Cogn. Neurosci.*, vol. 6, no. 3, pp. 256–266, 1994.

[168] S. Dikker, H. Rabagliati, T. A. Farmer, and L. Pylkkanen, "Early occipital sensitivity to syntactic category is based on form typicality," *Psychol. Sci.*, vol. 21, no. 5, pp. 629–634, May 2010.

[169] M. Alegre, I. G. Gurtubay, A. Labarga, J. Iriarte, A. Malanda, and J. Artieda, "Alpha and beta oscillatory changes during stimulus-induced movement paradigms: effect of stimulus predictability," *Neuroreport*, vol. 14, no. 3, pp. 381–385, 2003.

[170] C. Tallon-Baudry, "Oscillatory synchrony and human visual cognition," *J. Physiol.*, vol. 97, no. 2, pp. 355–363, 2003.

[171] M. Pesonen, C. H. Björnberg, H. Hämäläinen, and C. M. Krause, "Brain oscillatory 1–30Hz EEG ERD/ERS responses during the different stages of an auditory memory search task," *Neurosci. Lett.*, vol. 399, no. 1, pp. 45–50, 2006.

[172] A. D. Friederici, "Towards a neural basis of auditory sentence processing," *Trends Cogn. Sci.*, vol. 6, no. 2, pp. 78–84, 2002.

[173] G. Hickok and D. Poeppel, "Neural basis of speech perception," *Hum. Audit. Syst. Fundam. Organ. Clin. Disord.*, vol. 129, pp. 149–160, 2015.

[174] A. D. Friederici, S. A. Ruschemeyer, A. Hahne, and C. J. Fiebach, "The role of left inferior frontal and superior temporal cortex in sentence comprehension: localizing syntactic and semantic processes," *Cereb. cortex (New York, N.Y. 1991)*, vol. 13, no. 2, pp. 170–177, Feb. 2003.

[175] J. M. Ford *et al.*, "N400 evidence of abnormal responses to speech in Alzheimer's disease," *Electroencephalogr. Clin. Neurophysiol.*, vol. 99, no. 3, pp. 235–246, 1996.

[176] M. Kiang, I. Patriciu, C. Roy, B. K. Christensen, and R. B. Zipursky, "Test–retest reliability and stability of N400 effects in a word-pair semantic priming paradigm," *Clin. Neurophysiol.*, vol. 124, no. 4, pp. 667–674, 2013.

[177] E. F. Lau, K. Weber, A. Gramfort, M. S. Hämäläinen, and G. R. Kuperberg, "Spatiotemporal Signatures of Lexical–Semantic Prediction," *Cereb. Cortex*, vol. 26, no. 4, pp. 1377–1387, Apr. 2016.

[178] J. J. Ryan, L. A. Glass, J. M. Bartels, C. M. Bergner, and A. M. Paolo, "Predicting neuropsychological test performance on the basis of temporal orientation," *Aging, Neuropsychol. Cogn.*, vol. 16, no. 3, pp. 330–337, 2009.

[179] R. N. Dowler, B. A. Bush, T. A. Novack, and W. T. Jackson, "Cognitive orientation

in rehabilitation and neuropsychological outcome after traumatic brain injury," *Brain Inj.*, vol. 14, no. 2, pp. 117–123, 2000.

[180] E. O'Keeffe, O. Mukhtar, and S. T. O'Keeffe, "Orientation to time as a guide to the presence and severity of cognitive impairment in older hospital patients," *J. Neurol. Neurosurg. Psychiatry*, vol. 82, no. 5, pp. 500–504, May 2011.

[181] E. Guerrero‑Berroa *et al.*, "The MMSE orientation for time domain is a strong predictor of subsequent cognitive decline in the elderly," *Int. J. Geriatr. Psychiatry*, vol. 24, no. 12, pp. 1429–1437, 2009.

[182] S. Ghosh Hajra, C. C. Liu, X. Song, S. D. Fickling, T. P. L. Cheung, and R. C. N. D'Arcy, "Multimodal characterization of the semantic N400 response within a rapid evaluation brain vital sign framework," *J. Transl. Med.*, vol. 16, no. 1, p. 151, Jun. 2018.

[183] I. Winkler and I. Czigler, "Evidence from auditory and visual event-related potential (ERP) studies of deviance detection (MMN and vMMN) linking predictive coding theories and perceptual object representations," *International Journal of Psychophysiology*, vol. 83, no. 2. Elsevier, pp. 132–143, 01-Feb-2012.

[184] N. Fogelson, C. Loukas, J. Brown, and P. Brown, "A common N400 EEG component reflecting contextual integration irrespective of symbolic form," *Clin. Neurophysiol.*, vol. 115, no. 6, pp. 1349–1358, Mar. 2004.

[185] A. M. Proverbio and F. Riva, "RP and N400 ERP components reflect semantic violations in visual processing of human actions," *Neurosci. Lett.*, vol. 459, no. 3, pp. 142–146, Aug. 2009.

[186] M. Niedeggen, F. Rösler, and K. Jost, "Processing of incongruous mental calculation problems: Evidence for an arithmetic N400 effect," *Psychophysiology*, vol. 36, no. 3, pp. 307–324, 1999.

[187] L. Renoult *et al.*, "Autobiographically significant concepts: more episodic than semantic in nature? An electrophysiological investigation of overlapping types of memory," *J. Cogn. Neurosci.*, vol. 27, no. 1, pp. 57–72, 2015.

[188] P. Hagoort, L. Hald, M. Bastiaansen, and K. M. Petersson, "Integration of Word Meaning and World Knowledge in Language Comprehension," *Science (80-.).*, vol. 304, no. 5669, pp. 438–441, Apr. 2004.

[189] M. Brysbaert, A. B. Warriner, and V. Kuperman, "Concreteness ratings for 40 thousand generally known English word lemmas," *Behav. Res. Methods*, vol. 46, no. 3, pp. 904–911, 2014.

[190] M. Coltheart, "The MRC psycholinguistic database," *Q. J. Exp. Psychol.*, vol. 33, no. 4, pp. 497–505, 1981.

[191] T. Bardouille, S. V Krishnamurthy, S. G. Hajra, and R. C. N. D'Arcy, "Improved localization accuracy in magnetic source imaging using a 3-D laser scanner," *IEEE Trans. Biomed. Eng.*, vol. 59, no. 12, pp. 3491–3497, 2012.

[192] A. J. Bell and T. J. Sejnowski, "An information-maximization approach to blind separation and blind deconvolution," *Neural Comput.*, vol. 7, no. 6, pp. 1129–1159, 1995.

[193] D. J. Mitchell and R. Cusack, "The temporal evolution of electromagnetic markers sensitive to the capacity limits of visual short-term memory," *Front. Hum. Neurosci.*, vol. 5, p. 18, Feb. 2011.

[194] K. Joos, A. Gilles, P. Van de Heyning, D. De Ridder, and S. Vanneste, "From sensation to percept: The neural signature of auditory event-related potentials," *Neurosci. Biobehav. Rev.*, vol. 42C, pp. 148–156, Feb. 2014.

[195] V. Litvak *et al.*, "EEG and MEG data analysis in SPM8," *Comput. Intell. Neurosci.*, vol. 2011, p. 852961, 2011.

[196] C. C. Liu, S. G. Hajra, X. Song, S. M. Doesburg, T. P. L. Cheung, and R. C. N. D'Arcy, "Cognitive loading via mental arithmetic modulates effects of blink-related oscillations on precuneus and ventral attention network regions," *Hum. Brain Mapp.*, vol. 40, no. 0, pp. 377–393.

[197] R. Caldara, F. Jermann, G. L. Arango, and M. Van der Linden, "Is the N400 category-specific? A face and language processing study," *Neuroreport*, vol. 15, no. 17, 2004.

[198] A. Khateb, A. J. Pegna, T. Landis, M. S. Mouthon, and J.-M. Annoni, "On the Origin of the N400 Effects: An ERP Waveform and Source Localization Analysis in Three Matching Tasks," *Brain Topogr.*, vol. 23, no. 3, pp. 311–320, Sep. 2010.

[199] V. J. IRAGUI, M. KUTAS, M. R. MITCHINER, and S. A. HILLYARD, "Effects of aging on event-related brain potentials and reaction times in an auditory oddball task," *Psychophysiology*, vol. 30, no. 1, pp. 10–22, Jan. 2007.

[200] M. Kutas and V. Iragui, "The N400 in a semantic categorization task across 6 decades," *Electroencephalogr. Clin. Neurophysiol. Potentials Sect.*, vol. 108, no. 5, pp. 456–471, 1998.

[201] J. Kayser and C. E. Tenke, "In search of the Rosetta Stone for scalp EEG: converging on reference-free techniques.," *Clin. Neurophysiol.*, vol. 121, no. 12, pp. 1973–5, Dec. 2010.

[202] K. A. Paller, H. D. Lucas, and J. L. Voss, "Assuming too much from 'familiar'brain potentials," *Trends Cogn. Sci.*, vol. 16, no. 6, pp. 313–315, 2012.

[203] L. Renoult *et al.*, "Personal semantics: Is it distinct from episodic and semantic

memory? An electrophysiological study of memory for autobiographical facts and repeated events in honor of Shlomo Bentin," *Neuropsychologia*, vol. 83, pp. 242–256, 2016.

[204] D. Friedman, R. Simson, W. Ritter, and I. Rapin, "The late positive component (P300) and information processing in sentences," *Electroencephalogr. Clin. Neurophysiol.*, vol. 38, no. 3, pp. 255–262, 1975.

[205] E. L. Mazerolle, R. C. N. D'Arcy, Y. Marchand, and R. B. Bolster, "ERP assessment of functional status in the temporal lobe: Examining spatiotemporal correlates of object recognition," *Int. J. Psychophysiol.*, vol. 66, no. 1, pp. 81–92, 2007.

[206] A. Sousa, J. J. Gomar, T. E. Goldberg, and A. D. N. Initiative, "Neural and behavioral substrates of disorientation in mild cognitive impairment and Alzheimer's disease," *Alzheimer's Dement. Transl. Res. Clin. Interv.*, vol. 1, no. 1, pp. 37–45, 2015.

[207] M. Peer, R. Lyon, and S. Arzy, "Orientation and disorientation: lessons from patients with epilepsy," *Epilepsy Behav.*, vol. 41, pp. 149–157, 2014.

[208] M.-M. Mesulam, S. G. Waxman, N. Geschwind, and T. D. Sabin, "Acute confusional states with right middle cerebral artery infarctions.," *J. Neurol. Neurosurg. Psychiatry*, vol. 39, no. 1, pp. 84–89, 1976.

[209] L. R. Caplan *et al.*, "Infarcts of the inferior division of the right middle cerebral artery Mirror image of Wernicke's aphasia," *Neurology*, vol. 36, no. 8, p. 1015, 1986.

[210] E. Mori and A. Yamadori, "Acute confusional state and acute agitated delirium: Occurrence after infarction in the right middle cerebral artery territory," *Arch. Neurol.*, vol. 44, no. 11, pp. 1139–1143, Nov. 1987.

[211] D. L. Harrington, K. Y. Haaland, and R. T. Knight, "Cortical networks underlying mechanisms of time perception," *J. Neurosci.*, vol. 18, no. 3, pp. 1085–1095, 1998.

[212] H.-O. Karnath, "New insights into the functions of the superior temporal cortex," *Nat. Rev. Neurosci.*, vol. 2, no. 8, p. 568, 2001.

[213] M. T. de Schotten *et al.*, "Direct evidence for a parietal-frontal pathway subserving spatial awareness in humans," *Science (80-.).*, vol. 309, no. 5744, pp. 2226–2228, 2005.

[214] H.-O. Karnath, S. Ferber, and M. Himmelbach, "Spatial awareness is a function of the temporal not the posterior parietal lobe," *Nature*, vol. 411, no. 6840, p. 950, 2001.

[215] D. Bueti and V. Walsh, "The parietal cortex and the representation of time, space, number and other magnitudes," *Philos. Trans. R. Soc. B Biol. Sci.*, vol. 364, no. 1525, pp. 1831–1840, 2009.

[216] J. Davey *et al.*, "Exploring the role of the posterior middle temporal gyrus in semantic cognition: Integration of anterior temporal lobe with executive processes," *Neuroimage*, vol. 137, pp. 165–177, 2016.

[217] J. Davey *et al.*, "Automatic and Controlled Semantic Retrieval: TMS Reveals Distinct Contributions of Posterior Middle Temporal Gyrus and Angular Gyrus," *J. Neurosci.*, vol. 35, no. 46, pp. 15230–15239, Nov. 2015.

[218] P. Ramkumar, M. Jas, S. Pannasch, R. Hari, and L. Parkkonen, "Feature-specific information processing precedes concerted activation in human visual cortex.," *J. Neurosci.*, vol. 33, no. 18, pp. 7691–9, May 2013.

[219] T. W. Picton *et al.*, "Guidelines for using human event- related potentials to study cognition: Recording standards and publication criteria," *Psychophysiology*, vol. 37, no. 2, pp. 127–152, 2000.

[220] C. C. Liu, S. Ghosh Hajra, S. Fickling, G. Pawlowski, X. Song, and R. C. N. D'Arcy, "Novel Signal Processing Technique for Capture and Isolation of Blink-Related Oscillations Using a Low-Density Electrode Array for Bedside Evaluation of Consciousness," *IEEE Trans. Biomed. Eng.*, 2019.

[221] C. M. Fleck-Prediger *et al.*, "Point-of-care brain injury evaluation of conscious awareness: wide scale deployment of portable HCS EEG evaluation," *Neurosci. Conscious.*, vol. 2018, no. 1, p. niy011, 2018.

[222] S. D. Fickling *et al.*, "Brain vital signs demonstrate subconcussive impairment after a single season of ice hockey," in *BRAIN INJURY*, 2017, vol. 31, no. 6–7, pp. 942–943.

[223] P. M. Zeman, B. C. Till, N. J. Livingston, J. W. Tanaka, and P. F. Driessen, "Independent component analysis and clustering improve signal-to-noise ratio for statistical analysis of event-related potentials," *Clin. Neurophysiol.*, vol. 118, no. 12, pp. 2591–2604, Dec. 2007.

[224] C. D. McGillen, J. I. Aunon, and K. Yu, "Signals and Noise in Evoked Brain Potentials," *IEEE Trans. Biomed. Eng.*, vol. BME-32, no. 12, pp. 1012–1016, 1985.

[225] P. L. Nunez and R. Srinivasan, *Electric Fields of the Brain: The neurophysics of EEG*. 2009.

[226] G. D. Dawson, "A summation technique for the detection of small evoked potentials," *Electroencephalogr. Clin. Neurophysiol.*, vol. 6, pp. 65–84, Jan. 1954.

[227] E. S. Kappenman and S. J. Luck, "The effects of electrode impedance on data quality and statistical significance in ERP recordings," *Psychophysiology*, vol. 47, no. 5, pp. 888–904, 2010.

[228] J. Dien and A. M. Santuzzi, "Application of Repeated Measures ANOVA to High-Density ERP Datasets: A Review and Tutorial," *Event-Related Potentials. A Methods Handb.*, 2005.

[229] S. G. Hajra, C. C. Liu, X. Song, S. Fickling, G. Pawlowski, and R. C. N. D'Arcy, "DEVELOPING BRAIN VITAL SIGNS: INITIAL ASSESSMENTS ACROSS THE ADULT LIFESPAN," *Alzheimer's Dement.*, Jul. 2016.

[230] S. Ghosh Hajra, C. C. Liu, X. Song, S. D. Fickling, T. P. L. Cheung, and R. C. N. D'Arcy, "Accessing knowledge of the 'here and now': a new technique for capturing electromagnetic markers of orientation processing.," *J. Neural Eng.*, vol. 16, no. 1, p. 016008, Feb. 2019.

[231] K. M. Spencer, "Averaging, detection and classification of single-trial ERPs," in *Event-related Potentials: A Methods Handbook*, 2005.

[232] S. Hanslmayr *et al.*, "Alpha phase reset contributes to the generation of ERPs," *Cereb. Cortex*, 2007.

[233] S. Y. Tseng, R. C. Chen, F. C. Chong, and T. S. Kuo, "Evaluation of parametric methods in EEG signal analysis," *Med. Eng. Phys.*, 1995.

[234] N. Williams, S. Nasuto, and J. Saddy, "Evaluation of Empirical Mode Decomposition for Event-Related Potential Analysis," *EURASIP J. Adv. Signal Process.*, 2011.

[235] B. Blankertz, S. Lemm, M. Treder, S. Haufe, and K. R. Müller, "Single-trial analysis and classification of ERP components - A tutorial," *Neuroimage*, 2011.

[236] P. Kidmose, D. Looney, M. Ungstrup, M. L. Rank, and D. P. Mandic, "A study of evoked potentials from ear-EEG," *IEEE Trans. Biomed. Eng.*, 2013.

[237] S. Debener, R. Emkes, M. De Vos, and M. Bleichner, "Unobtrusive ambulatory EEG using a smartphone and flexible printed electrodes around the ear," *Sci. Rep.*, 2015.

[238] J. J. S. Norton *et al.*, "Soft, curved electrode systems capable of integration on the auricle as a persistent brain–computer interface," *Proc. Natl. Acad. Sci.*, 2015.

[239] A. M. Beres, "Time is of the essence: A review of electroencephalography (EEG) and event-related brain potentials (ERPs) in language research," *Appl. Psychophysiol. Biofeedback*, vol. 42, no. 4, pp. 247–255, 2017.

[240] N. N. Thigpen, E. S. Kappenman, and A. Keil, "Assessing the internal consistency

of the event-related potential: An example analysis," *Psychophysiology*, vol. 54, no. 1, pp. 123–138, 2017.

[241] S. J. Luck, "Ten Simple Rules for Designing and Interpreting ERP Experiments.[In:] Event-Related Potentials: A Methods Handbook," *Handy, TC*, 2004.

[242] S. D. Fickling *et al.*, "Brain vital signs detect concussion-related neurophysiological impairments in ice hockey," *Brain*, vol. 142, no. 2, pp. 255–262, Jan. 2019.

[243] Z. Qi *et al.*, "Native-language N400 and P600 predict dissociable language-learning abilities in adults," *Neuropsychologia*, vol. 98, pp. 177–191, 2017.